

Experimental Investigations and Modelling Studies on Performance of Spark Ignited Engine with Varied Composition of Producer gas

THESIS

Submitted in partial fulfilment
of the requirements for the degree of

DOCTOR OF PHILOSOPHY

by

METIKELA SREEDHAR BABU

Under the Supervision of

Prof. Shibu Clement

&

Dr. N. K. S. Rajan



BITS Pilani

Pilani|Dubai|Goa|Hyderabad

BIRLA INSTITUTE OF TECHNOLOGY AND SCIENCE, PILANI

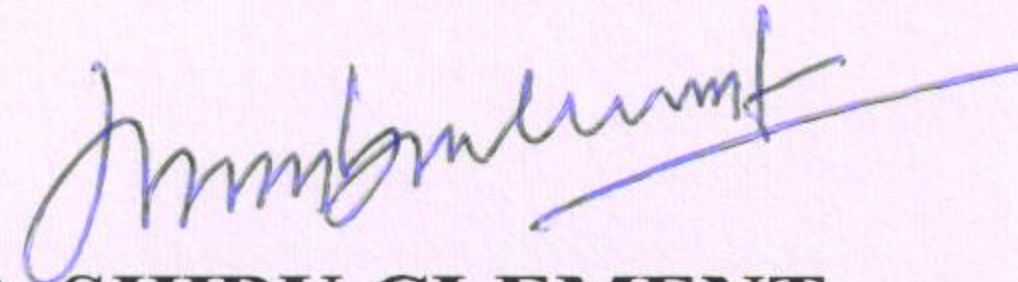
2016

BIRLA INSTITUTE OF TECHNOLOGY AND SCIENCE, PILANI

CERTIFICATE

This is to certify that the thesis entitled: **Computational and experimental analyses of alternative fuel based internal combustion engine**. Submitted by **Metikela Sreedhar Babu**, ID No **2009PHXF424G** for the award of Ph.D. of the Institute embodies original work done by him/her under my supervision.

Signature of the Supervisor:



Name in capital letters:

DR. SHIBU CLEMENT

Designation:

Associate Professor and Head of Department

Mechanical Engineering

BITS Pilani, K.K. Birla Goa Campus, Goa - 403726

Signature of the Co-Supervisor:



Name in capital letters:

DR. N.K.S. RAJAN

Designation:

Chief Research Scientist

Institute:

Combustion Gasification & Propulsion Laboratory

Department of Aerospace Engineering

Indian Institute of Science, Bengaluru - 560012

Date: November 2016

Dedicated to my

Brothers

&

Sisters

Acknowledgements

I would like to express my heartfelt gratitude to my PhD supervisor, Prof. Shibu Clement for his continuous guidance, immense patience, thoughtfulness, motivation and support throughout my research work. My deepest gratitude to my co-supervisor Dr. N.K.S. Rajan, for guiding me successfully towards the completion of this thesis work. His patience, technical discussions and timely inputs greatly helped my thesis work and made it enjoyable journey.

I am grateful to Prof. Souvik Bhattacharyya, Vice Chancellor, BITS Pilani and Prof. Raghurama G., Director of BITS Pilani KK Birla Goa Campus. Prof. Sasikumar Punnekkat, and Prof. K. E. Raman, Former Directors, BITS, Pilani - KK Birla Goa Campus, Prof. Sanjay Kumar Verma, Dean, Academic Research, BITS, Pilani for giving me an opportunity and necessary infrastructure to carry out my research work at Goa campus.

Thanks to Prof. P.M. Singru, former Head, Department of Mechanical Engineering, BITS Pilani, K. K. Birla Goa Campus, for allowing to use laboratory facilities. My heartfelt thanks to Dr. S.S. Baral and Dr. Ranjit S. Patil for their comments and valuable suggestions in enhancing the quality of the thesis. I am grateful to Dr. Prasantha Kumar Das, Associate Dean Academic Research Division and Dr. S.D. Manjare, Former Faculty-In charge, Research and Consultancy and Education Development Division, BITS Pilani - KK Birla Goa Campus for their encouragement throughout the course of this study. I also thank my faculty colleagues Dr. PL. Ramkumar, Dr. Kiran D. Mali, Dr. Vikas Chaudhary, Dr. Sachin Waigoankar, Dr. Varinder Singh, Dr. Gaurav Singh, Dr. G. Karthikeyan, Mr. A.C. Kulkarni, Mr. Abhilash Kumar, Mr. Ravindra Singh and Mr. Amal of Mechanical Engineering Department for providing moral support during critical phases of my research work.

I am also thankful to Prof. M.K. Gajendra Babu, Emeritus Professor, IIT-Madras for the technical interactions and suggestions on manuscripts. Sincere thanks to Dr. Rajaram Lakkaraju for his timely help in sharing research papers. I am grateful to Mr. G. J. Desai, Superintendent of Workshop and Mr. Vijay Suryavamshi, Assistant superintendent of Workshop for their immense help in procurement of equipment. My sincere thanks to Mr. Shailesh and Mr. Surendra Kinlekar, Purchase officer, for helping me in paper work and approvals. Thanks to Mr. Jitendranath Nayak, Mr. Ajay, Mr. Viraj of BITS Pilani – KK Birla Goa Campus and Mr. Venu

of CGPL., IISc for assisting me in experimental work. Thanks to research scholars Mr. Abhijith Padhiary, Mr. Prashant Mewani, Mr. Dhananjay Gupta, Mr. Atul Kumar, Mr. Vishal Garg, Mr. Siddhant Rathore, Mr. Bhaswat and Mr. Gaurav Gude for helping in engine experiments.

I extend my gratitude to Dr. Ravi Fernandez, Mr. Sonal Kumar, Ms. Prajuktha and Ms. Rupali of Aachen University, Germany for helping me with combustion properties related to producer gas fuel. I am also grateful to engine suppliers “Legion Brothers”, Bengaluru for their timely online service.

Last but not least, my sincere thanks to my wife, Tabitha and daughter Shiphrah for their patience and inspiration in completing this thesis work. Heartfelt thanks to my parents and in-laws for their blessings and constant prayer support. Finally, I wish to record my sincere thanks to all my well-wishers and my friends, especially Mr. Anurag Devarapalli for their support.

M. Sreedhar Babu

Abstract

Internal combustion engines have been a major source for power generation worldwide over many decades. The utility of engines powering the generator sets (gensets) has been a tremendous benefit to society but at the cost of degradation to environment due to harmful emissions. In this context, as a part to combat climate change and to reduce dependency on fossil fuels, major research is focused on (i) improving the existing engine design, (ii) improving the combustion process (iii) after treatment of exhaust gases and (iv) adoption of renewable fuels. Among the alternative fuels, Producer gas (PG) is one such renewable and eco-friendly fuel, having a potential to meet the twin requirement of improving the in-cylinder combustion process and also an ability to undergo a cleaner combustion resulting in lower emission levels. PG is derived from a thermo-chemical energy conversion route. Here the biomass undergoes a gasification process (air as gasification agent) in a gasifier, giving rise to a multi component fuel called Producer gas. PG is a mixture of three combustibles and two non-combustibles gases namely, hydrogen, methane, carbon monoxide and carbon-di-oxide, nitrogen respectively. The composition and calorific value of PG varies widely depending upon the type of feed stock used and gasifier design. Among the reactor units, downdraft gasifiers are most suitable for engine application due to their ability to break down higher hydrocarbons like tar and clinkers.

Based on above discussion, in the present work the dynamics associated with engine combustion process against the fluctuating trend in producer gas fuel composition is taken up. In order to assess the magnitude of variation in engine combustion and performance parameters, bottled fuel gas was considered. However, interfacing highly pressurized PG bottle is challenging. This arrangement requires great control and systematic handling of induction system for safe operation of PG engine. Owing to typical A/F mass ratio, the PG engine requires tailor made carburetor other than conventional types. These challenges of developing suitable induction system and also designing gas carburetor have been successfully addressed in this work. The selected combinations of PG fuel sets based on moisture variation in biomass were formulated to investigate the effect of hydrogen and methane concentration on engine performance and combustion parameters. The variation of combustible gases considered was, H₂ (16 - 22%), CH₄ (1 – 4%), CO (18%), CO₂ (12%) and

N₂ (Balance) by volume basis. Experiments were conducted on single cylinder, four stroke converted spark ignition engine of 359 cm³ with a compression ratio of 11:1 and at constant speed of 1500 rpm. The results indicated a knock free engine operation with 1.35 bar/CA and the optimal ignition time varied from -18 to -14° CA, -20 to -16° CA and -23 to -20° CA at full, 75% and 50% engine load respectively. On emission front CO, HC and NO were well within prescribed CPCB-2016 norms.

To estimate the effect of hydrogen concentration at higher compression ratio and to arrive at optimized the compression ratio for the present engine (Model #1533), the engine was tested at constant speed of 1500 rpm at 11:1, 15:1 and 18:1. The test results were encouraging and did not show up any sign of knocking even with 22% vol. hydrogen in PG. On the other side, fuel sets like B set (19% H₂ + 2.5% CH₄), C set (22% H₂ + 2.5% CH₄) were found to promote fuel economy. The influence of hydrogen at higher compressions ratios (11:1 to 18:1) was successfully assessed and optimum compression ratio for the present engine configuration based on brake thermal efficiency and brake specific fuel consumption was identified as 15:1. On emission front at higher compression ratio, producer gas was found to be an environmental benign.

The last objective of the work is to model the burn rate of PG blends through double stage Wiebe combustion model. Literature in the field of combustion modelling was reviewed. It was found that Wiebe correlation was extensively used in zero and one dimensional cycle simulation study both in SI and CI engines. Wiebe model is a well-known mass fraction burn formulation and is a function of shape factor (m) and efficiency factor (a). The combustion parameters like mass fraction burnt (MFB) and rate of heat release (ROHR) are important in research and development of engines to study the overall engine performance, efficiencies and emissions. The mass fraction burn (MFB) profiles were estimated based on well- established Rassweiler and Withrow method. The parametric study reveals that, presence of higher concentration of hydrogen in PG causes significant variations in burn angles during primary combustion phase and thus results in higher in-cylinder temperatures. On the other hand, the concentration of methane in PG was found to shorten the duration of secondary combustion phase and thus reduce the prolonged combustion durations which is generally the case with PG engine operation.

Table of Contents

| | |
|------------------------------------|-------------|
| <i>Acknowledgements</i> | <i>i</i> |
| <i>Abstract</i> | <i>iii</i> |
| <i>Table of contents</i> | <i>v</i> |
| <i>List of figures</i> | <i>ix</i> |
| <i>List of tables</i> | <i>xi</i> |
| <i>List of symbols</i> | <i>xiii</i> |
| <i>List of abbreviations</i> | <i>xiii</i> |

Chapter 1

Introduction

| | |
|----------------------------------------------------------|---|
| 1.1 Perspective | 1 |
| 1.2 Indian scenario in bio-energy..... | 1 |
| 1.3 Prospects of biomass gasification technology..... | 3 |
| 1.4 Downdraft gasifier for Producer gas generation | 5 |
| 1.5 Issues related to Producer gas fuel combustion | 6 |
| 1.6 Scope of the present work..... | 7 |
| 1.7 Organization of thesis | 7 |

Chapter 2

Literature Review

| | |
|-----------------------------------------------------|----|
| 2.1 Introduction..... | 9 |
| 2.2 Routes for energy conversion..... | 9 |
| 2.2.1 Brief history of gasification..... | 9 |
| 2.3 Open-top downdraft gasifier | 11 |
| 2.4 Issues related to producer gas quality | 11 |
| 2.4.1 Suitable gasifier for engine application..... | 12 |

| | |
|-------------------------------------------------------------------|----|
| 2.4.2 Factors affecting producer gas quality or composition | 13 |
| 2.5 Producer gas as a fuel in IC engines | 14 |
| 2.6 Effect of hydrogen and methane composition | 18 |
| 2.7 Emission trend | 19 |
| 2.8 Modelling studies on combustion characteristics | 21 |
| 2.9 Natural gas fuelled engines | 22 |
| 2.10 Gaps in the existing research work | 23 |
| 2.11 Objectives of present work | 24 |

Chapter 3

Materials and methodology

| | |
|--------------------------------------------------------------------|----|
| 3.1 Introduction | 26 |
| 3.2 Producer gas mixture formulation (PG fuel sets) | 26 |
| 3.3 Estimation of producer gas quantity | 28 |
| 3.4 Methodology to acquire engine data | 28 |
| 3.4.1 Engine instrumentation | 28 |
| 3.4.2 Significance of combustion pressure versus crank angle | 29 |
| 3.4.3 Engine combustion parameters | 30 |
| 3.4.4 Engine performance parameters | 32 |
| 3.5 Variation of compression ratio | 33 |
| 3.6 Exhaust gas measurement | 35 |
| 3.6.1 Emission analyzer | 35 |
| 3.6.2 Emission conversion | 36 |
| 3.7 Uncertainty analyses | 36 |
| 3.8 Summary | 37 |

Chapter 4

Experimental set-up and procedure

| | |
|----------------------------------------------|----|
| 4.1 Introduction | 38 |
| 4.2 Description of engine set-up | 38 |
| 4.3 Developmental activity of test-rig | 40 |

| | |
|------------------------------------------------|----|
| 4.3.1 Elements of induction system..... | 40 |
| 4.3.2 Testing of induction system..... | 44 |
| 4.3.3 Engine testing | 46 |
| 4.4 Optimum fuel line operating pressure | 48 |
| 4.5 Summary..... | 49 |

Chapter 5

Influence of Hydrogen and Methane Concentration in Producer Gas Fuelled SI Engine .

| | |
|----------------------------------------------------------------------------------------|----|
| 5.1 Introduction..... | 50 |
| 5.2 Variation of H ₂ and CH ₄ concentration in producer gas..... | 50 |
| 5.3 Experimental set-up..... | 51 |
| 5.4 Experimental procedure..... | 52 |
| 5.5 Analysis of engine performance parameters..... | 53 |
| 5.6 Analysis of combustion parameters..... | 56 |
| 5.7 Variation of emissions levels at full, 75% and 50% load points..... | 63 |
| 5.8 Summary..... | 66 |

Chapter 6

Effect of Hydrogen Concentration at Higher Compression Ratios in Producer gas Fuelled SI Engine

| | |
|-----------------------------------------------------------------|----|
| 6.1 Introduction..... | 68 |
| 6.2 Producer gas fuel formulation for higher CRs | 68 |
| 6.3 Experimental set-up for higher compression ratio work | 69 |
| 6.4 Experimental procedure..... | 70 |
| 6.5 Analysis of engine performance parameters..... | 70 |
| 6.6 Analysis of combustion parameters..... | 73 |
| 6.7 Analysis of emissions | 78 |
| 6.8 Summary | 80 |

Chapter 7

Modeling of Mass Fraction Burn Curves and Parametric Studies

| | |
|------------------------------------------------------------------|----|
| 7.1 Introduction | 82 |
| 7.2 Methodology | 82 |
| 7.3 Inadequacy of Wiebe single stage function for PG fuel | 83 |
| 7.4 Suitability of double stage Wiebe function for PG fuel | 87 |
| 7.5 Result and discussions | 88 |
| 7.6 Summary..... | 97 |

Chapter 8

Conclusions

| | |
|-------------------------------------------------------------------------|-----|
| 8.1 Introduction | 99 |
| 8.2 Work flow | 99 |
| 8.3 Development of induction system for bottled fuelled PG engine | 100 |
| 8.4 Influence of variation in hydrogen and methane concentration..... | 100 |
| 8.5 Effect of hydrogen at higher compression ratios | 102 |
| 8.6 Modelling of mass fraction burn curves | 102 |
| 8.7 Contribution of the thesis..... | 104 |
| 8.8 Recommendations | 104 |
| 8.9 Scope for future work | 105 |

| | |
|-------------------------|-----|
| References | 106 |
|-------------------------|-----|

| | |
|-----------------------------------|-----|
| List of publications | 115 |
|-----------------------------------|-----|

Appendices

| | |
|------------------------------------------------------------------------------------------|-----|
| Appendix-A : Estimation of producer gas requirement | 116 |
| Appendix-B : Technical details of pressure transducer | 117 |
| Appendix-C : Technical details of crank angle encoder | 119 |
| Appendix-D : MATLAB code for in-cylinder data processing..... | 121 |
| Appendix-E : Technical details of flue gas analyzer | 135 |
| Appendix-F : Demonstration of uncertainty calculation | 137 |
| Appendix-G : a) Calibration certificate of air flow orificemeter for gasoline operation. | |

| | |
|---------------------------------------------------------------------------|-----|
| | 138 |
| b) Calibration certificate for PG based orificemeter | 139 |
| c) Calibration certificate of air flow orificemeter for CNG operation.... | 140 |
| Appendix-H: MATLAB code for curve fitting (Wiebe model) | 141 |
| Appendix-I: Data table for MBT spark time and brake power | 142 |
| Biography of supervisor | 143 |
| Biography of Co-supervisor | 143 |
| Biography of Scholar | 144 |

List of Figures

| | |
|-----------------------------------------------------------|----|
| Fig.1.1 Total primary energy consumption of India | 2 |
| Fig.1.2 Gasifier and engine system | 6 |
| Fig. 2.1 Biomass energy conversion pathways..... | 10 |
| Fig. 2.2 Types of gasifier | 12 |
| Fig. 2.3 Carburetors for PG induction..... | 15 |
| Fig. 3.1 Calibrated producer gas bottles..... | 28 |
| Fig. 3.2 Piezoelectric pressure transducer | 29 |
| Fig. 3.3 Photographic view of engine gasket..... | 34 |
| Fig. 3.4 Flue gas analyzer (AVL-444) | 36 |
| Fig. 4.1 Photographic view of engine set-up..... | 38 |
| Fig. 4.2 Toroidal piston shape | 39 |
| Fig. 4.3 PG-Air mixer | 41 |
| Fig. 4.4 Air gas regulator..... | 42 |
| Fig. 4.5 Air flow measurement | 43 |
| Fig. 4.6 Piping network and entire induction system..... | 44 |
| Fig. 4.7 PG reservoir | 44 |
| Fig. 4.8 Optimum port diameter of air-gas regulator..... | 45 |
| Fig. 4.9 Location of optimum port diameter | 46 |
| Fig. 4.10 Peak combustion pressure at MBT spark time..... | 48 |

| | |
|---------------------------------------------------------------------------------------------------------------------|----|
| Fig. 4.11 Work output of producer gas over gasoline | 48 |
| Fig. 5.1 Schematic view of experimental set-up..... | 52 |
| Fig. 5.2 Head gasket and compression rings for CR:11 | 52 |
| Fig. 5.3 Flue gas sampling system | 53 |
| Fig. 5.4 Variation of BSFC at CR: 11, 1500 rpm and $\phi \approx 1$ | 54 |
| Fig. 5.5 Energy consumption at CR:11 and 1500 rpm..... | 55 |
| Fig. 5.6 Brake thermal efficiencies at CR:11 | 56 |
| Fig. 5.7 In-cylinder pressure variations at full, 75% and 50% load,..... | 58 |
| Fig. 5.8 Overall engine response at CR:11, full load for 16 to 22% H ₂ and 1 to 4% CH ₄ | 60 |
| Fig. 5.9 Overall engine response at CR:11, 75% load for 16 to 22% H ₂ and 1 to 4% CH ₄ | 60 |
| Fig. 5.10 Overall engine response at CR:11, 50% load for 16 to 22% H ₂ and 1 to 4% CH ₄ .. | 61 |
| Fig. 5.11 Variation in combustion duration at full load, CR:11 and 1500 rpm..... | 62 |
| Fig. 5.12 Mass fraction burnt variation at 75% load..... | 62 |
| Fig. 5.13 Variation in ROPR at CR:11 and 1500 rpm | 63 |
| Fig. 5.14 Emissions at full load, CR:11, 1500 rpm..... | 64 |
| Fig. 5.15 Emissions at 75% load, CR:11, 1500 rpm..... | 65 |
| Fig. 5.16 Emissions at 50% load, CR:11, 1500 rpm..... | 65 |
| Fig. 6.1 Head gasket and compression rings for CR:11, 15 and 18..... | 69 |
| Fig. 6.2 A view of forced convection to support higher CR operation | 70 |
| Fig. 6.3abc Brake thermal efficiencies at CR: 11, 15 and 18 | 72 |
| Fig. 6.4 Brake specific fuel consumption at CR: 11, 15 and 18 | 72 |
| Fig. 6.5 Cylinder pressure variation at full load for various CRs..... | 74 |
| Fig. 6.6 Asymmetrical late valve overlap..... | 74 |
| Fig. 6.7 Cylinder pressure variation at 75% load for various CRs | 75 |
| Fig. 6.8 Mass fraction burnt trend at full load | 76 |
| Fig. 6.9 Mass fraction burnt trend at 75% load | 77 |
| Fig. 6.10 Mass fraction burnt trend at 50% load | 77 |
| Fig. 6.11 Mass fraction burnt profiles at CR:15 and 75% load point | 78 |
| Fig. 6.12 Emissions at full load engine operation..... | 79 |
| Fig. 6.13 Emissions at 75% engine load | 80 |
| Fig. 7.1 Single Wiebe coefficients for Gasoline fuel at full load | 84 |

| | |
|---------------------------------------------------------------------------------------|----|
| Fig. 7.2 Single Wiebe coefficients for CNG fuel at full load | 85 |
| Fig. 7.3 Single Wiebe coefficients for PG: (Set-A) fuel at full load..... | 85 |
| Fig. 7.4 Unsymmetrical negative valve overlap | 86 |
| Fig. 7.5 Inadequacy of single stage Wiebe model for heavy valve overlap engines | 87 |
| Fig. 7.6 Phases of combustion process..... | 88 |
| Fig. 7.7 Model constants for PG: Set-A, B and C..... | 90 |
| Fig. 7.8 Model constants for PG: Set-D, E and F | 91 |
| Fig. 7.9 Model constants for PG: Set-G, H and I..... | 92 |
| Fig. 7.10 Effect of hydrogen with 1% methane concentration | 93 |
| Fig. 7.11 Effect of hydrogen with 2.5% methane concentration | 93 |
| Fig. 7.12 Effect of hydrogen with 4% methane concentration | 94 |
| Fig. 7.13 Effect of methane with 16% hydrogen..... | 95 |
| Fig. 7.14 Effect of methane with 19% hydrogen..... | 96 |
| Fig. 7.15 Effect of methane variation with 22% hydrogen | 97 |
| Fig. 8.1 Block diagram of research work | 99 |

List of Tables

| | |
|---------------------------------------------------------------|----|
| Table 1.1 IEA, Energy indicator statistics – 2012 | 2 |
| Table 1.2 Fuel usage in India and purpose 2007–2008..... | 4 |
| Table 2.1 Emissions at full load..... | 20 |
| Table 2.2 Emissions under dual fuel and gas alone mode..... | 20 |
| Table 2.3 Gas engine emission (off road vehicles norms) | 21 |
| Table 3.1 Producer gas range considered in present work..... | 26 |
| Table 3.2 Producer gas formulation strategy | 27 |
| Table 3.3 Optimal combinations of producer gas mixtures | 27 |
| Table 3.4 Thickness of compression rings | 35 |
| Table 3.5 Accuracy and uncertainties of instruments | 37 |
| Table 4.1 Engine specifications | 39 |
| Table 4.2 Settings of flow parameters..... | 46 |

| | |
|-----------------------------------------------------------------------------|----|
| Table 4.3 Producer gas composition | 47 |
| Table 4.4 Combustion properties of PG and Gasoline | 47 |
| Table 5.1. Formulation of PG fuel sets | 51 |
| Table 5.2 Calculated combustion properties of PG blends & other fuels | 51 |
| Table 5.3 Load carrying ability of PG blends..... | 53 |
| Table 5.4 BSFC and BSEC values of all fuels | 55 |
| Table 5.5 Engine response at 50%, 75% and Full Load for various CR's | 57 |
| Table 5.6 Emissions at full load against CPCB-2016 norms (CPCB-2016) | 65 |
| Table 5.7 Emissions at 75% load against CPCB-2016 norms (CPCB-2016) | 65 |
| Table 5.8 Emissions at 50% load against CPCB-2016 norms (CPCB-2016) | 66 |
| Table 6.1 Formulation of PG fuel sets | 68 |
| Table 6.2 Combustion properties of fuels | 69 |
| Table 6.3 Emissions at 75% load against (CPCB-2016 norms) | 80 |
| Table 6.4 Emissions at 50% load operation | 80 |
| Table 7.1 Optimal combinations of PG fuel sets | 82 |
| Table 7.2 Combustion properties of PG blends..... | 83 |
| Table 7.3 Combustion properties of fuels (M.S. Babu, et al., 2017) | 88 |
| Table 7.4 Curve fitted model constants at full load | 89 |
| Table 7.5 Variation of Wiebe model constants..... | 89 |

List of symbols

- ϕ : Equivalence ratio, based on fuel to air basis
- x_b : mass fraction burnt
- a : Wiebe efficiency factor
- m : Form or shape factor
- ρ_{PG} : Density of producer gas
- ρ_{AIR} : Density of atmospheric air
- γ : Ratio of specific heats
- H₂ : Hydrogen
- CO : Carbon monoxide
- CH₄ : Methane
- \emptyset : Port diameter of air-gas regulator

List of abbreviations

- ATDC : After top dead center
- BTDC : Before top dead center
- ABDC : After bottom dead center
- BBDC : Before bottom dead center
- CA : Crank angle
- CR : Compression ratio
- BTE : Brake thermal or fuel conversion efficiency
- BSFC : Brake specific fuel consumption
- MFB : Mass fraction burnt

mmt : Million metric ton

ROHR : Rate of heat release

ROPR : Rate of pressure rise

PG : Producer gas

MBT : Minimum spark time advance for maximum torque

SFC : Specific fuel consumption

Chapter 1

Introduction

1.1 Perspective

The need for energy conservation or an effective utilization of available energy sources was first felt worldwide after oil crisis in 1973 (Horton, 1973) and oil shock in 1979. This energy crisis has laid a platform to explore alternative fuels in order to substitute baseline fossil fuels. The depletion of fossil fuel reserves like coal, oil, and issues like climate change has raised the quest to search and develop the alternative fuels - which are both renewable and eco-friendly. Biomass derived producer gas (PG) is one such renewable and eco-friendly fuel. Biomass, with its short carbon cycle (hence renewable) and their near zero carbon addition to atmosphere, makes it attractive in thermal power plants in generating power via gasifier-engine systems. Furthermore, according to literature, combustion science has a huge role to play in improving the biomass based combustion systems (Bilger, 2000) like engines or burners. The internal combustion (IC) engines are primarily designed for fossil fuels like gasoline or Diesel. Therefore, there exists a scope for combustion and power output optimization when new fuels are used on base frame derived gasoline or diesel engines. In view of this, the present work is taken up to understand and address the complex in-cylinder combustion behavior and its influence on various engine response parameters when fuelled with varied composition of Producer gas.

1.2 Indian scenario in bio-energy

Normally, consumption of a large segment of energy in any country implies increased energy activities within the country. This may include advancement in basic infrastructure like raising of living standards of the citizens, transportation system, expansion of industries and agriculture, gross domestic product (GDP) being a representative index for economic size. According to 'U.S. World Bank' Statistics - 2012, India has a steady growth of 6.5% in its GDP_purchasing power parity (GDP_PPP) value almost every year. However, the magnitude of growth in its GDP is much lesser compared to USA, China and the world

average. Referring to Table 1.1 with reference to GDP, the energy consumption comparatively shows less. In 2012, the average annual energy consumption of the world was estimated to be 75.29 EJ, out of which 19.45% was consumed by USA, having about 4.46% of world's population; whereas, India having 17.57% of world's population consumed only 4.49% of average world's energy. This reflects as one of the reasons for lower GDP value of India. The per capita electricity consumption of India in 2012 was 0.76 MWh/Capita. Comparatively, USA consumes 17 times higher as compared to India and China 4.5 times higher with 9% more population than India. These facts prove that India's development and growth trend can be improved. Furthermore, Fig. 1.1 shows that India is heavily dependent on fossil fuels with a share of 73% as compared to a supply of 5.89% primary energy sources (US EIA, 2014).

Table 1.1 IEA, Energy indicator statistics – 2012

| Country | Population (Millions) | GDP_PPP (Billion 2005 USD) | Electricity consumption (TWh) | CO ₂ emission from fuel combustion (Mt) | Per capita elec. Consumption (MWh/Capita) |
|-----------------|-----------------------|----------------------------|-------------------------------|----------------------------------------------------|-------------------------------------------|
| USA | 314.28 | 14231.58 | 4069.06 | 5074.14 | 12.95 |
| China | 1350.70 | 12968.57 | 4693.68 | 8205.86 | 3.48 |
| India | 1236.69 | 5567.13 | 939.78 | 1954.02 | 0.76 |
| World's average | 7037.07 | 82900.58 | 20915.39 | 31734.35 | 2.97 |

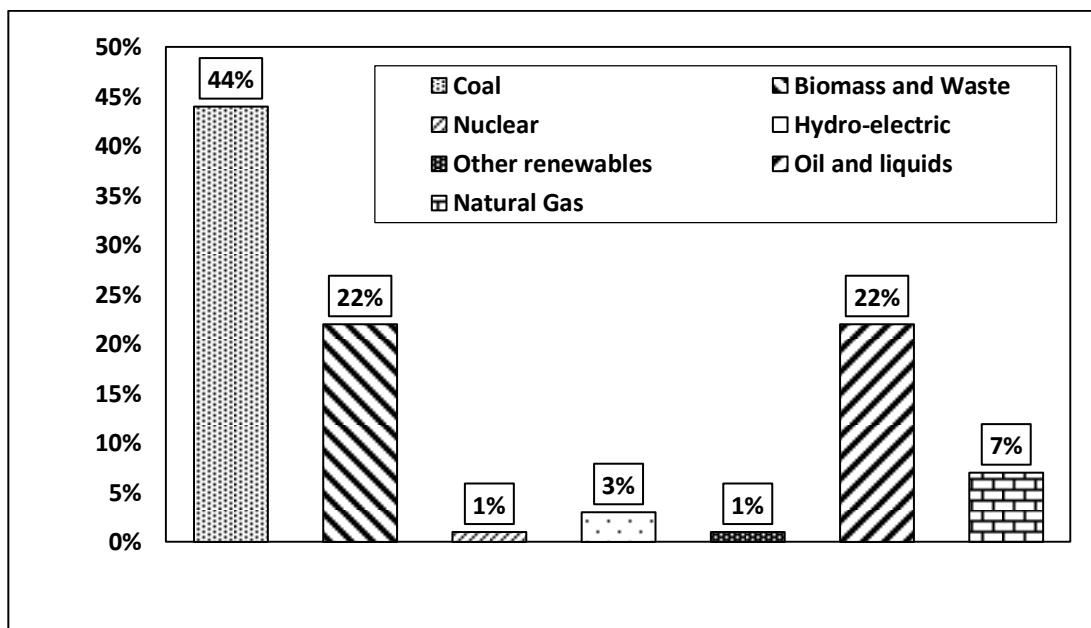


Fig.1.1 Total primary energy consumption of India (Energy statistics, 2012)

From the above Fig.1.1 it is also clear that, besides baseline fossil fuels especially oil, renewable energy (from biomass) are also comparable. India, being an agriculturally dominated land with surplus amount of biomass and approximately 70% of population in villages and hamlets, is suitable for biomass-based technologies (Dasappa et.al, 2004). Estimates have indicated that 15 to 50% of the world's primary energy use could come from biomass by the year 2050 (Kumar et. al. 2010). By 2020, estimates reveal that India requires 400,000 MW of electricity because of rapid growth in population (Poonam, 2011). According to Energy Statistics-2012, the potential of biomass derived energy, stands at second highest 17,538 MW (19%) after wind energy potential 49,130 MW which amounts to 55 % (Energy Statistics, 2013). In 2014, the installed capacity of biomass power in India was 4013.55 MW which amounts to 12.66% (Energy Statistics, 2014). The state-wise availability of biomass (of various kinds) can be found in 'Biomass Atlas' launched online by CGPL, IISc, Bangalore, as a project under MNRE, Govt. of India. Thus, biomass as an energy source is attractive and promising to meet partial forecasted energy targets for India.

1.3 Prospects of biomass gasification technology

Gasification process is used to convert biomass (organic matter) into combustible gaseous fuel called Producer gas (PG). Gasification process was quite popular during the Second World War (WW-II) and diminished when liquid fuel became easily available after WW-II (FAO report, 1972). The interest in gasification technology has undergone many ups and downs till date. Recently, because of depletion in fossil fuels, frequent change in fuel prices and also because of environmental concerns, there is a renewed interest in century old gasification technology and considered as modern and sophisticated technology (Babu et al., 2011).

The merits of biomass gasification technology are as follows:

- Provides all forms of energy namely, electrical, mechanical and thermal
- Net addition of CO₂ into atmosphere is almost negligible (carbon neutral technology)
- Advantageous for remote areas having plenty of biomass but no electrical power
- Useful for power level ranging from 3 kW to few MW

Some of the applications of power derived from Producer gas are (Tewari et al., 2001):

- Water pumping for irrigation
- Local power generation

- Flour mill grinding and
- Brick kiln operations

Energy from renewable sources like biomass is very important in meeting the growth targets in power sectors. Biomass in an energy mix is comparable, from utilization view point, over other conventional fuels, and stands out, next to major conventional fuel (coal) as shown in Table 1.2 (Mukunda, 2011).

Table 1.2 Fuel usage in India and purpose 2007–2008

| Fuel | LCV (MJ/kg) | Usage (mmt/year) | Purpose |
|-------------------------|-------------|------------------|----------------------------------------------|
| Coal | 20 | 400 20 | Electricity Steam raising/Heating |
| Natural Gas | 50 | 12 | Electricity, transport, cooking |
| High speed diesel | 42 | 40 | Heavy vehicle transport |
| Naphtha | 42 | 12 | Stationary power generation |
| Light diesel oil | -- | 02 | |
| Fuel oil | 40 | 14 | Electricity via diesel engine |
| Gasoline | 42 | 09 | Vehicle transport |
| Kerosene | 42 | 12 | Cooking/transport |
| Liquefied Petroleum Gas | 45 | 10 | Cooking, urban transport |
| Firewood | 16 | 250 | Cooking, electricity Industry and rituals |
| Agro residues | 14 | 120 | |
| Cowdung | 13 | 40 | |

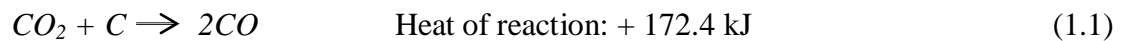
Biomass is any plant and plant-derived material obtained from photosynthetic reaction of carbon-dioxide with water vapor. In the context of energy source, biomass can also include woody plants, residues from agriculture or forestry and the organic component of municipal and industrial wastes. Since the biomass based feed stock is cyclic (renewable), it qualifies as a sustainable source of energy as long as it is consumed at a rate comparable to or less than the rate of production. The energy derived from plant or plant-derived materials is called as Bio-energy, which can be produced using gasification technology coupled with an engine route (Babu, 2011). Recently the interest in using biomass as an energy source has increased and it represents approximately 14% of the world's final energy consumption. Biomass based power generation in India is an industry that attracts investments of over Rs.600 crores every year, generating more than 5000 million units of electricity and yearly employment of more

than 10 million man-days in the rural areas (Kumar et. al. 2010). One can harness bio-energy in two ways namely: Bio-chemical route (BCR), which gives rise to biogas fuel as a result of anaerobic digestion, and the thermo-chemical route (TCR), which leads to generation of Producer gas fuel as a result of partial combustion in a gasifier. However, the present thesis work is focused to study the influence of bottled Producer gas composition (resembling the PG through gasification via TCR route) on combustion characteristics of IC engine. In the following section, a discussion on thermo-chemical based gasification process is presented.

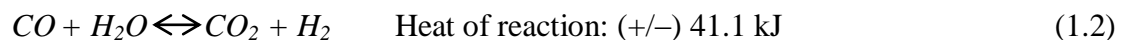
1.4 Downdraft gasifier for Producer gas generation

The gasification process takes place in a reactor unit called gasifier. Here the biomass fed from top of a downdraft gasifier with approximately 10 - 15% of moisture level undergoes complex chemical oxidation and reduction reactions in a reactor, passing through different zones, namely, drying zone, pyrolysis zone, oxidation zone and reduction zone. Producer gas is a mixture of combustible gases (hydrogen, methane and carbon-monoxide) and non-combustible gases. The major reactions which aid in generation of combustible gases of Producer gas are listed below (Mukunda, 2011 & Khan, 2014).

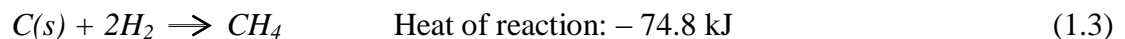
- The Boudouard reaction



- Water-gas shift reactions



- Methanation reaction



- Water Gas reaction



Furthermore, gasifier also contains a train of cooling and cleaning systems as shown in Fig. 1.2. Cleaning system includes ‘cyclone separator’ to separate heavy dust/ash particles by adopting a principle of centrifugal action. Fabric filter, after cooling process, filters the raw PG to much lower level of contaminants of the order of micro level. The cooling systems includes ‘scrubbers’ and ‘chiller’ to cool and filter the contaminants like, particulate matter (PM) and tar associated with raw PG exiting from gasifier outlet.

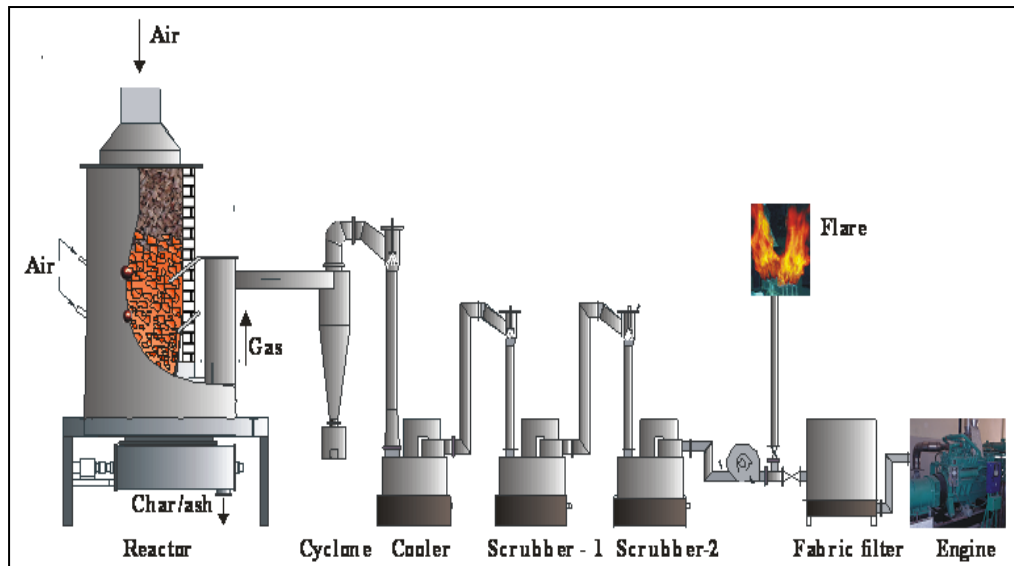


Fig.1.2 Gasifier and engine system (Courtesy: CGPL)

This cooling is required to bring down the gasifier outlet exit temperature of PG approximately from 800 K to 300 K so as to undergo safe secondary combustion in an IC engine as shown in Fig. 1.2. The typical composition of PG based on Open top downdraft gasifier (developed by Combustion Gasification & Propulsion Laboratory (CGPL), Indian Institute of Science, Bangalore) using Causurina wood with moisture content between 12% and 15% on dry basis (sun-dried wood) is $19 \pm 1\%$ H₂; $19 \pm 1\%$ CO; 2% CH₄; $12 \pm 1\%$ CO₂; $2 \pm 0.5\%$ H₂O and rest, N₂. The mean calorific value of gas varied around 4.65 ± 0.15 MJ/Nm³ (Sridhar, 2003).

1.5 Issues related to Producer gas fuel combustion

It has been reported in the literature (Rajvanshi, 2014, Kumar et al., 2010, Roy et al., 2009, Kishore et al., 2008) that, PG has a tendency to undergo variation in its composition (thus its fuel quality). Among the influential parameters, biomass properties and gasifier design greatly affect the quality of PG fuel. Detailed study on this aspect will be covered in literature review section.

The experimental study on combustion properties of PG fuel (H₂, CO and CH₄) indicates that, hydrogen is a highly reactive component and has a flame speed (2.37 m/sec) which is almost 80% faster as compared to methane (0.42 m/sec). A computational work reported by Sridhar et al., 2005c shows a 7% reduction in flame speed of PG due to 1% reduction in hydrogen concentration in PG at an equivalence ratio of 0.9. Further, the minimum ignition energy of

hydrogen is 0.02 mJ as compared to 0.29 mJ of methane, indicating an ability to undergo quick chemical reaction. The diffusion coefficient of hydrogen is 0.61 cm²/sec as compared to 0.16 cm²/sec of methane. Indicating an ability to diffuse 3.8 times faster as compared to methane. From heating value view point, hydrogen contains 120 MJ/kg and methane 50.2 MJ/kg (Andrea et al., 2004 and Bauer et al., 2001), typically signifying the potential to take up higher engine loads, though the CO component in combustion process is known to suppress the chemical reactivity of mixture (Cha et al., 2015). Furthermore, the inert gases like CO₂ and N₂ in PG hinders the pre-flame reactions and act like thermal buffer (Jonas et al., 2011). From the above discussion, it is quite clear that, PG undergoes dynamic variations in the combustion process owing to variation in its composition. From engine operation point of view, optimal spark time is of paramount interest, as it dictates the power output and also influences the emission characteristics. Therefore, setting the Maximum Brake Torque (MBT) spark time against fluctuating PG trend is a challenging task.

1.6 Scope of the present work

From the above discussions, it is clear that Producer gas as a fuel is gaining much prominence among renewable fuels, mainly due to its potential to mitigate global warming, climate change and also to meet partially the forecasted energy demand in India. According to literature (Bilger, 2000), combustion science has a significant role to play in improving biomass technology and combustion systems (like engines). Researcher, Yaliwal et al., 2014, also suggested that, combustion characteristics of a Producer gas fuelled engines need extensive research for long term use in both gas alone and dual fuel mode. Thus, pursuing PG as a potential renewable fuel over other baseline fossil fuels in Indian scenario, present study is motivated to explore its utilization in modified spark ignited (SI) engine considering gas alone mode and to address few technical gaps associated with PG engines against varied composition of Producer gas.

1.7 Organization of thesis

Chapter 1: Introduction

This chapter presents an overview of Indian energy scenario. The biomass gasification technology, merits of gasification technology and applications of Producer gas and scope of present work is also described.

Chapter 2: Literature Review

A comprehensive literature review is presented in this chapter. It includes discussion on factors affecting the composition of Producer gas (fuel quality). This chapter also covers various combustion, performance and emissions parameters of Producer gas fueled engines. Simulation studies related to combustion process of PG are also brought out. Finally, objectives for the proposed research work are presented.

Chapter 3: Materials and methods

This chapter describes the methodology followed to achieve the list of research objectives and experimental methodology with relevant mathematical background.

Chapter 4: Experimental set-up and procedure

In this chapter, details related to design and development of induction system is presented. The testing features of flow control systems are also discussed. Finally, the engine testing and comparison of results against published work are presented.

Chapter 5: Influence of hydrogen and methane concentration in PG fuelled SI engine

In this chapter, the effect of optimal PG fuel sets on various engine parameters is presented. The key PG fuel sets promoting fuel economy are identified. The MBT spark times based on spark sweep test is also identified and presented.

Chapter 6: Effect of hydrogen concentration at higher compression ratios in PG fuelled SI engine

In this chapter, the experimental results pertaining to higher compression ratios (11, 15 and 18) are presented. The response of the engine was studied with reference to brake thermal efficiency, specific fuel consumption, rate of pressure rise, heat release and combustion duration. Finally, emissions trend at various CRs are also covered and the robust combustion parameter for closed loop engine operation is proposed.

Chapter 7: Modelling of mass fraction burn curves and Parametric Studies

This chapter includes the modelling studies on MFB curves of PG combustion based on double stage Wiebe model. Parametric studies to understand the effect of hydrogen and methane concentration in PG combustion is also presented.

Chapter 8: Conclusions

This chapter summarizes various findings that emerged from the experimental investigation. It also brings out the important conclusions drawn from each objective and the scope for future work.

Chapter 2

Literature Review

2.1 Introduction

The main aim of the present work was to study the in-cylinder combustion behavior of an engine and its impact on engine response parameters due to the fluctuating tendency of producer gas composition. Literature addressing in-cylinder combustion, performance and emission trends were explored. Based on the literature review, research objectives were framed. In this chapter, a brief overview on biomass to energy conversion, factors affecting producer gas fuel quality are presented.

2.2 Routes for energy conversion

Biomass is basically any organic matter available either in liquid or in solid form. Depending upon the moisture content in the biomass, it gets qualified either for bio-chemical conversion (if moisture > 70%) or for thermo-chemical conversion (if moisture < 30%). The bio-chemical route leads to production of biogas (rich in methane) through anaerobic digestion process which is further used to generate electricity via IC engines. The thermo-chemical conversion through oxygen / steam gasification process yields synthesis gas (also called as Syngas) which is rich in CO and H₂. Further, when Syngas is subjected to Fischer-Tropsch (FT) process it yields hydrocarbon fuels and synthetic products like diesel, gasoline, methane, ethane, LPG and waxes etc. (Hackett et. al., 2004). Thermo-chemical conversion with air blown gasification leads to generation of producer gas, which is further subjected to secondary combustion in engines to generate electricity. The other conversion routes are shown in Fig. 2.1.

2.2.1 Brief history of gasification

According to literature (Kaupp, 1984), gasification emerged more than 200 years ago. A remarkable progress in this technology was witnessed in last few decades as shown below:

- **19th century** – Gasification was first used to produce “town gas” from coal for community lighting and cooking applications.

- **Early 20th century** – During WW-II, German engineers developed a pathway to produce synthetic fuel via gasification of wood and other biomass fuel sources. This method migrated to South Africa after the war, and the technology continued to advance to create liquid fuels.
- **Late 20th century** – The U.S. government provided financial support for several R&D facilities following the Arab Oil Embargo of 1973 with the goal to convert coal to liquid fuel. Along with these, the European governments also made investments in medium-size gasification plants for electricity production.
- **21st century** – Many commercial manufacturers and suppliers have begun building gasification power plants. Some facilities are advancing from electricity and chemical production to liquid fuels for transportation, such as gasoline, diesel and jet fuel.

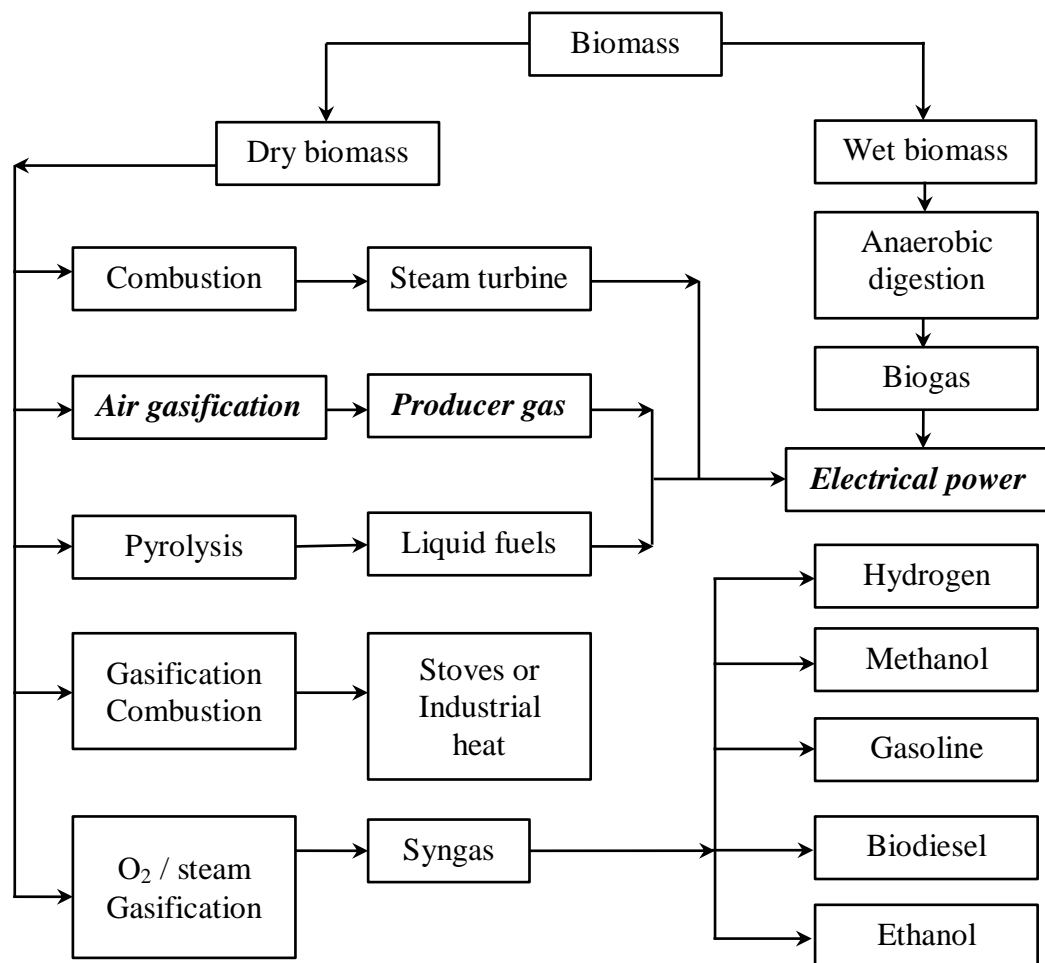


Fig. 2.1 Biomass energy conversion pathways

Gasification is a partial oxidation process which takes place in a reactor vessel (gasifier) and thereby converts carbonaceous material (biomass or coal) into a ‘fuel gas’. This fuel gas is a

mixture of combustible gases like hydrogen, methane and carbon-monoxide, and non-combustible gases like carbon-dioxide and nitrogen. Based upon the gasifying agent, the quality (composition) of fuel gas varies. In the present work, gasification with air blown method was considered and hence the fuel gas is referred as ‘producer gas’ throughout the thesis.

Gasification (air or oxygen blown):

- Fuel + limited air \longrightarrow producer gas (fuel gas) + heat + char/ash + tar
- Fuel + limited oxygen \longrightarrow Syngas (fuel gas) + heat + char/ash + tar

2.3 Open-top downdraft gasifier

The bottled PG quality (composition) considered in the present work closely resembles the quality of producer gas produced through a downdraft gasifier developed by IISc, Bangalore. Therefore, few important features of an open-top gasifier system are presented in this section. The gasifier design enables a twin staged air entry – one at the top and others at the sides of a reactor as shown in Fig. 1.2 of Chapter 1. This arrangement of air inlets enables higher biomass to gas conversion efficiency without ash-fusion. A dual effect of not leading to formation of ash-fusion and at the same time ensuring tar cracking at desired turn-down ratio is an integral part of this design. The reaction zone has a cylindrical chamber with ceramic lining to ensure long life and good insulation. The ash and char is extracted from a screw located at the base of a gasifier. Further, the design enables to accommodate multi-fuel (wooden chips, coconut shells, agro-residue briquettes or in pellet form and municipal solid waste) for gasification process (Mukunda, 2011). The gasifier with cooling and cleaning train is Cⁿ patented technology (S. Dasappa et. al., 2008). This gasifier is known for its ultra-clean and superior quality of producer gas with energy content of 4.65 ± 0.15 MJ/Nm³ (Sridhar, 2003). The other details of this industrially proven gasifier system capable of generating superior gas quality are presented in (Mukunda, et al., 1993 and Mukunda, et al., 1994).

2.4 Issues related to producer gas quality

In order to understand the issues related to producer gas fuel quality, a study on types of gasifiers as shown in Fig. 2.2 and their suitability for engine operation was imperative.

2.4.1 Suitable gasifier for engine application

Depending upon direction of air flow within reactor, fixed bed gasifiers are classified as, updraft or counter current gasifier, downdraft or co-current gasifier and cross-draft gasifier.

Updraft gasifier: - In this gasifier, the feedstock is fed from top of the gasifier and eventually moves in the downward direction as the feedstock bed gets consumed; whereas, the product end gas moves upwards (counter flow) and exits from the gasifier accordingly. However, this type of gasifier is known to produce higher level of tar and particulate matters and therefore not suitable for engine application.

Downdraft gasifier: - In the downdraft gasifier, the feedstock is fed from top of the gasifier and the bed moves in the downward direction as it get consumed. Similarly, the product end gas also moves downward and eventually exits from gasifier. The advantage associated with downdraft gasifiers are production of lower level of tar and particulate matters and hence most suitable for engine application.

Crossdraft gasifier: - In case of cross-draft gasifier, the feedstock moves in the downward direction similar to up-draft or downdraft gasifier, whereas, the product gas exits from the oxidation zone and exits perpendicular to gasifier. However, these gasifiers are not suitable for engine application due to higher level of tar and particulate matters. Many other combinations of gasifiers were developed and these are not relevant for present study.

From the above discussion, it is clear that downdraft gasifier is most suitable for engine application. The permissible limit of tar concentration and particulate matter for satisfactory engine operation, as given by (Laurence et al., 2012) are to be less than 100 mg/Nm^3 and 50 mg/Nm^3 respectively.

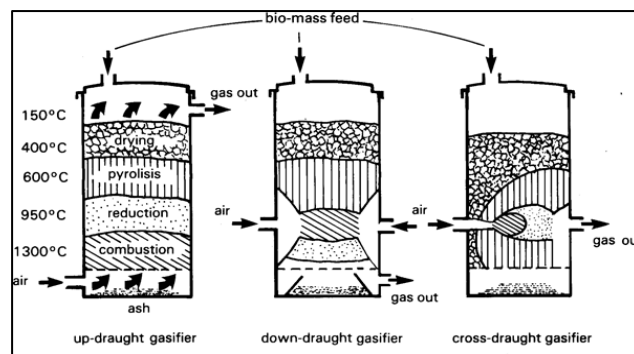


Fig. 2.2 Types of gasifier (FAO Report, 1986)

2.4.2 Factors affecting producer gas quality or composition

Though the gasification process appears simple, it is very sensitive to changes in a few factors. The important factors affecting gasification process and eventually causing variation in gas quality are as follows (Rajvanshi, 2014 and Sheth et al., 2005),

- 1) Type of feedstock
- 2) Moisture level in the feedstock
- 3) Size of feedstock
- 4) Feed rate
- 5) Design of gasifier

- **Type of feed stock**

The type of feedstock employed for a given gasifier is important from long lasting charge. This need gets sufficed if the employed feedstock has higher bulk density and energy content to tap more power with single charge. The consumption time intervals of different energy crops / agro-residue differ based on its structural composition make-up like hemi-cellulose, cellulose, lignin, ash and crude protein. Hence a biomass feedstock with higher densities and calorific value is preferred, subjected to local availability for economic reasons.

- **Moisture level in the feedstock**

During the process of thermo-chemical conversion in a gasifier, the two important reactions namely, Water-shift and Water gas reactions expressed by eq.1.2 and 1.4 in Chapter 1 contribute towards production of hydrogen content in a producer gas. Furthermore, according to literature, a linear increase in H₂ and CO₂ concentration was observed with increase in moisture percentage in a biomass feedstock. On the other hand, the CO yield was found to decrease with increase in moisture levels in a biomass feedstock (Sheth et al., 2005).

- **Size of feedstock**

In biomass gasification, normally the feedstock comes in a range of sizes. This feedstock has to be processed to arrive at uniform shape or size. This process helps in overcoming (i) bridging action within gasifier as the bed gets consumed in downward direction, and (ii) effectively gasify the biomass and reduce to lower level of hydrocarbon across oxidation zone.

- **Feed rate**

The feed rate of biomass is also one important factor, which needs to be maintained on a timely basis. Any discontinuity in biomass bed level will result in a pressure drop across gasifier. Thus, the production of producer gas suffers and thereby the end utility.

- **Design of gasifier**

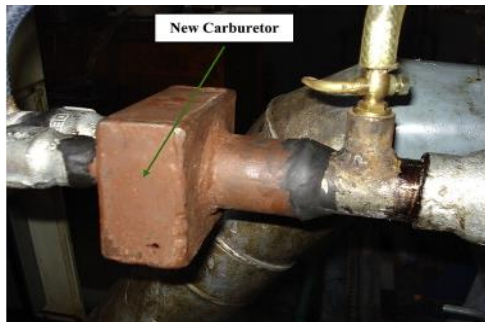
The gasifiers are designed depending on the type of feedstock and end utility. For an application like power generation via IC engine route, primary concern will be of quality (energy content) and purity (free from tar and particulate matters) of producer gas.

2.5 Producer gas as a fuel in IC engines

In this section, studies related to PG engine with higher compression ratio and varying hydrogen concentration in PG fuel is reviewed. The relevant and key findings are presented below as a summary. From historical perspective, the most important gaseous fuel used in the first century of industrial development was town gas (produced from coal). The first application of town gas was illumination. It was followed by heating and then as a raw material for chemical industry. Lately through technological development, producer gas (produced from biomass gasification) is used for power generation application through IC engine route. The drawback of producer gas was that the heating value was relatively low and highly fluctuating in its chemical composition. The first vehicle powered through town gas in 1901 was built by Thomas. Wood gas vehicles were used during WW-II and in Germany alone, 5 million vehicles such as buses, trucks, motor cycles, ships and trains equipped with wood gasification were powered through producer gas. 73,000 in Sweden, 65,000 in France, 10,000 in Denmark and 8,000 in Switzerland were fueled with producer gas. However, load falling ability with engines and inconsistency in PG composition was witnessed. The utilization of PG was explored both in Compression Ignition (CI) engines (as a dual fuel mode) and Spark Ignited (SI) engines (as a gas alone mode operation), owing to higher auto-ignition temperature (625°C) of PG (Tewari et al., 2001). To exercise complete freedom from baseline fossil fuels, engine operation under gas alone mode is greatly encouraged. According to FAO Report (1972), the utilization and development activity of PG engines was largely witnessed during WW-II. However, no much data on optimization of these engines for a given PG quality (composition dependent) was present. It is reported that issues like heating value and poor volumetric efficiencies limited the power output of PG engines (Hagos et al., 2014). Work with higher compression ratio (CR) was also limited due to presumption of

knocking tendency. According to (FAO-72 report), the power output of PG engines mainly depends on factors such as (i) heating value of the fuel and air mixture – which leads to power loss of approximately 35% due to the differences in lower mixture heating value against fuels like gasoline (ii) Amount of mixture supplied to cylinder – only 0.65 to 0.8 times the theoretical maximum is expected to enter the cylinder due to pressure loss across induction system (iii) Engine efficiency – thermal efficiency depends on CR. Further, CR is limited based on octane number of the gas (iv) Engine speed – the engine efficiency drops when burning speed of mixture equals the average piston speed. This phenomenon was estimated to occur around 2500 rpm. Therefore, PG engines were suggested to operate below 2500 rpm.

Further, due to non-availability of commercial PG gas carburetors in market, researchers (Tewari, 2001 and Shashikantha et. al., 1999, Banapurmath et. al. 2008, 2009) have developed their own gas carburetors as shown in Fig. 2.3 However, no much information on design guidelines and effective operation of these carburetors were presented.



Box type



Venturi type



Y-Shape



Parallel flow type

Fig. 2.3 Carburetors for PG induction

In 2001, Sridhar et al. adopted a modified CI engine for a gas alone mode operation and presented a knock-free engine operation at CR:17 with PG having 19 ± 1 % H₂ and mean calorific value of 4.65 ± 0.15 MJ/Nm³. The work also involved a systematic study by varying CR from 11.5 to 17. An improvement of 13% in power output, optimal spark time of 14 to 16° CA BTDC at CR 11:5 and 6 to 10° CA BTDC at CR 17 was reported. Homdoun et al., 2014, presented a work by examining the effect of optimal spark time under different speeds (1100 to 1900 rpm) and load conditions by using a small capacity, single cylinder, modified CI engine under gas alone mode operation. Optimum CR was achieved at 14:1 with charcoal based PG having a calorific value of 4.64 MJ/Nm³ with 8.5 ± 2 % H₂ and 30.5 ± 2 % CO. 35° CA BTDC at 1500 rpm was determined as optimal spark time with approximately 18% brake thermal efficiency. The coefficient of variance (COV) of brake mean effective Pressure (BMEP) increased with increase in engine speed (1.75 to 3%). The overall exhaust gas temperature was observed within 298 to 420° C.

In 2015, Gobbato et al. reported work on PG by considering 21.927 liters, 250 kW at 1500 rpm heavy duty NG engine. The engine performance and emissions was examined by considering CR:12.5 at several air fuel ratios and spark timing. The volumetric efficiencies were found to vary from 31 to 39% and a power loss of 50% was recorded. The engine was operated up-to a lean limit of (A/F) of 2:1. The fuel conversion efficiency was found to reduce when lean limit exceeded 1.3 because of reduced flame speed, however stable engine operation was noticed. On emission front, both CO and NO_x were found to reduce. The PG had a calorific value (CV) of 4.3 MJ/Nm³ with 18% H₂ and 20% CO concentration.

Tewari et al. in 2001, conducted experiments on a single cylinder, four stroke, air cooled, 0.661 liters with bowl in piston. The engine was operated close to stoichiometry at CR: 7.5, 11.5 and 12 with 1500 rpm. On comparison with gasoline performance, a 9% reduction in BTE was observed and it was attributed to lower flame speed of PG due to variation in composition. Therefore, advancement in spark time was suggested. The BTE was observed within 18 to 22% for PG and 24 to 28% for gasoline. The COV of peak pressure was found to be on higher side (19.4%) due to variation in PG fuel quality. The CO and HC emissions were much lesser than gasoline operation.

In 1999, Shashikantha et al. reported work with CI engine modified to SI engine to operate on gas alone mode at CR: 11.5 for both PG and compressed natural gas (CNG). For PG operation, 35° before TDC was considered as best spark time by considering shorter

combustion duration and occurrence of peak pressure between 5 to 10° CA after TDC. For CNG, spark time at 22° CA before TDC was found as optimum based on maximum power output. The part load operation was observed to be problematic for both the fuels. On emission front, CO and NO_x were found within safe limits and thus proven as environmental safe fuel. However, the information on calorific value of PG was not made very clear.

In 2015, Nakazono et al. presented work by considering a four cylinder with 3.317 liters and having a rated power output of 20 kW at 1900 rpm. The engine was operated at CR:12 with a stoichiometry ($\phi = 0.998$ to 1.008). Two sets of bottled PG having CV of 4.3 and 5.3 MJ/Nm³ with 15 to 18% H₂ and 16 to 19% CO were tested and compared with onsite down draft gasifier based PG. The onsite based PG fluctuated in its composition between 3.8 and 5.5 MJ/Nm³. The thermal efficiencies (up-to 30%) and supply of PG mixture at different load points were found to be almost similar. One of the underlining outcomes of this work was the sensitivity and variation of CO and NO_x when A/F ratio departed slightly away from stoichiometry condition. The author suggested a three-way catalyst to minimize the harmful emissions.

In 2015, Shivapuji et al. conducted experiments by considering four sets of syngas (oxy-steam gasification agent) on two cylinder, naturally aspirated, 1.67 liter capacity engine. CV was found to vary from 3.14 to 7.15 MJ/Nm³ with 12.8 to 37.2% H₂ and 11.5 to 16.4% CO. The optimal spark time was retarded with increase in the percentage of H₂. The researcher found an increase in combustion duration (CD) after 90% of heat release (terminal duration) and it was attributed to enhanced thermal conductivity and diffusivity of unburnt mixture at the vicinity of cylinder wall. Further, this terminal phase CD was found to increase with increase in hydrogen concentration. A 10% higher cooling load as compared to base hydrocarbon powered engines was presented due to thermo-physical properties of syngas.

Cha et al. in 2015, presented experimental work to study the influence of syngas concentration on methane with main parameters being the fuel conversion efficiency and NO_x emissions for power generation utility. Four cylinder, turbocharged, 2.28 liter capacity SI engine with CR:13 and 1800 rpm was tested with syngas mixing ratio ranging 5%, 10% and 15% in methane. This translates to volume ratio of CH₄:H₂:CO as 86:7:7, 74:13:13 and 64:18:18 respectively. The study reveals an increase in flame speed with increase in percentage of H₂ in CH₄+CO mixture. On the counter side, increase in CO% in CH₄+H₂ brings down the flame propagation speed. The improvement in combustion process resulted

in higher cylinder pressures. But the rate of variation in cylinder pressures was not linear with mixing ratios. Therefore, identification of optimum mixing ratios and production of syngas which is serving as an additive was suggested to weigh economically.

In 2014, Flekiewicz et al. conducted experiments at $\phi=1$ and 2500 rpm and full load to study the influence of gaseous fuel types like CH₄ with H₂ and LPG with DME on energy conversion. The researcher used electronic injection to maintain charge at stoichiometry state. The H₂ enrichment of CH₄ was 5, 15, 30 and 50%. The mixture blend with H₂ > 15% was found to influence the cylinder peak pressures, rate of pressure rise and exhaust gas temperature. The CD within 10% MFB was found to be on lesser side with increase in percentage of H₂, thus proving that H₂ is a combustion activator. Further, percentage of H₂ greater than 15% increased the exhaust gas temperatures. The emission levels were found to reduce by 37% as compared to gasoline with a blend of 70% CH₄ and 30% H₂.

2.6 Effect of hydrogen and methane composition

For air gasification, the producer gas quality or composition varies widely depending on the gasifier configuration, chemical composition of the feedstock, moisture, ash content, size, density, equivalence ratio, reaction temperature profile and turn down of power level (Sharma, 2011, Roy et al., 2009 and Sharma, 2006). The most sensitive components of PG are hydrogen and methane. In view of this, literature pertaining to these components was explored and the outcomes of the most relevant studies are discussed below in brief.

In 1999, Shrestha et al., reported a work on performance of SI engine running on methane with hydrogen blends. The hydrogen was added mainly to bring the stability to engine combustion process and to offset few disadvantages in general, encountered with lean engine operations. The results have shown improvement in engine performance for low equivalence ratio mixtures. In 2006, Tinaut et. al., presented a work based on an observation of drastic power drop after the stoichiometric value. Therefore, a new parameter called “Engine Fuel Quality” was proposed to estimate the power that can be attained with the known fuel composition. Such parameters emerged because of fluctuating tendency of producer gas composition.

In 2007, Melgar, introduced a thermo-chemical equilibrium model to predict the producer gas composition. This model helps to predict the behavior of different biomass types and proposed a tool for optimizing the design and operation of downdraft biomass gasifiers. In

2007, Akansu et al., presented a work on SI engine by varying hydrogen from 0, 10, 20 and 30% by volume in methane. The engine was operated between 0.6 to 1.2 equivalence ratio and compression ratio 10:1. The results have shown an increase in NO emissions with increase in hydrogen percentage and with $\phi < 0.75$, the NO emissions were on lower side. Rest of the emissions HC, CO, CO₂ were on lower side. Furthermore, lean mixtures resulted in increase of brake thermal efficiencies with increase in hydrogen percentage. The highest thermal efficiency was identified at $\phi = 0.85$.

In 2008, Kishore et al., studied the effect of varying the producer gas composition using mathematical code RUN-1DL on unstretched burning velocity and sensitivity of the laminar burning velocity to stretch. Three sets of producer gas compositions were investigated. Methane, hydrogen and carbon monoxide was varied from 0 to 48% and carbon dioxide and nitrogen was kept constant to 10% and 42% by volume. The peak burning velocity of flame increased with rise in hydrogen and the equivalence ratio shifted towards lower values with increase in hydrogen and decrease in carbon monoxide. In 2009, Ceper et al., conducted experiments at constant speed of 2000 rpm and compression ratio 10. The aim of the study was to study the engine performance and pollutant formation by operating a four stroke SI engine on natural gas (methane) – hydrogen blends at several load points with variation in excess air ratios. The results showed a decrease in CO and CO₂ with increase in excess air ratio.

2.7 Emission trend

Since biomass based feedstock is cyclic (therefore renewable), it remains as a sustainable energy source as long as it is consumed at a rate comparable to or less than the rate of biomass growth or production. Further, considering biomass cycle in nature and its net impact, biomass gasification technology is carbon neutral and therefore environmental friendly (Babu et al., 2011). Number of studies was reported to describe the emission trend of PG when used in IC engines. Shivapuji et al., 2011, conducted experiments on multi-cylinder natural gas engine fuelled with producer gas. The emission readings obtained during experiments are shown in Table 2.1. The CO emission was found to be on higher side and it was attributed to partial or incomplete combustion at full load. Further a need for identifying suitable catalytic converter to reduce CO emissions was expressed. A work based on years of experience conducted at different time on dual fuel and 100% PG mode was reported by Sridhar et al., 2005b. The results are summarized as shown in Table 2.2. Under dual fuel mode, NO_x was found to be under limit due to lower combustion pressures and CO was

above the existing limits due to combustion inefficiencies. Whereas under 100% gas mode (12-cylinder turbo charged mode), both NO_x and CO were within norms.

Table 2.1 Emissions at full load

| Norms | NO _x (g/MJ) | HC (g/MJ) | CO (g/MJ) |
|---------------------|------------------------|-----------|-----------|
| Indian | 2.56 | 0.360 | 0.970 |
| European | 1.30 | 1.30 | 1.390 |
| Experimental values | 0.22 | 0.011 | 4.904 |

Table 2.2 Emissions under dual fuel and gas alone mode

| Parameter | European | U.S.A | India | PG (100%) | Dual fuel |
|------------------------|-------------|-------|-----------|------------|-----------|
| CO (g/MJ) | 1.4 – 1.8 | 3.06 | 1.25 | 0.58-1.2 | 3.1 -3.5 |
| NO _x (g/MJ) | 2.56 | 2.56 | 2.22 | 0.32 – 0.7 | < 0.25 |
| PM (g/MJ) | 0.15 – 0.24 | 0.15 | 0.1 – 0.2 | <0.0005 | < 0.01 |

On similar account, a case study was presented by Sridhar et al., 2005, to bring out the experience on gasifier-engine based power plant to support textile industry. The emissions (HC, CO, NO_x) were within permissible limits against off road diesel engine norms applicable to Europe Stage-II. The readings obtained for the above applications are summarized in Table 2.3. A work by Jonas et al., 2011, indicates PG as a good knock resistant and excellent lean burn fuel. Results were compared with NG engine operation. PG was produced from onsite Viking gasifier having H₂:30, CO:20 and CH₄:1 along with CO₂ & N₂ inerts with 6 MJ/Nm³ energy content. This work also shows an adaptation of high swirl based fast burn design piston (quartette piston). Emission analysis on single cylinder, four stroke NG engine with CR 12.6 and 1050 rpm revealed that NO_x values are comparatively low against NG at lambda (λ) = 1 and reduces greatly when λ is 1.8 due to low combustion temperatures as a result of inerts in PG mixture. The total hydrocarbons (THC) for PG was low (less than 30 ppm) as compared to that of NG (approx. 300 ppm) and increased marginally above λ (air to fuel ratio) = 2.5. This observation was attributed to lower % contribution of CH₄ in PG fuel. However, CO emissions were found to be on higher side away from λ = 1 due to the presence of higher amount of CO in PG fuel itself. In summary,

from the above emission studies it is clear that CO emissions were found to be on higher side as compared to NO_x and HC with a PG engine operation. A concern remains, as CO by itself is a fuel having chemical energy. A suitable catalytic convertor may have to be identified for oxidation of CO to CO₂.

Table 2.3 Gas engine emission (off road vehicles norms)

| Parameter | Europe Stage II | PG engine |
|-----------------|-----------------|--------------|
| CO | 0.97 | 0.5 – 0.7 |
| NO _x | 1.67 | 0.2 – 0.3 |
| PM | 0.083 | Below limits |

2.8 Modelling studies on combustion characteristics

With the advancement in computational capabilities in the present day world, complex fluid flow interaction studies are being handled relatively easy. The combustion process associated with IC engines are more complicated, owing to turbulence level, engine dynamics, flame propagation and energy conversion. Simulation work ranging from full fledge three dimensional (3D) to zero dimensional (0D) thermodynamic based studies are being explored for better understanding of complex combustion processes in engines. For quick assessment and to carryout parametric studies, zero dimensional models are gaining much importance. In view of this, literature in the field of combustion modelling through zero dimensional studies was reviewed.

In 0D studies, the popular combustion model used to estimate burn rate of engine combustion process is represented by Wiebe function (single stage) as shown by eq.2.1

$$x_b = 1 - \exp \left[-a \left(\frac{\theta - \theta_o}{\Delta\theta} \right)^{m+1} \right] \quad (2.1)$$

where, x_b is the mass fraction burnt, θ is the crank angle, θ_o is the start of combustion, $\Delta\theta$ is the total combustion duration, efficiency factor a and form factor m are adjustable. For conventional hydro-carbon fuels like gasoline, efficiency factor $a = 5$ and form factor $m = 2$ have been reported based on experimental observations (Pundir, 2010 and Ferguson, 2011). However, the coefficients depend on engine load and speed as well.

It was found that Wiebe correlation was extensively used in CI and SI engines to study engine combustion process. Miyamoto et al.,1972, used single Wiebe function for predicting the in-cylinder pressure and thermal efficiency of diesel engine. In 1979, Heywood, studied the effect of Wiebe function on four stroke SI engine to study the effect of operating conditions on engines performance and NO emissions. Further, specialized applications like trinitrotoluene (TNT) explosions were studied by Kuhl et al., 1999, and to generate catalytic conversion efficiency maps (Shaw, et al., 2002), the single Wiebe function was used. However, single stage Wiebe function was well suited only for limited applications (Ghojel, 2010) mostly dominated by conventional fuels. However, according to recent study by Shivapuji et al., 2015, owing to thermo-physical properties of PG fuel (due to presence of hydrogen) like heating value, flame speed, adiabatic flame temperature etc., the heat release curve was different from conventional baseline fuels like gasoline. He observed a change in slope of MFB curve from 50% MFB point and therefore, coefficients a and m were curve fitted accordingly as 2.4 and 0.7. However, the exact PG composition for which the MFB curves were analyzed was not clear. The work was carried out on two multi-cylinder engines, one under naturally aspirated mode and the other on turbocharged mode.

For estimating burn rate in diesel and dual fuel engine operation, double stage Wiebe function are extensively used (Miyamoto et al., 1972 and Liu et al.,1997). The double stage Wiebe function is expressed as shown by below eq.2.2

$$x_b = x \left(1 - \exp \left[-a_1 \left(\frac{\theta - \theta_o}{\Delta\theta} \right)^{m_1+1} \right] \right) + (1-x) \left(1 - \exp \left[-a_2 \left(\frac{\theta - \theta_o}{\Delta\theta} \right)^{m_2+1} \right] \right) \quad (2.2)$$

Where, a_1 , a_2 are model constants, m_1 and m_2 are index variables and x is a scaling factor. The advantage of Wiebe function lies in modelling the complicated mass fraction burnt curves by adjusting the coefficients of above eq. 2.2. In 2007, Meyer, reported a work considering gasoline fuelled engine operation, in which, double stage Wiebe function was found most suitable to estimate the burnt rate due to heavy valve overlap condition.

2.9 Natural gas fuelled engines

Natural Gas (NG) can be extracted from oil and gas wells located at different depths below the earth (Catania et al., 2004). NG is treated as the promising alternative fuel due to number of benefits it offers as compared to gasoline fuel. These benefits include, cleaner

exhaust gas emissions, low cost and higher knocking resistance. Therefore, an increasing usage of NG vehicles are seen (Poulton et al., 1994, Pischinger et al., 2003). Furthermore, NG fuel is safer than gasoline in many respects (Cho and He, 2007, Ganesan, 1999). The ignition temperature of NG is higher than gasoline fuel and NG is lighter than air and thus ascends upward readily, where as fuels like diesel and gasoline do not dissipate readily. However, the utilization of NG as an alternative fuel in engines is considered as beneficial, owing to limited supply of liquid fuels and higher cost (Catania, 2004, Sera, 2003). NG is a cleaner fuel than gasoline or diesel and considered environmentally friendly (Cho and He, 2006, Shashikantha and Parikh, 1999, Wayne, 1998). Other advantages associated with NG is its remarkable performance on SI and at higher compression engines (Ganesan, 1999).

According to literature (Bakar et al., InTech Report, 2012), four types of NG engines were explored, namely: the traditional premixed charge spark ignition engine, the port injection lean burn engine, the dual-fuel/pilot injection engine and the direct injection engine (Ouellette, 2000; Shashikantha and Parikh, 1999). Shashikantha and Parikh (1999), studied a 17 kW, stationary, direct injection diesel engine, converted to operate as a gas engine, using producer-gas and NG as the fuels on two different operational modes, called SIPGE (Spark Ignition Producer Gas Engine) and DNGE (Compressed NG Engine). Shashikantha and Parikh (1999) results of conversion to SIPGE (or DNGE) is appreciated since comparable power and efficiency could be developed. NG operation of SIPGE yielded almost comparable power and higher efficiency, which establishes the fuel flexibility of the machine under spark ignition performance. The spark advance needed for producer-gas operation was suggested much higher of 35° BTDC as compared to NG operation which is 22° BTDC, with a compression ratio of 11.5:1. However, the composition of PG fuel considered was not clear, and it appears that the presence of hydrogen concentration in PG is on lower side, to set such a higher spark advance of 35° CA. Since NG engines have reached matured technological status, the reference for development of PG engines is largely compared with NG (CNG) fuel and engines (Mukunda, 2011).

2.10 Gaps in the existing research work

Based on the literature survey and findings reported by various researchers, it is clear that PG fuel is sensitive to a number of factors such as properties of biomass, operational or process parameters of gasification process. Estimation of optimal combustion criteria (MBT spark time) for the PG derived from specific gasifier design, considering the variation of

hydrogen concentration, was lacking. Furthermore, due to non-availability of commercial PG carburetor and owing to vast difference in air to fuel ratio of PG ($\approx 1.2:1$) as compared to conventional fuels like Natural gas (17.2:1) and gasoline (15:1), development of customized PG-air mixer (PG carburetor) is much needed. For a fixed range of PG composition, the dynamics associated with PG engine both at in-cylinder front and shaft end was not adequately addressed. Finally, the influence of hydrogen and methane concentration on modified SI engine (derived from CI base frame) was not addressed through modelling studies. Therefore, the main aim of the present research work was to address the in-cylinder combustion aspects of Producer gas fuel causing dynamics in combustion and performance parameters against the varied composition of producer gas.

2.11 Objectives of present work

Based on the literature review and the research gaps in the area of producer gas fuelled engines, the following objectives are framed accordingly:

1. To design and develop the induction system suitable for bottled producer gas fuelled SI engine operation
2. To study the influence of variation in hydrogen and methane concentration of producer gas on engine combustion, performance and emissions parameters at compression ratio 11:1 and to compare the results with CNG ($\text{CH}_4 = 95\%$ by volume) and gasoline
3. To experimentally investigate the effect of hydrogen (in producer gas) on engine response parameters at higher compression ratios (CR: 11:1, 15:1 and 18:1)
4. To model the mass fraction burn curves and the parametric studies to understand the effect of hydrogen and methane concentration for producer gas fuelled SI engine with heavy valve overlap configuration.

2.12 Summary

In this chapter, a review on existing literature was pursued to frame the research objectives for the present thesis work. Literature was explored in three areas namely, producer gas combustion characteristics, performance characteristics and the emission characteristics. It was found that, number of researchers designed and fabricated their own gas carburetors for their end application. However, no sufficient information on design guidelines and their effectiveness was presented. PG engine performance was also investigated by number of

researchers and reported poor volumetric efficiency (30 to 40%) and huge power loss (upto 50%). Due to variation in PG quality, the MBT spark time was also studied considering high quality PG with least composition variation. The emission characteristics were found to be within Indian norms except CO emissions at higher loads due to incomplete combustion.

Some of the potential research gaps identified based on the existing literature review were, a need for development of induction system due to non-availability of commercial test rigs. Quantifying the effect of hydrogen and methane on in-cylinder aspects. Considering a comprehensive range of PG composition variation, predicting the heat release and thus engine performance is an area to explore. The possible objectives to explore includes, methodological development of induction system to suit bottled fuelled small capacity engine operation, analyzing the effect of hydrogen and methane concentration on engine characteristics through parametric studies and to develop a combustion model for predicting heat release and thus the PG engine performance.

Chapter 3

Materials and Methods

3.1 Introduction

In the previous chapter, a detailed discussion on the literature review pertaining to producer gas fuelled IC engines and the influence of hydrogen and methane on engine response was presented. In the present chapter, various engine instrumentation and the methodology followed to quantify engine response parameters are presented. Based on McClintock approach (Kline et al., 1953) the uncertainty associated with measuring instruments is also obtained.

3.2 Producer gas mixture formulation (PG fuel sets)

The range of PG composition derived from open-top downdraft gasifier considering sun dried Causurina wood chips with 12 to 15% moisture and bottled producer gas considered in present work is set out in Table 3.1.

Table 3.1 Producer gas range considered in present work

| PG composition | (Kanitkar et al., 1993) % Volume | (Sridhar, 2003) % Volume | Present work % Volume |
|------------------------------------|-------------------------------------|-----------------------------|--------------------------|
| Hydrogen (H ₂) | 18 to 20 | 18 to 20 | 16 to 22 |
| Carbon monoxide (CO) | 18 to 20 | 18 to 20 | 18 |
| Methane (CH ₄) | 2 to 3 | 2 | 1 to 4 |
| Carbon di-oxide (CO ₂) | 12 | 11 to 13 | 12 |
| Water Vapour (H ₂ O) | 2.5 | 1.5 to 2.5 | -- |
| Nitrogen (N ₂) | Balance | Balance | Balance |

3.2.1 Variation of hydrogen concentration in producer gas

One of the issues related to gasification process is the variation in moisture content of biomass (Rajvanshi, 2014). The moisture content in PG plays an important role in production of H₂ concentration in gasifier unit. Generally, the moisture range lies between 14 to 24%. A sun dried biomass approximately contains 14% of moisture level. A 5 to 10% moisture in biomass yields 16% of H₂, and 15 to 25% of moisture content yields 24% of H₂. Based on the

literature and information available on hydrogen yield with moisture content, in the present work, a comprehensive range of 16 to 22% of H₂ variation in PG was considered for experimentation as shown in Table 3.1.

3.2.2 Variation of methane concentration in producer gas

The variation of methane concentration in the producer gas is dependent on hydrogen and solid carbon (exothermic) reaction taking place in the reactor. This reaction is called as methanation reaction as expressed below by balanced chemical eq.3.1. The range of methane variation considered in the present work was 1 to 4%. Further, the following PG formulation strategy is carried out with specific reference to PG derived from the downdraft gasifier with air as a gasification agent. This work is pursued to understand the influence of constituents (hydrogen and methane) concentration in PG engines. In order to have a complete control on producer gas range composition, bottled PG fuel was formulated with mid-point strategy as shown in Table 3.2. Furthermore, to precisely quantify the effect of individual gases like H₂, CO and CH₄ on engine combustion process the optimal combinations of producer gas mixtures are chosen and presented in Table 3.3. The combustion properties of individual producer gas fuel sets are presented in the next chapters.

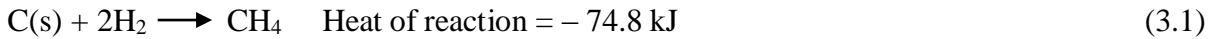


Table 3.2 Producer gas formulation strategy

| Input parameters | Lower limit | Mid-point | Upper limit |
|----------------------------|-------------|-----------|-------------|
| Hydrogen (H ₂) | 16 % | 19 % | 22 % |
| Methane (CH ₄) | 1 % | 2.5 % | 4 % |

Table 3.3 Optimal combinations of producer gas mixtures

| PG composition (% Vol.) | A | B | C | D | E | F | G | H | I | CNG |
|-------------------------|----|------|----|----|------|----|----|------|----|-----|
| Hydrogen | 16 | 16 | 16 | 19 | 19 | 19 | 22 | 22 | 22 | -- |
| Carbon-monoxide | 18 | 18 | 18 | 18 | 18 | 18 | 18 | 18 | 18 | -- |
| Methane | 1 | 2.5 | 4 | 1 | 2.5 | 4 | 1 | 2.5 | 4 | 95 |
| Carbon-dioxide | 12 | 12 | 12 | 12 | 12 | 12 | 12 | 12 | 12 | -- |
| Nitrogen | 53 | 51.5 | 50 | 50 | 48.5 | 47 | 47 | 45.5 | 44 | -- |
| Ethane | -- | -- | -- | -- | -- | -- | -- | -- | -- | 5 |

In the present study, the variation of CO was not considered because of its lowest energy content as compared to hydrogen and methane in PG. Also, the CO fraction does not vary as strongly as hydrogen and methane with the variation in moisture and densities of biomass.

3.3 Estimation of producer gas quantity

The procedure followed to estimate the total number of PG bottles required for taking 3 trials on PG engine was estimated by considering the engine compression ratio of 11:1, speed 1500 rpm and approximate volumetric efficiency of 0.45 is considered under full load. From the calculations given in Appendix-A, it is clear that PG engine requires almost 7 m³ of gas per hour. According to general gas industry standards in India, the medium capacity (47 liters) cylinder (bottle) holds 7 m³ of gas. It was estimated that, to complete 3 trials on each PG composition considering 4 engine load points (25%, 50%, 75% and full load), approximately 14 m³ of gas was required. Therefore, 2 bottles per composition was needed. The photographic view of calibrated PG bottles is shown in Fig. 3.1.



Fig. 3.1 Calibrated producer gas bottles

3.4 Methodology to quantify the various engine parameters

3.4.1 Engine instrumentation

The engine cylinder head was fitted with a flush mounted piezoelectric pressure transducer (Kistler make # 6613CA). The photographic view of pressure transducer is shown in Fig. 3.2 (The technical details of pressure transducer are given in Appendix-B). The position of piston motion was measured through crank angle encoder (Kuebler make # 8.5000.8352.0360) of 1° CA resolution (the technical details are given in Appendix-C). The crank angle resolution of the encoder is 1°, which is the minimum crank angle required for in-cylinder analysis as per literature (Roger, 2010). The in-cylinder data from pressure sensor and encoder are acquired through a high speed (1 MHz, sampling rate) data acquisition system (SAM3X8E-MCU). Further, the conversion of pressure signals from differential to

absolute mode was made through intake absolute manifold pressure. The exhaust gas was measured through AVL-444 Digas analyzer.

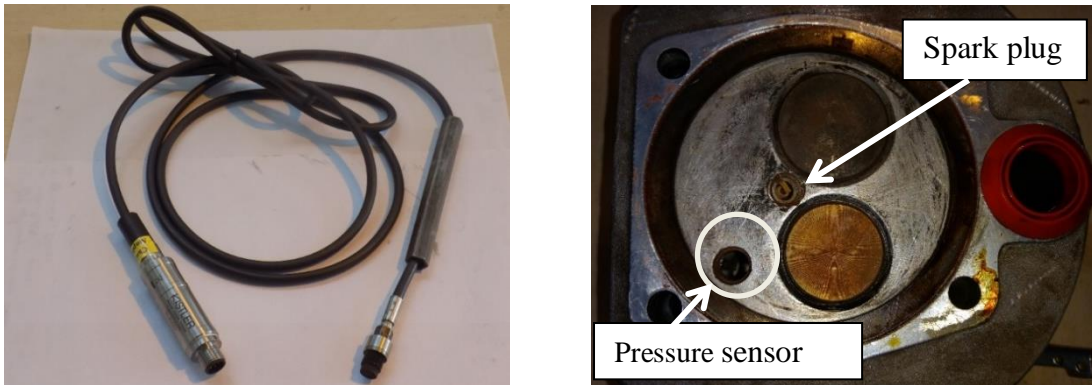


Fig. 3.2 Piezoelectric pressure transducer

3.4.2 Significance of combustion pressure versus crank angle

In this work, engine combustion parameters are derived from in-cylinder pressure and crank angle data. It was reported by Amann, 1985, and Lancaster et al., 1975, that in-cylinder pressure and its cyclic variation is of paramount interest for the combustion analysis. Therefore, cylinder pressure indicator stands as the first diagnostic tool in this work for understanding PG fuelled engine behavior. It was brought out by Lancaster, 1975, that cylinder pressure is the basic engine variable for the combustion study. He further reports that many researchers (Krieger et al., 1966, Cornelius et al., 1952, Rifken et al., 1952, Patterson, 1967, Chen et al., 1973, Gish et al., 1958, Brown et al, 1973) have used cylinder pressure to study cyclic variation, pumping losses, engine friction and NO_x emission. Today, the modern engines with good fuel economy and fewer emission are an outcome of engine development that came through basic pressure measurement.

The various advantages of cylinder pressure versus crank angle are listed below:

- Qualitative description on the progress of combustion can be seen
- The instantaneous pressure value at every crank angle inside the cylinder can be monitored
- Compared to pressure volume curve, the pressure and crank angle provides combustion events occurring closer to top dead center
- Optimization of valve opening and closing can be studied through pressure-crank angle information

- Vital information such as peak pressure value and its occurrence, IMEP, rate of pressure rise and its position etc. can be visualized

3.4.3 Engine combustion parameters

Based on the acquired in-cylinder data, the following engine parameters can be evaluated.

The rate of heat release

It is the analysis of cylinder pressure from a firing engine to determine the burn rate of the combustion event on crank angle to crank angle basis. From the first law of thermodynamics in differential form as shown below, the steps involved in deriving the heat release equation are shown below (Pundir, 2010). In present work for heat release analysis, the energy equation based on single zone model was followed, where, crevice, blow-by effects and heat losses from cylinder walls are neglected. The polytropic index (n) was taken as 1.35 based on literature for calculation of pressure developed due to piston motion.

$$d(Q - Q_w) = dW + dU$$

$$dW = PdV \text{ and } dU = m C_v dT$$

$$dQ = PdV + m C_v dT + dQ_w$$

Differentiating the equation of state for ideal gas $PV = mRT$

$$mdT = \frac{1}{R}(PdV + VdP)$$

Substituting dT in the energy equation

$$dQ = PdV + \frac{C_v}{R}(PdV + VdP) + dQ_w$$

Expressing it in terms of crank angle (θ)

$$\frac{dQ}{d\theta} = \frac{\gamma}{\gamma-1} \cdot P \cdot \left(\frac{dV}{d\theta} \right) + \frac{1}{\gamma-1} \cdot V \cdot \frac{\partial P}{\partial \theta} \quad (3.2)$$

where, Q is the heat release during combustion, γ is the ratio of specific heat, p is the cylinder pressure, $\frac{dP}{d\theta}$ is the pressure variation with crank angle and $\frac{dV}{d\theta}$ is the volume variation with reference to crank angle and dQ_w is heat loss from the cylinder walls.

Using engine geometry data, the instantaneous piston position in differential form is given as

$$\frac{dV}{d\theta} = \frac{V_d}{2} \sin \theta \left[1 + \cos \theta (R^2 - \sin^2 \theta)^{-0.5} \right]$$

where V_d is the swept volume of engine and $R = (2.l/B)$, l = connecting rod length

Combustion duration

The crank angle duration from 10% mass fraction burnt (MFB) to 90% MFB is called as the Combustion Duration (CD).

Rate of pressure rise (ROPR)

Rate of pressure rise implies pressure load on cylinder head due to combustion process and to a large extent it determines structural design (Murugan et al., 2008) and also noisy operation. It is given by eq.3.3

$$ROPR = \left(\frac{dQ}{d\theta} \right) \text{ kJ/}^\circ\text{CA} \quad (3.3)$$

Mass fraction burnt

Based on experimental observation, the pressure rise ΔP is proportional to the heat added to the in-cylinder medium during the crank angle interval. The mass fraction burned at the end of i^{th} interval was calculated as shown below (Shayler et al, 1990 and Stone et al., 1987), where ‘SOC’ denotes the start of combustion, ‘N’ end of combustion.

$$MFB = \frac{m_b(i)}{m_b(\text{total})} = \frac{\sum_{SOC}^i \Delta p}{\sum_{SOC}^N \Delta p} \quad (3.4)$$

Indicated Mean Effective Pressure (IMEP)

The pressure – volume indicator diagram is very important because, work produced by the cylinder gas can effectively be quantified with the below equation on per unit mass basis (Pulkrabek, 2004),

$$w = \int P(dv) \text{ kJ/kg} \quad (3.5)$$

Thus, when pressure is plotted against volume, the area under the pV curve signifies indicated work done by the cylinder gas. From the indicated diagram one can calculate the IMEP value directly as shown by the following expression,

$$IMEP = \frac{\text{Net work done}}{\text{Change in cylinder volume}} \text{ kPa} \quad (3.6)$$

Cycle to cycle variation – Combustion variability

The measured pressure crank angle data history for several successive cycles indicates cycle by cycle variation in combustion pressure. The combustion variability also signifies smoothness of engine operation. Various in-cylinder parameters have been used to characterize cycle to cycle combustion variation. Examples for parameters based on cylinder pressure are peak pressure and its crank angle, maximum rate of pressure rise and its angle of occurrence, IMEP. Parameters related to combustion rate are maximum rate of heat release, flame development angle, flame propagation etc. The most widely used parameters to characterize the cycle to cycle combustion are peak pressure (maximum pressure) and IMEP. The index for cyclic variability is called as Coefficient of Variance (COV) expressed by the eq.3.7.

$$(COV_{P_{max}}) = \frac{\sigma_{p_{max}}}{P_{max}} \times 100 \quad (3.7)$$

where, $\sigma_{p_{max}}$ is the standard deviation in pressure. The data collected for 200 to 300 consecutive cycles provide a realistic measure of combustion variability.

3.4.4 Engine performance parameters

The performance of an engine influencing shaft output power can be analyzed by various parameters as follows (Heywood, 2011):

Brake power

The power available at the engine shaft is called as the brake power. It is given by the following equation,

$$\text{Brake power}(BP) = \frac{2 \times \pi \times N \times T}{60 \times 1000} \text{ kW} \quad (3.8)$$

where, T is the engine torque in N-m, N is the engine speed in rpm, the 1000 in the denominator is the conversion factor to express in kW.

Brake thermal efficiency

The effective utilization of thermal energy is quantified by brake thermal efficiency equation.

$$\text{Brake thermal efficiency} = \frac{\text{Brake power}}{\text{mass flow rate of fuel} \times \text{LHV}_{\text{fuel}}} \quad \text{kW} \quad (3.9)$$

Brake mean effective pressure

The engine output torque at the crank shaft when related to the engine displacement is BMEP. It is the measure of work output from an engine and not of the pressures in the engine cylinder. BMEP is used to compare the performance of different engine capacities and the number of cylinders.

$$\text{BMEP} = \frac{BP \times 60 \times 1000}{L \times A \times (N/2) \times k} \quad \text{kPa} \quad (3.10)$$

Brake specific fuel consumption (BSFC)

BSFC is an important parameter which determines the fuel consumption rate to develop unit brake power. It is expected to keep the SFC value as minimum as possible for fuel economy.

$$\text{BSFC} = \frac{\text{Mass flow rate of fuel}}{\text{Brake power}} \quad \text{kg/kWhr} \quad (3.11)$$

Brake specific energy consumption (BSEC)

BSEC is yet another engine performance parameter, which reflects the energy consumed to develop unit power output. The lower values of BSEC indicates how efficiently the fuel energy is obtained from fuel.

$$\text{BSEC} = \frac{\text{Mass flow rate of fuel} \times \text{LHV}_{\text{fuel}}}{\text{Brake power}} \quad \text{kJ/kWhr} \quad (3.12)$$

A MATLAB code was written to process and calculate engine combustion properties based on acquired in-cylinder pressure and crank angle data. For more details, refer to Appendix–D.

3.5 Variation of compression ratio

In the present investigation, compression ratio was changed by changing the clearance volume of engine by inserting rings of different thicknesses between the cylinder and cylinder head in place of gasket. The photographic view of gasket is shown in Fig. 3.3. The

producer gas fuelled engine was tested under three different CR's 11:1, 15 and 18 to understand its combustion characteristics, performance and emission trends.



Fig. 3.3 Photographic view of engine gasket

The steps involved in calculating the Compression Ratio is as follows,

$$\text{Compression Ratio} = \frac{\text{Maximum cylinder volume}}{\text{Clearance volume}} = \frac{(V_s + V_c)}{V_c} \quad (3.13)$$

Swept volume = $\frac{\pi}{4} \times d^2 \times L$, where bore diameter $d = 82 \text{ mm}$, stroke length, $L = 68 \text{ mm}$.

$$\text{Swept volume} = 359 \text{ cm}^3$$

Gasket inner diameter = 84 mm and area = 55.41 cm^2 .

Clearance volume without gasket (constant) = 17.31 cm^3

Using above compression ratio equation, for CR=11:1

$$11 = \frac{V_s + V_c}{V_c}$$

$$V_c = \frac{V_s}{10} = 35.9$$

$$V_c = 17.31cc + \left[\left(\frac{\pi}{4} \right) \times d^2 \times L \right]$$

where L is the thickness of compression ring thickness

$$\text{Gasket volume} = 35.9 - 17.31 = 18.59 \text{ cm}^3$$

$$\text{Thickness of ring} = \frac{18.59}{55.41} = 0.335 \text{ cm}$$

Following the similar procedure, the thickness for the rest of the CR's 15 and 18 is calculated and listed in Table 3.4

Table 3.4 Thickness of compression rings

| CR | Clearance volume (cm ³) | Gasket volume (cm ³) | Ring thickness (cm) |
|------|-------------------------------------|----------------------------------|---------------------|
| 11:1 | 35.90 | 18.59 | 0.335 |
| 15:1 | 25.64 | 8.33 | 0.15 |
| 18:1 | 21.11 | 3.80 | 0.068 |

3.6 Exhaust gas measurement

3.6.1 Emission analyzer

The exhaust gas sample was analyzed by a Five Gas analyzer (Make: AVL India, Model: 444) fitted with a Digas sampler, it is calibrated as per Automotive Research Association of India (ARAI) norms. The technical specifications and calibration certificate are given in Appendix-E. The principle used for measuring the CO & CO₂ was the Nondispersive Infrared (NDIR), HC was measured through Flame Ionization Detector (FID), NO was with Chemiluminescence detector (CLD) and O₂ was measured through electro-chemical sensor. The CO, CO₂, O₂ emissions were measured in volume percentage, while the unburnt hydrocarbon (HC) was measured in ppm (vol.) of n-hexane equivalent and the NO emission was measured in ppm (vol.) during each run of the engine operation. The photographic view of the AVL-444 Digas analyzer is shown in Fig. 3.4.



Fig. 3.4 Flue gas analyzer (AVL-444)

3.6.2 Emission conversion

The formulae used to convert the raw emissions (ppm) to g/kWh is given below.

HC emissions in g/kWh

$$HC \text{ (g/kWhr)} = 6 \times (m_f + m_a) \times \left(\frac{13}{29} \right) \times \left[\frac{HC \text{ ppm} \times 3600}{BP \text{ in kW} \times 10^6} \right] \quad (3.14)$$

CO emissions in g/kWh

$$CO \text{ (g/kWhr)} = \frac{28}{29} \times \frac{CO \text{ (% vol.)}}{100} \times \left(\frac{(m_f + m_a) \times 3600}{BP \text{ in kW}} \right) \quad (3.15)$$

NO emissions in g/kWh

$$NO \text{ (g/kWhr)} = \frac{30}{29} \times \frac{NO \text{ (ppm)}}{1000000} \times \left(\frac{(m_f + m_a) \times 3600}{(BP \text{ in kW})} \right) \quad (3.16)$$

where, mass flow rate of fuel (m_f) and air (m_a) are expressed in g/sec.

3.7 Uncertainty analysis

Uncertainty is the measure of 'goodness' of a result. Without such a measure, it is impossible to judge the fitness of the value. An uncertainty or error analysis is necessary to establish the bounds on the accuracy of the estimated parameters. The evaluations of some

unknown uncertainties from known physical quantities were obtained using the following equation (Kline and McClintock F.A, 1953 and Holman, 2015).

$$U_u = \sqrt{\left(\frac{\partial U}{\partial E_1} \times e_1\right)^2 + \left(\frac{\partial U}{\partial E_2} \times e_2\right)^2 + \dots + \left(\frac{\partial U}{\partial E_n} \times e_n\right)^2} \quad (3.17)$$

In the above equation, U is the physical parameter that is dependent on the parameters E_1, E_2, \dots, E_n . The symbol U_u denotes the uncertainty in U. Table 3.5 gives the instruments used in the present study and their uncertainties. The calculations involved in determining the uncertainty of selected parameters are given in Appendix-F.

Table 3.5 Accuracy and uncertainties of instruments

| Instrument | | Range | Accuracy | Uncertainty |
|-------------------------------------|------------|---------------|-----------|-------------|
| 5 Gas analyzer | HC | 0 – 20000 ppm | ± 10 | 0.11 |
| | CO | 0 – 10 % | 0.03 | 0.75 |
| | NO | 0 – 5000 ppm | ± 50 | 0.5 |
| Pressure transducer | | 0 – 100 bar | ± 0.01 | 0.1 |
| Crank angle encoder | | 0 – 360° | ± 1° | 1 |
| Gasoline | Burette | 0 – 20 cc | ± 1 cc | 0.05 |
| | Stop watch | 0 – 300 sec | ± 1 sec | 0.06 |
| Manometer (For air flow rate) | | 0 – 250 mm | ± 1 mm | 0.33 |
| Electronic scale (For NG flow rate) | | 0 – 75 kg | ± 10 gram | 0.027 |
| Manometer (For PG flow rate) | | 0 – 500 mm | ± 1 mm | 0.25 |
| Thermocouple (K-Type) | | 0 – 800° C | ± 1° C | 0.005 |

3.8 Summary

In this chapter, a discussion on the variation of hydrogen and methane concentration in producer gas was presented. Formulation of optimal combinations of producer gas fuel sets was also covered. The methodology adapted to analyze engine data is presented along with relevant mathematical relations. Finally, details of instrumentation and uncertainties associated with measuring devices are also discussed. In the next chapter, design and development of induction system suitable to operate bottled producer gas engine is described.

Chapter 4

Experimental Set-up and Procedure

4.1 Introduction

In the previous chapter, a detailed description on producer gas fuel set formulation and methodology followed to quantify various in-cylinder combustion and performance parameters was presented. In this chapter, an in-depth discussion on development of producer gas induction system is presented. Apart from this, the procedure followed to operate the engine at naturally aspirated mode is also elaborately discussed.

4.2 Description of engine set-up

The photographic view of the experimental test rig is shown in Fig. 4.1. The test rig considered in the present work was a retrofitted diesel engine base frame with CR:18. Hereafter, this engine is referred as “modified SI engine”. The benefit of working on higher CR’s using low energy density fuel like PG lies in drawing higher thermal efficiencies (Babu et al., 2012). Work with higher CR is possible due to higher Octane number (> 100) of producer gas (Banapurmath et al., 2009). Further, this set-up was operated on three fuels namely, gasoline, CNG and producer gas. The specifications of the engine are listed in Table 4.1.

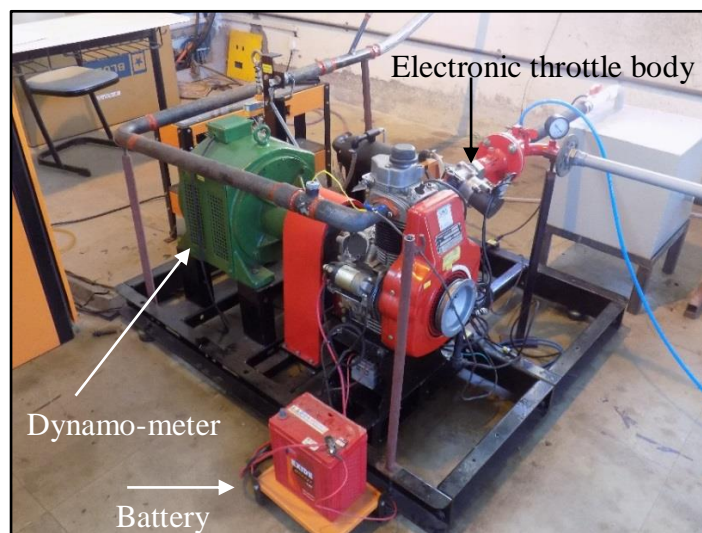


Fig. 4.1 Photographic view of engine set-up

Table 4.1 Engine specifications

| Parameters | Specification |
|-------------------------------|-----------------------------------------------------------------------------------------------------|
| Make and model | Greaves Cotton Pvt. Ltd., # 1533 |
| Engine type | Naturally aspirated, air cooled and 4-Stroke |
| Number of cylinders | Single cylinder |
| Bore and Stroke | 82 mm × 68 mm |
| Swept volume | 359 cm ³ |
| Rated power in Diesel mode | 4.32 kW with CR:18 at 1500 rpm |
| Power output in Gasoline mode | 2.2 kW with CR: 11 at 1500 rpm |
| Combustion chamber | Flat cylinder head and toroidal piston type |
| Ignition system | Battery operated – Coil-on-plug (COP) system with computer control to advance and retard spark time |
| Dynamometer | Eddy current with 58.80 N (6 kg) capacity loading |
| Valve timing | Inlet valve opening – 5° BTDC |
| | Inlet valve closing – 38° ABDC |
| | Exhaust valve opening – 36° BBDC |
| | Exhaust valve closing – 35° ATDC |

The toroidal shape piston cavity is shown in Fig. 4.2. The cavity is offset slightly away from piston center. Further, these type of piston shapes are known to cause higher turbulence and thus promote better mixing of air and fuel – for diesel engine operation.

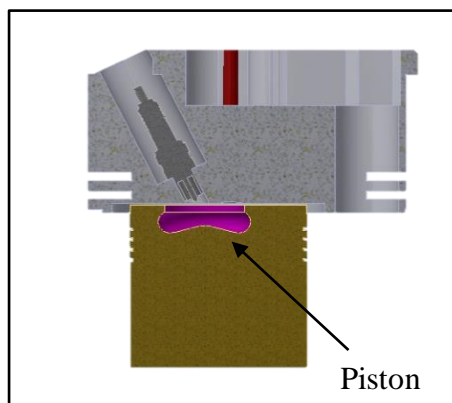


Fig. 4.2 Toroidal piston shape

4.3 Developmental activity of test-rig

Generally, the design of commercial test-rig packages for conventional fuels like gasoline and diesel are standardized and are readily available in the market. However, the challenge was encountered when a multi component fuel (producer gas with unique thermo-physical properties) is to be used in the base diesel engine test-rig. In such situations, the entire fuel and air induction design and the operating parameters to support the test rig may change. In this context, to interface a bottled PG, a systematic approach was followed to arrive at an integrated induction system to operate in conjunction with the retrofitted diesel engine test-rig. The developmental activity was carried out in three phases namely. Phase-1: Involves sizing of induction system (various circuitry elements) to suit bottled producer gas operation. Phase-2: The engine was tested with step wise engine loading from no load to full load operation. A closed loop arrangement of PG-air mixer and air-gas regulator was essential to enable stoichiometry engine operation. Phase-3: Deals with setting operating pressure for various engine loading conditions and corresponding mass flow measurements to ensure satisfactory engine operation.

4.3.1 Elements of induction system

The PG-mixer outlet diameter of 43 mm was taken as a base reference (due to available port diameter of engine inlet manifold) for entire design and development activity. The induction system basically consists of the following elements,

- a) PG-air mixer
- b) Air-gas regulator
- c) Orifice - meters
- d) PG reservoir and
- e) Piping network along with flow control valves

4.3.1.a PG-air mixer

A comparison of air-fuel mass ratio of fuels like NG (17.2:1), Liquefied petroleum gas (15.5:1) and gasoline (14.7:1) and PG (1.5:1) shows a vast difference in existing A/F ratios. Therefore, available conventional carburetors are not suitable for the application of producer gas engine operation. With this requirement, there was a need to design and fabricate a customized PG-air mixer. The air and fuel port diameter of mixer was designed based on the

principle of area ratio matching with stoichiometry air to fuel ratio for producer gas fuel. On average basis, the air to fuel volume ratio 1.2:1 was considered. Based on the area ratio, the port diameters of air and gas side were estimated as 31.75 and 28.99 mm respectively as shown below.

$$\left(\frac{Area_{Air}}{Area_{PG}} \right) = \frac{\left(\frac{\pi}{4} \right) \times d_{air}^2}{\left(\frac{\pi}{4} \right) \times d_{pg}^2} = \frac{1.2}{1}$$

$$\text{Fuel port diameter} = \left(\sqrt{\frac{(43\text{mm})^2}{(1.2+1)}} \right) = 28.99\text{mm}$$

$$\text{Air port diameter} = \left(\sqrt{(28.99\text{mm})^2 \times 1.2} \right) = 31.75\text{mm}$$

$$\left(\frac{Area_{Air}}{Area_{PG}} \right) = \frac{\left(\frac{\pi}{4} \right) \times 31.75^2}{\left(\frac{\pi}{4} \right) \times 28.99^2} = 1.2:1$$

Further, the PG-air mixer houses a flap arrangement at the junction of two (air and gas) flow streams as shown in Fig. 4.3. This flap arrangement enables fine tuning of air to fuel ratio either for maximizing the power output (fuel rich condition) or to limit emissions (lean condition).

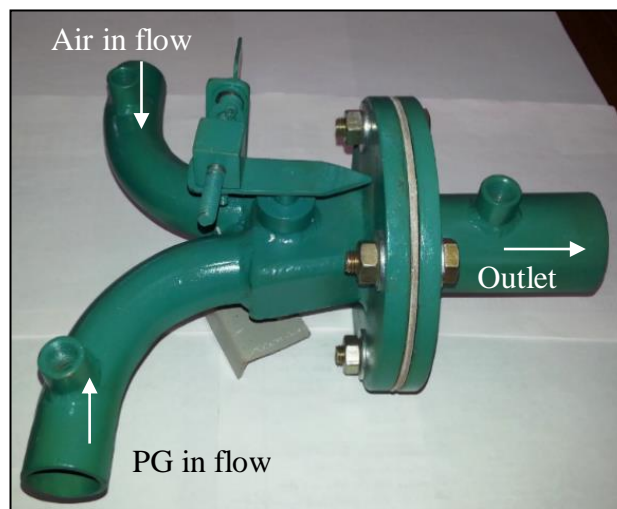


Fig. 4.3 PG-Air mixer

4.3.1.b Air-gas regulator

To ensure supply of right quantity of charge (for stoichiometry operation) to the engine at all engine load conditions, the air-gas regulator is arranged before PG-air mixer. It has a gas diaphragm, which regulates the flow of fuel gas based on the reference pressure prevailing along the air flow passage at all engine load conditions as shown in Fig. 4.9. Based on engine capacity, stoichiometry operation and specific gravity of PG fuel, a suitable regulator model (7218-2) was selected from manufacturer's (Wesman Thermal Engg. Pvt. Ltd., Kolkata) list, the photographic view of air-gas regulator is shown in Fig. 4.4.

Sometimes, one may have to reset gas diaphragm valve lift position to support higher engine loads. Else, engine may starve from lack of required quantity of fuel supply. Furthermore, the advantage of adapting such an air-gas regulator helps in supporting varying engine load with stoichiometry operation as described by Dasappa, 2011.



Fig. 4.4 Air gas regulator

4.3.1.c Flow measurement

For PG and air flow measurements, calibrated orifice-meters were employed in the present work. Along the air flow passage line, the pipeline was connected to a calibrated orifice-meter with an inclined tube manometer (15° inclination) to measure the differential pressure across the orifice-meter. A red oil based manometric fluid (SG: 0.83) was used in the manometer. The photographic view of air flow measurement system is shown in Fig. 4.5. The orifice-meter along the PG fuel line is connected to water column differential manometer as shown in Fig. 4.6. Both the orifice meters were primarily designed for air flow. However, to account for the PG fuel flow, a suitable density ratio correction factor was incorporated in the mass flow rate mathematical expression as demonstrated below by eq.4.1.



Fig. 4.5 Air flow measurement

$$\text{Correction factor} = \sqrt{\frac{\rho_{PG}}{\rho_{AIR}}} \quad (4.1)$$

$$\text{Mass flow rate of PG} = K\sqrt{\Delta h} \times \text{correction factor} \quad \text{kg/hr}$$

where, K is the geometry constant accounting for orifice bore diameter, coefficient of discharge and pipe diameter(s). The Δh is the liquid column height which depends on differential pressure ΔP and density of fluid flow. The maximum variation of column height was observed to be ± 3 mm during engine operation and considered in uncertainties. The calibration details of orifice-meters are given in Appendix-G.

4.3.1.d Producer gas reservoir and piping network

The critical flow parameters encountered while working with bottled producer gas were operating pressure and mass flow of fluid. Normally, a standard 47-liter capacity PG cylinder is supplied with 7 m^3 gas at 130 bar pressure. Thus, a small storage cylinder serving as a reservoir to enhance mass availability was fabricated and arranged ahead in-line with orifice-meters as shown in Fig. 4.5 and 4.6. With this arrangement, it becomes necessary to limit and control PG flow pressure, at the same time ensuring a sufficient quantity of mass flow along the fuel passage. The piping network connecting the PG bottle, PG reservoir, air gas regulator, PG-air mixture and the intake port of engine is shown in Fig. 4.6. The right position of the main valve opening (Fig. 4.7) after PG reservoir is of paramount interest to ensure no discontinuity in mass flow along fuel passage during engine operation. Further, a right setting of valve positions with required mass flow of fluid along passages (gas and air) resulted in dynamic balancing of air-gas regulator in conjunction with PG-air mixer.



Fig. 4.6 Piping network and entire induction system

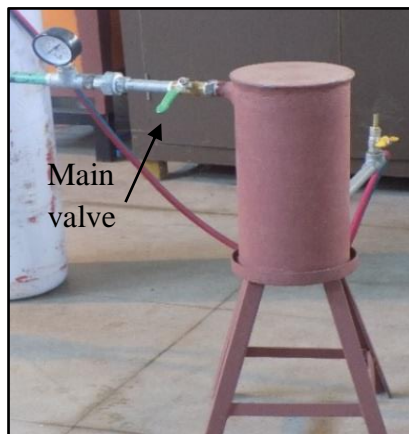


Fig. 4.7 PG reservoir

4.3.2 Testing of induction system

In this section, setting and testing of flow parameters (pressure and mass flow) across orifice meter and air-gas regulator are described. Fire safety devices like flame arrester at supply cylinder end and dry chemical multipurpose extinguisher of class A-B-C type were in place to arrest any fire hazards during testing and experimentation. A 130 bar supply gas pressure was conditioned to 2 bar (gauge) along pipeline connecting PG reservoir using a two-stage gas regulator. The benefit of using two-stage gas regulator lies in knowing the prevailing pressure within supply cylinder throughout the engine run. One can notice an erratic and lean operation of engine during the consumption of remainder 10 to 15 % of left over gas in the reservoir. It was also observed that after every 30 min of engine operation an

increase of 0.5 bar of supply gas cylinder pressure was required to ensure supply of desired mass flow to engine.

Further, a main valve (ball valve throttling device) was in place ahead of orifice-meters to limit the mass flow based on engine load demand. Moreover, the air-gas regulator had a constraint of maximum allowable inlet flow pressure of 13789.5 Pa (1400 mm WC). Any violation of this pressure limit would lead to rupture of diaphragm. However, with 7218-2 model less than 20 mm WC before regulator was noticed at peak load engine operation and this was not desirable to ensure trouble free operation. This inadequate differential pressure of 20 mm WC was due to higher port diameter existing within the air-gas regulator. Therefore, a lower size regulator model (7218-1) was tested – since it had a reduced port diameter as compared to 7218-2 model.

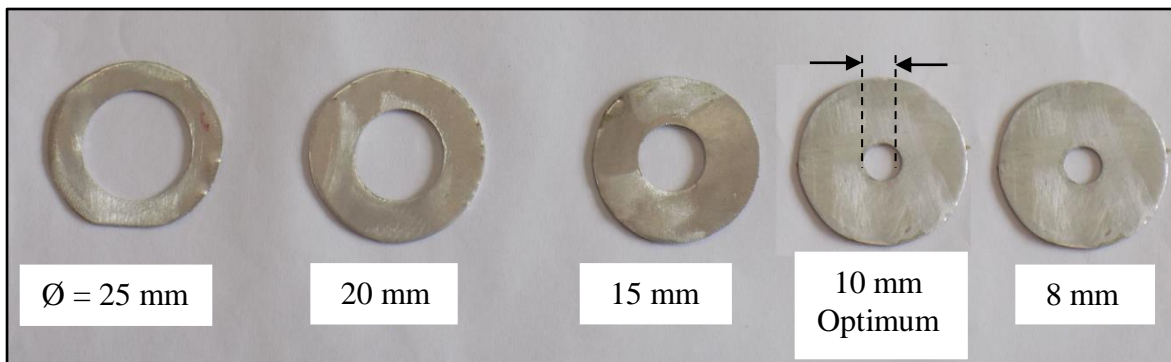


Fig. 4.8 Optimum port diameter of air-gas regulator

However, it did not yield desirable outcome, because the port diameter enabled a higher level of flow pressure magnitudes (>1400 mm WC) before regulator. This was crossing the safe limit of regulator operation. Further, to overcome this bottle neck situation, five different port diameters in the form of aluminum washers were placed on existing original port of 30 mm and tested, as shown in Fig. 4.8 on 7218-2 model. An optimum port diameter was found by reducing the existing original diameter of 30 mm to 33.33% on 7218-2 model as shown in Fig. 4.9 and therefore 10 mm port diameter plate was selected for further study. This modification enabled satisfactory engine operation with 100 mm WC ahead of ZPR. Engine response at various flow conditions are summarized in Table 4.2.

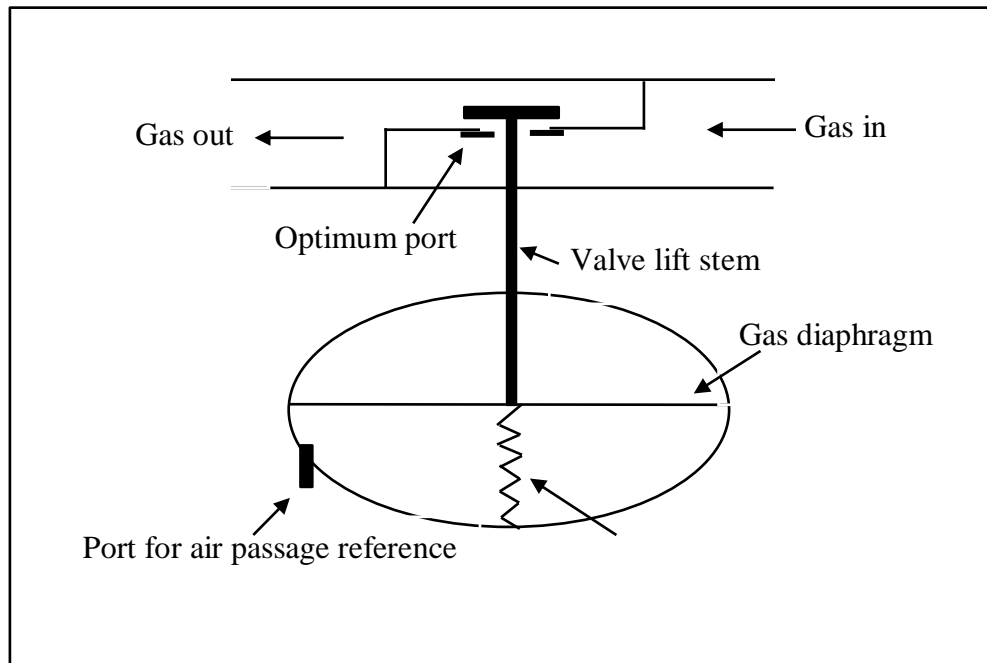


Fig. 4.9 Location of optimum port diameter

Table 4.2 Settings of flow parameters

| Flow parameter setting | Before air-gas regulator | Engine response |
|------------------------|--------------------------|---------------------------------------------|
| Water column in mm | 10 | Unstable engine operation |
| Water column in mm | 50 | Unstable engine operation |
| Water column in mm | > 100 | Stable operation up-to peak load |
| | | |
| Flow pressure | At orifice inlet | Engine Response |
| Inlet pressure in bar | 1 bar gauge | Did not support beyond 50% load |
| Inlet pressure in bar | 2 bar gauge | Supported full load for 1 st run |
| Inlet pressure in bar | 2.5 bar gauge | Supported full load for 2 nd run |
| Inlet pressure in bar | 3 bar gauge | Supported full load for 3 rd run |

4.3.3 Engine testing

Evaluation of engine performance is one of the key aspects during any engine testing activity. In the present work, the engine speed was maintained constant at 1500 rpm by adapting an electronic throttle body (Woodward make: L-series ITB 25mm). Further, during entire engine testing no trace of any back fire was observed at the vicinity of intake manifold (no fumes or burnt effect was visualized). Back fire may exist at times and can extend towards carburetor (air and fuel mixer) due to poor ignition time control. For a fuel like PG having higher flame speed of 0.5 m/s (Dasappa et al., 2011) as compared to gasoline (Shivapuji et al., 2014) is quite hazardous.

Table 4.3 Producer gas composition

| Producer gas composition | % volume basis |
|--------------------------|----------------|
| Hydrogen | 19 |
| Methane | 4 |
| Carbon-monoxide | 18 |
| Carbon-dioxide | 12 |
| Nitrogen | Balance |

Table 4.4 Combustion properties of PG and gasoline

| Combustion property | Unit | PG (Calculated values) | Gasoline (Shivapuji et al., 2013) |
|---------------------------|-------------------|---------------------------------------------------------------------|--------------------------------------|
| Chemical formula | -- | H ₂ ,CH ₄ ,CO ₂ ,CO,N ₂ | C ₈ H ₁₈ |
| Density | kg/m ³ | 0.96 | -- |
| Air to fuel mass ratio | kg/kg | 1.5:1 | 14.7:1 |
| Lower heating value | MJ/kg | 5.25 | 44.4 |
| Mixture heating value | MJ/kg | 2.11 | 2.82 |
| Product to reactant ratio | -- | 0.91 | 1.05 |

However, since the engine was equipped with modern plug-on-coil ignition system, a release of an electric discharge at the required time without any scope for misfires was ensured, unless there is some hot spot (carbon deposit) within combustion chamber.

During engine testing at no-load condition, a hunting behavior was observed. This gradually disappeared with step wise engine loading and no trace of hunting was observed after 20% engine load condition. Furthermore, a smooth engine operation was witnessed at peak power corresponding to 85 % against gasoline with a maximum brake torque (MBT) timing of 16° Crank Angle (CA) before top dead center (BTDC) at 1500 rpm and CR 11:1. A peak combustion pressure of 33 bar and 38 bar for producer gas with mid-point composition listed in Table 4.3 and gasoline was obtained as shown in Fig. 4.10.

Similarly, the area under the pressure – volume diagram shown in Fig. 4.11 depicts a 24.8% reduced potential work output against gasoline. The corresponding net mean effective pressure developed in combustion chamber for PG and gasoline were 6.55 and 8.72 bar respectively. Furthermore, the engine delivered a brake power of 1.87 kW (85%) against 2.2 kW gasoline mode. A 15 % power loss was noticed and it was attributed to 25 % lower mixture heating value of PG as compared to Gasoline. These observations are in good agreement with literature as discussed in chapter 2. Based on the above comparable results, the present induction system ensured a trouble free and satisfactory engine performance under naturally aspirated mode.

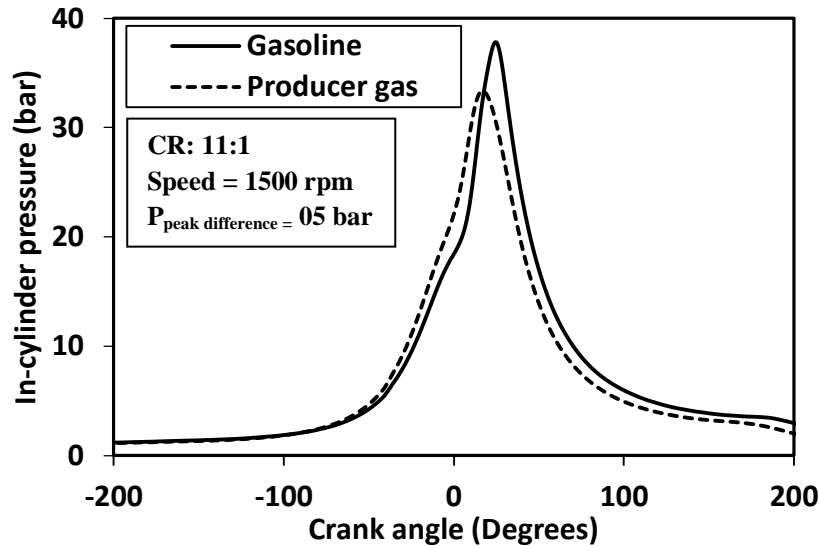


Fig. 4.10 Peak combustion pressure at MBT spark time

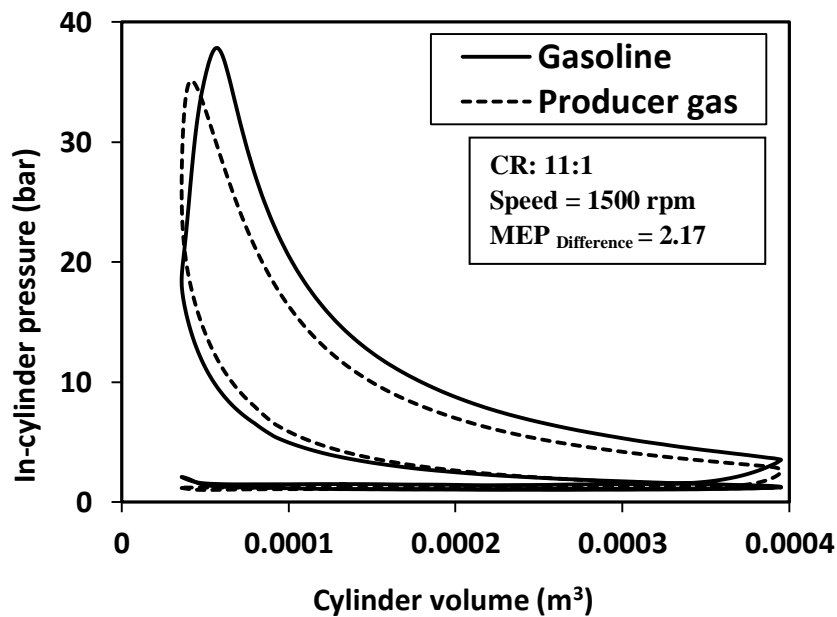


Fig. 4.11 Work output of producer gas over gasoline

4.4 Optimum fuel line operating pressure

The lack of literature in providing sufficient information on operating a bottled PG engine with conventional (without electronic controlling devices) settings for the induction system was the motivating factor to explain the following procedure. It was utmost important to figure out the initial workable line pressure at the outlet of PG cylinder. Depending on this pressure, the required amount of mass of fluid gets stored in PG reservoir, else engine fails to take up higher loads. In the present work, a fresh bottle for the first run, 2 bar flow line

pressure was found to support up to a full load engine operation. Based on this need, the observations as out-lined in Table 4.2 were presented earlier. Therefore, estimating the range of fluid flow parameters for the step wise engine loading is essential. Further, for the fresh second run, a 2.5 bar flow line pressure helped to take up maximum load. Hence it was observed that for every fresh engine start depending on the amount of gas consumption, PG bottle pressure also varies and therefore the flow line pressure gets affected which dictates the availability of fluid mass. Likewise, for the third run, 3 bar flow line pressure sufficed a safe engine operation up to full load range. Other important requirement was to fix up the position of main valve as shown in Fig. 4.7, once the engine reaches maximum or full load condition. This helped in uninterrupted flow pressure ahead of PG orifice meter. Depending on the estimated mass flow rate calculations corresponding to stoichiometry condition, the differential pressure was accordingly adjusted for the given load point in conjunction with engine speed and water column (gas pressure) ahead of regulator. All readings were recorded after engine attained a stable operation corresponding to MBT spark time operation.

4.5 Summary

In this chapter, a systematic development and testing of induction system suitable for bottled PG fuelled IC engine was discussed. The salient points from the induction system developmental activity are given below:

- A closed looping of PG-air mixer with an air-gas regulator was essential to enable stoichiometry engine operation. This type of looping in conjunction with circuit elements provides a dynamic self-adjustment of air to fuel ratio against varying engine loads.
- The performance evaluation of the engine shows that PG operated with brake power of 84.54% as compared to gasoline with an MBT spark timing of 16° BTDC. Further, a power loss of 15% was observed due to 25% lower mixture calorific value of PG against gasoline. These results are in good agreement with literature. A peak pressure of 33 bar against 38 bar of gasoline was observed because of lower product to reactant ratio of PG combustion.
- With the above testing methodology, observations and findings, the induction system suitable for bottled producer gas was designed and tested successfully for the retrofitted CI engine (Babu et al., 2016).

Chapter 5

Influence of Hydrogen and Methane Concentration in Producer Gas Fuelled SI Engine

5.1 Introduction

In the previous chapter, a detailed discussion was presented on experimental set-up of the modified SI engine fuelled by bottled Producer gas. It was also brought out from literature review that extensive research on PG combustion characteristics was required for long-term use in both gas alone and dual fuel mode engine operation (Yaliwal et al., 2014). In this chapter, the influence of hydrogen and methane concentration of PG on various engine response parameters (combustion, performance and emissions) is discussed. The results are compared with the engine parameters for same engine fuelled with CNG and gasoline.

5.2 Variation of H₂ and CH₄ concentration in Producer gas

The moisture content in biomass plays an important role in production of H₂ concentration in a gasifier unit. Generally, the moisture range lies between 14 to 24%. A sun dried biomass approximately contains 14% of moisture level. Generally, 5 to 10% moisture in biomass yields 16% of H₂, and 15 to 25% of moisture content yields 18 to 24% of H₂, with reference to downdraft gasifier, considering air as oxidizing agent. Considering the availability and typical moisture content of biomass used in gasification systems, a comprehensive range of 16 to 22% of H₂ was considered. Furthermore, based on hydrogen production in gasifier and associated equivalence ratios within, the production of methane is directly influenced, as shown by balanced chemical equation 5.1 (Mukunda, 2011), and therefore, a comprehensive range covering 1 to 4% of CH₄ was considered. Assuming no variations in rest of the PG fuel components, hydrogen was varied from 16 to 22%, and methane from 1 to 4% in the experiments, to quantify various engine response parameters. To exercise a precise control on Producer gas composition, bottled PG fuel formulated with mid-

point strategy as discussed in section 3.2.2 of Chapter 3 was considered. Based on mid-point strategy, nine optimal PG blends were formulated resembling design of experiments (2 factors {H₂&CH₄} and 3 levels {Low: Mid: High}: 3² = 9 sets) and listed in Table 5.1. The calculated combustion properties of the PG fuel sets, bottled CNG and gasoline are shown in Table 5.2.

Methanation reaction

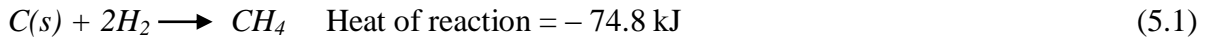


Table 5.1. Formulation of PG fuel sets

| PG composition (% Vol.) | A | B | C | D | E | F | G | H | I | CNG |
|----------------------------|----|------|----|----|------|----|----|------|----|-----|
| Hydrogen | 16 | 16 | 16 | 19 | 19 | 19 | 22 | 22 | 22 | -- |
| Carbon-monoxide | 18 | 18 | 18 | 18 | 18 | 18 | 18 | 18 | 18 | 95 |
| Methane | 1 | 2.5 | 4 | 1 | 2.5 | 4 | 1 | 2.5 | 4 | -- |
| Carbon-dioxide | 12 | 12 | 12 | 12 | 12 | 12 | 12 | 12 | 12 | -- |
| Nitrogen | 53 | 51.5 | 50 | 50 | 48.5 | 47 | 47 | 45.5 | 44 | -- |
| Ethane | -- | -- | -- | -- | -- | -- | -- | -- | -- | 5 |

Table 5.2 Calculated combustion properties of PG blends & other fuels

| Properties | Units | A | B | C | D | E | F | G | H | I | CNG | Gasoline (C ₈ H ₁₈) |
|-----------------------|-------------------|-------|-------|-------|-------|-------|-------|-------|-------|-------|-------|-----------------------------------------------|
| Mol. Wt | g/mole | 25.61 | 25.43 | 25.25 | 24.86 | 24.66 | 24.55 | 24.02 | 23.90 | 23.74 | 16.73 | 114 |
| Density | kg/m ³ | 1.065 | 1.058 | 1.05 | 1.034 | 1.026 | 1.021 | 0.999 | 0.994 | 0.987 | 0.695 | 4.73 |
| (A/F) _{stoi} | kg/kg | 1.028 | 1.189 | 1.36 | 1.133 | 1.308 | 1.484 | 1.276 | 1.438 | 1.614 | 17:1 | 14.7:1 |
| AFT | K | 1800 | 1850 | 1890 | 1850 | 1890 | 1920 | 1900 | 1930 | 1960 | 2230 | 2280 |
| LHV | MJ/kg | 3.850 | 4.318 | 5.066 | 4.224 | 4.742 | 5.257 | 4.738 | 5.204 | 5.717 | 49.88 | *44.4 |
| MHV _{stoi} | MJ/kg | 1.898 | 1.973 | 2.044 | 1.98 | 2.055 | 2.116 | 2.082 | 2.135 | 2.187 | 2.771 | 2.828 |

* adapted from A.M. Shivapuji et al., 2014, Mol.Wt: Molecular weight, AFT: Adiabatic flame temperature, LHV: Lower heating value, MHV_{stoi}: Mixture heating value at stoichiometry.

5.3 Experimental set-up

The schematic view of experimental apparatus is shown in Fig. 5.1. The nine combinations of PG bottles were interfaced with test rig one after the other. The desirable compression ratio 11 was set by varying the thickness of engine head gasket volume as shown in Fig. 5.2. More details on calculations of compression ratios are presented in Chapter 3. The PG bottle flow pressure was set to 2 bar which sufficed for full load engine operation. Further, through flow control valves, the PG flow rate was adjusted for safe and stoichiometry operation. A pressure head of 120 to 180 mm Water Column (WC) was maintained before air-gas regulator to ensure sufficient availability of PG for continuous engine operation, especially during load change or variation. The cylinder walls surface temperature (thus the heat losses) was not accounted in the present work. The other

mandatory arrangements like instrumentation for acquiring engine data are described in chapter 3. The engine performance was also tested for CNG and gasoline fuels.

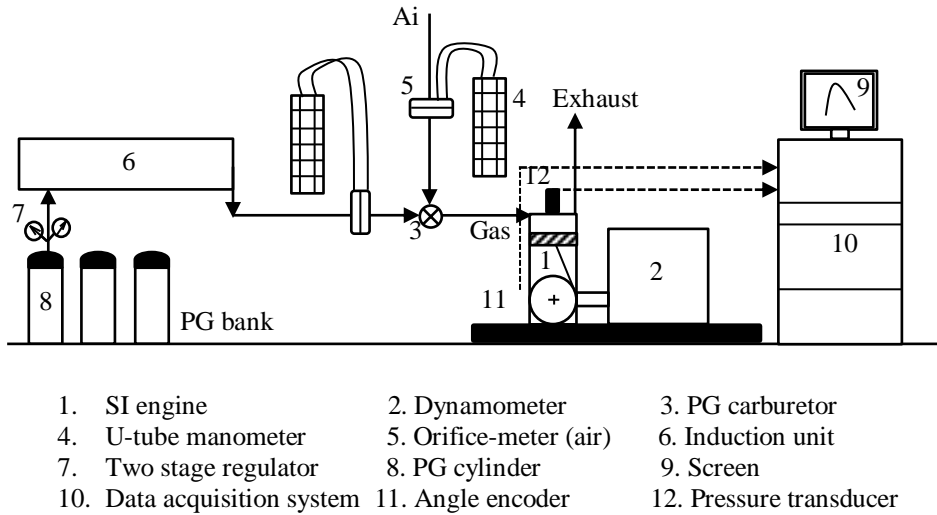


Fig. 5.1 Schematic view of experimental set-up



Fig. 5.2 Head gasket and compression rings for CR:11

5.4 Experimental procedure

In the present work, the combustion pressure traces and their derived parameters are of ensemble average values of 200 consecutive pressure cycles. All experiments were conducted at CR: 11:1, 1500 rpm and close to stoichiometry condition. The engine was tested with steps ranging from no-load, 25%, 33.33%, 50%, 75% and full load against rated dynamometer load of 14 Nm. The experiments were conducted at MBT spark time (minimum spark advance for best torque) through spark sweep test as discussed in Heywood, 2011. Pollutants like CO, HC and NO were measured through AVL-444 Digas analyzer (five gas analyzer) as discussed in

Chapter 3. The flue gas analyzer was interfaced to engine tail pipe. The flue gas sampling system as shown in Fig. 5.3 was designed and fabricated as per the emission standards.



Fig. 5.3 Flue gas sampling system

Table 5.3 Load carrying ability of PG blends

| PG blend | Stoichiometry mixture heating value (MJ/kg) | Maximum supported load (Nm) | Variation against rated load (14Nm) |
|----------|---------------------------------------------|-----------------------------|-------------------------------------|
| A | 1.89 | 11.10 | 79.28 % |
| B | 1.97 | 10.8 | 77.14 % |
| C | 2.04 | 11.8 | 84.28 % |
| D | 1.98 | 11.50 | 82.14 % |
| E | 2.05 | 11.80 | 84.28 % |
| F | 2.11 | 10.90 | 77.85 % |
| G | 2.08 | 11.60 | 82.85 % |
| H | 2.13 | 11.70 | 83.57 % |
| I | 2.18 | 12.10 | 86.42 % |
| CNG | 2.77 | 12.70 | 90.71 % |
| Gasoline | 2.82 | 12.73 | 90.42 % |

Peak supported load for each PG blend

The load carrying ability of engine varied from 10.80 to 12.10 Nm against rated load of 14 Nm (translates to 77.14 to 86.4%) as shown in Table 5.3. The NG and gasoline engine was operated upto 12.70 and 12.73 Nm against rated load (14 Nm) for safety reasons. A maximum power loss of 14% was observed against NG. This power loss is attributed to variation in mixture heating value of respective fuels against baseline fuels as shown in Table 5.2

5.5 Analysis of engine performance parameters

5.5.1 Brake specific fuel consumption (BSFC)

From Fig. 5.4, it is observed that the curves approach minimum values of BSFC with step wise increase in engine load at constant speed of 1500 rpm. In the present work, the overall BSFC at 75% load varied from 1.82 to 4.41 kg-gas/kW-hr (variation of 58.7%). This includes estimated BSFC values for F (2.34 kg/ kW-hr) and I of PG fuel sets (1.82 kg/kW-hr). Otherwise H, C and G sets have consumed lowest fuel at 75% engine load and translates to 1.41, 1.49 and 1.56 kg-biomass/kW-hr based on IISc designed gasifier performance (1 kg of biomass = 2.2 kg of producer gas). This indicates that the fuel blends with higher concentration of H₂% have a greater potential to consume lesser amount of fuel, owing to mixture heating value of hydrogen (3.407 MJ/kg) as compared to methane (2.77 MJ/kg) and gasoline (2.82 MJ/kg). Furthermore, the rapid level of flame speed (85% greater than NG) and mixture reactivity of hydrogen (minimum ignition energy 12 times less than that of NG) leads to efficient and quick completion of combustion process. From the above discussion, it is quite clear that, the variation trend of H₂ concentration (16 to 22%) in PG is significant from engine performance view point.

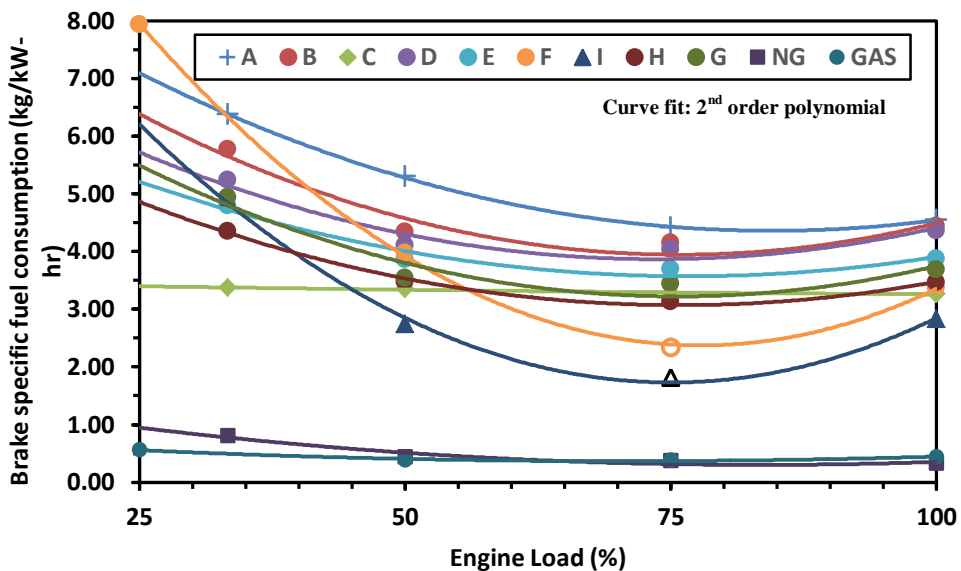


Fig. 5.4 Variation of BSFC (kg-gas/ kW-hr) at CR: 11, 1500 rpm and $\phi \approx 1$

Table 5.5 shows the BSFC values obtained at full, 75% and 50% load points for each of the PG blends, CNG and gasoline. A list of optimal spark time for maximum brake torque and equivalence ratio maintained across each load point is also presented.

5.5.2 Brake specific energy consumption (BSEC)

The variation of brake specific energy consumption for all PG fuel sets and conventional baseline fuels is shown in Fig. 5.5. The 75% load point was found to consume lowest fuel for

unit brake power output as compared to 50% and full load and indicating the maximum energy conversion regime (75% load) for the present engine.

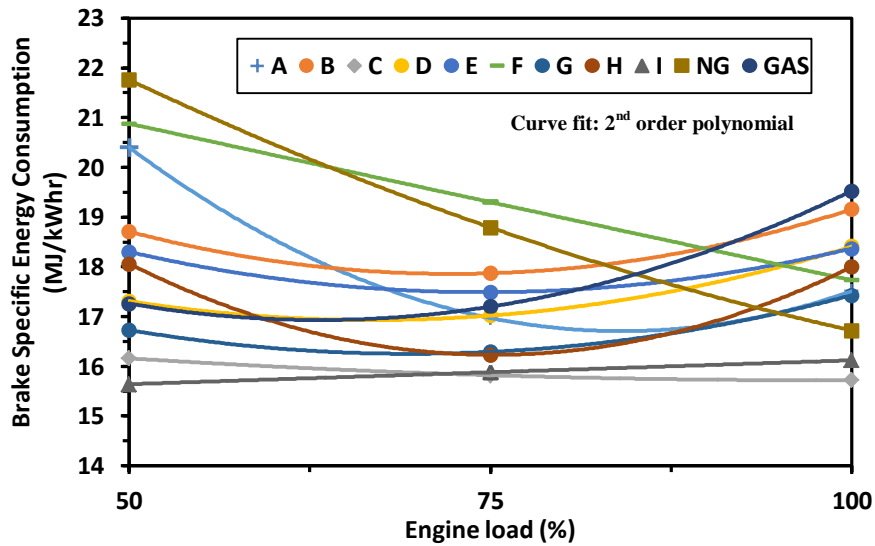


Fig. 5.5 Energy consumption at CR: 11, 1500 rpm

Table 5.4 BSFC and BSEC values of all fuels

| Fuel sets | Phi (ϕ) on (F/A) basis | | | MBT spark time (CA) | | | BSFC (kg-gas/kW-hr) | | | BSEC (MJ/kW-hr) | | |
|-----------|----------------------------------|------|------|------------------------|-----|-----|------------------------|-------|-------|-----------------|-------|-------|
| | Full | 75% | 50% | Full | 75% | 50% | Full | 75% | 50% | Full | 75% | 50% |
| A | 1.09 | 1.07 | 1. | -18 | -19 | -23 | 4.55 | 4.41 | 5.30 | 17.51 | 16.97 | 20.40 |
| B | 1.06 | 0.96 | 1.08 | -18 | -20 | -22 | 4.43 | 4.14 | 4.33 | 19.16 | 17.87 | 18.71 |
| C | 0.94 | 1.05 | 0.99 | -16 | -18 | -20 | 3.26 | 3.28 | 3.35 | 15.72 | 15.82 | 16.16 |
| D | 1.15 | 1.08 | 0.98 | -18 | -19 | -20 | 4.36 | 4.03 | 4.10 | 18.41 | 17.02 | 17.31 |
| E | 1.13 | 1.01 | 1.08 | -15 | -17 | -19 | 3.87 | 3.69 | 3.86 | 18.37 | 17.49 | 18.30 |
| F | 1.16 | -- | 1.17 | -16 | -- | -23 | 3.37 | -- | 3.97 | 17.73 | -- | 20.88 |
| G | 1.15 | 1.02 | 0.98 | -14 | -16 | -19 | 3.68 | 3.44 | 3.53 | 17.43 | 16.29 | 16.73 |
| H | 1.18 | 1.04 | 1.07 | -15 | -17 | -20 | 3.46 | 3.12 | 3.47 | 18.00 | 16.23 | 18.06 |
| I | 0.97 | -- | 0.9 | -15 | -- | -20 | 2.82 | -- | 2.74 | 16.12 | -- | 15.64 |
| NG | 1 | 1.02 | 0.95 | -16 | -22 | -24 | 0.33 | 0.37 | 0.43 | 16.72 | 18.79 | 21.76 |
| GAS | 1.44 | 1.21 | 0.99 | -10 | -17 | -22 | 0.44 | 0.387 | 0.388 | 19.53 | 17.20 | 17.26 |

Furthermore, it is also clear that except F set, all other PG blends consumed less energy for developing comparable thermal efficiencies. The fuel sets F, B and E consumed slightly higher energy as compared to gasoline. The fuel sets G, C and I consumed almost constant energy at all load point with 13%, 15.8% and 15.48% lesser amount of energy, as compared to NG at 75% load. The BSEC values also depict lower consumption of energy except B and E set as compared to NG and gasoline. Therefore, for economic reasons, it is desirable to operate the present PG engine at 75% load point taking advantage of the fuel conversion

efficiency over baseline NG and gasoline fuels. The BSFC and BSEC against MBT spark time is presented in Table 5.4.

5.5.3 Brake thermal efficiency (%)

The effective utilization of supplied thermal energy is quantified by brake thermal efficiency (BTE). With the tested fuels as shown in Fig. 5.6, BTE was found to vary from 18.22 to 22.85 %, 19.16 to 22.73% and 16.46 to 23% at full, 75% and 50% load respectively as shown in Table 5.5. Efficient energy conversion was seen at 75% engine load, however due to lower mixture heating value the BTE values drop on either side of 75% load point.

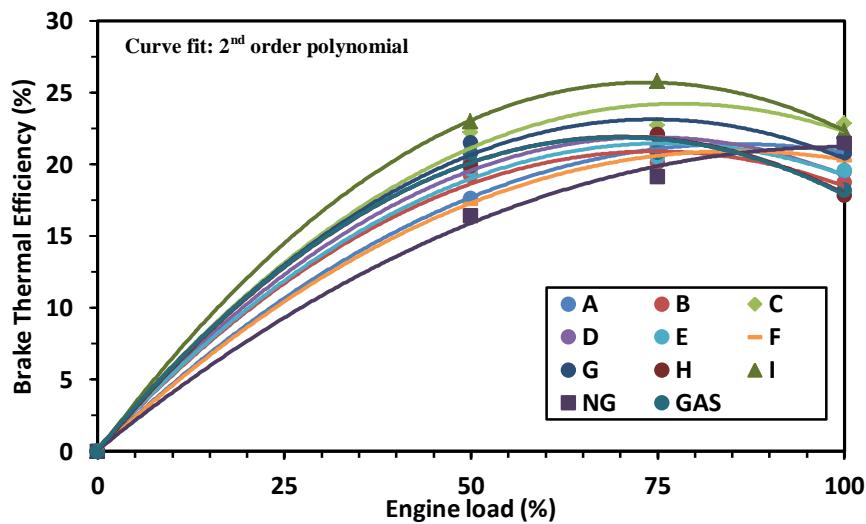


Fig. 5.6 Brake thermal efficiencies at CR:11

The C (16% H₂+4% CH₄), H (22% H₂+2.5% CH₄) and I (22% H₂+4% CH₄) sets have shown potential for achieving higher BTE's, perhaps due to higher heating value of hydrogen (2.38 times greater than methane) and methane (0.12 times higher than gasoline), enabling higher load carrying ability of 7.14% against the rest of PG fuel sets.

5.6 Analysis of combustion parameters

5.6.1 Variation of in-cylinder peak pressure

According to literature, PG fuelled engines have a tendency to undergo variation in their torque values due to variation in fuel composition (Litak et al., 2009). Torque (and therefore power), being an output parameter, is governed by peak in-cylinder pressure influenced by MBT spark time. Thus the study of in-cylinder pressure was important. Table 5.5 shows the MBT spark time and peak pressures for the formulated PG fuel blends. The MBT spark time

through combustion phasing was obtained by spark sweep test (Heywood, 2011) at various loads and constant speed of 1500 rpm. The optimal spark time was observed to retard with increase in H₂% and it is in good agreement with the literature. Load throw-off conditions or drop in engine speed was noticed especially at full loads depending on mixture strength.

Table 5.5 Engine response at 50%, 75% and Full Load for CR:11

| Fuel Set | MBT spark time (°CA) BTDC | | | Peak in-cylinder pressure (bar) | | | Occurrence of peak pressure crank angle (ATDC) | | | Brake thermal efficiency (%) | | |
|----------|---------------------------|----------|----------|---------------------------------|----------|----------|------------------------------------------------|----------|----------|------------------------------|----------|----------|
| | Full load | 75% load | 50% load | Full load | 75% load | 50% load | Full load | 75% load | 50% load | Full load | 75% load | 50% load |
| A | 18 | 19 | 23 | 31.96 | 31.35 | 26.34 | 15 | 14 | 11 | 20.78 | 21.2 | 17.63 |
| B | 18 | 20 | 22 | 31.33 | 31.08 | 24.57 | 15 | 14 | 14 | 18.78 | 20.14 | 19.23 |
| C | 16 | 18 | 20 | 31.39 | 29.41 | 21.99 | 15 | 15 | 14 | 22.85 | 22.73 | 22.26 |
| D | 18 | 19 | 20 | 37.36 | 34.34 | 25.34 | 12 | 12 | 12 | 19.54 | 21.11 | 20.17 |
| E | 15 | 17 | 19 | 34.18 | 32.48 | 24.34 | 15 | 14 | 13 | 19.61 | 20.55 | 19.7 |
| F | 16 | -- | 23 | 33.13 | -- | 26.52 | 15 | -- | 11 | 20.29 | -- | 17.23 |
| G | 14 | 16 | 19 | 35.69 | 33.79 | 26.76 | 14 | 13 | 11 | 20.82 | 22.03 | 21.51 |
| H | 15 | 17 | 20 | 35.87 | 33.67 | 26.30 | 14 | 13 | 11 | 19.93 | 22.11 | 19.91 |
| I | 15 | -- | 20 | 34.84 | -- | 25.26 | 15 | -- | 12 | 22.32 | -- | 23.00 |
| NG | 16 | 22 | 24 | 33.29 | 29.52 | 20.94 | 18 | 17 | 15 | 21.50 | 19.16 | 16.46 |
| GAS | 10 | 17 | 22 | 32.32 | 32.57 | 21.88 | 21 | 16 | 15 | 18.22 | 20.87 | 20.80 |

Where, MBT – Maximum brake torque, GAS – Gasoline, NG – Natural Gas

Fig. 5.7 shows a smooth variation of pressure at full load, 75% and 50% load. The peak pressures shift towards TDC with increase in hydrogen concentration, indicating quick combustion of mixtures due to higher flame speeds of hydrogen (2.5 m/s) compared to methane (0.35 m/s) (Sridhar, 2001). These observations are consistent with the literature (Ceper et al., 2009 and Christodoulou et al., 2013). Differences in maximum pressures of all blends were 6.03, 4.93 and 4.77 bar at full, 75% and 50% engine load respectively. The peak pressures at full load for G, H and I set were 2 to 2.5 bar higher when compared to baseline NG and gasoline.

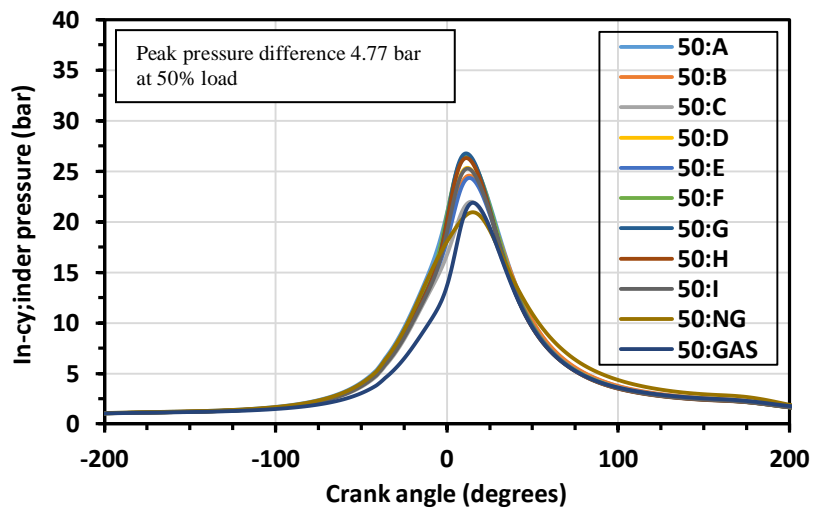
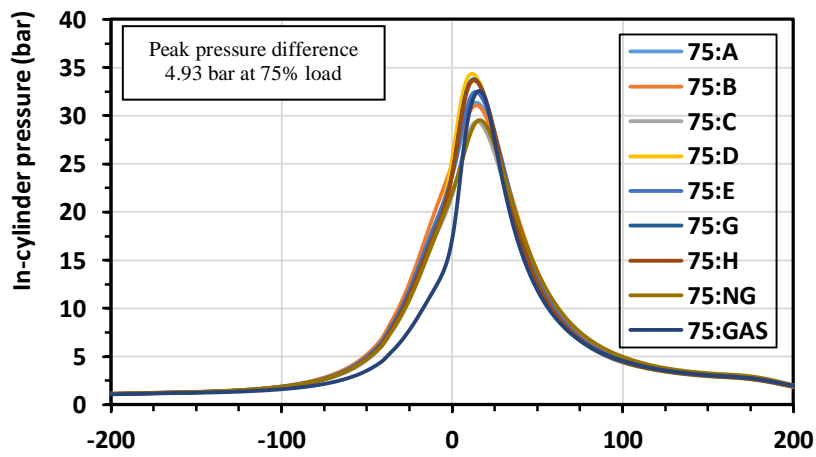
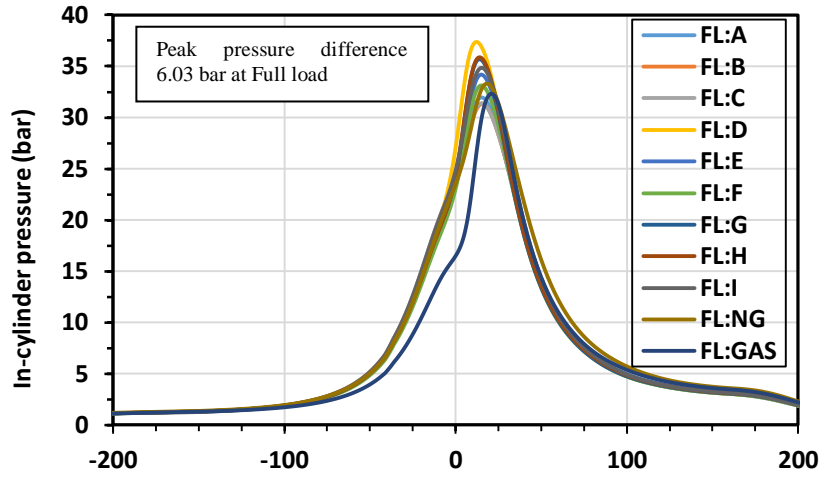


Fig. 5.7 In-cylinder pressure variations at full, 75% and 50% load

5.6.2 Effect of hydrogen (16 - 22%) and methane (1 - 4%) concentration on PG engine

*Analysis at full load point**

- 1) At full load, the effect of 16 to 22% H₂ variation with 1% CH₄ (set A, D and G) resulted in overall 14.45% increase in peak pressure, 19.12% reduction in BSFC, 31% reduction in CO, 42% reduction in HC and 73.5% increase in NO emissions.
- 2) With 2.5% CH₄ (set B, E and H) an overall 12.65% increase in peak pressure, 22% reduction in BSFC, 73% increase in CO, 13% reduction in HC and 91% increase in NO emissions were observed. The increase in CO may be due to dissociation effect at higher engine loads.
- 3) Similarly, with 4% CH₄ (set C, F and I) an overall 9.9% increase in peak pressure, 16.32% reduction in BSFC and 39.5% increase in CO, 25.58% reduction in HC and 84% increase in NO emission was noticed. In summary, a decreasing trend of BSFC and increasing trend of NO emissions with increase in H₂% was observed. However, the variation in IMEP, BMEP and BP was insignificant as shown in Fig. 5.8.

Analysis at 75% load point

- 1) At 75% load point, the effect of 16 to 22% H₂ variation and 1% CH₄ (set A, D and G) resulted in overall 8.70% increase in peak pressure, 22% reduction in BSFC, 51.7% reduction in CO, 29.6% reduction in HC and 39.6% increase in NO emissions.
- 2) With 2.5% CH₄ (set B, E and H) an overall 7.69% increase in peak pressure, 24.6% reduction in BSFC, 27.8% decrease in CO, 34.2% reduction in HC and 87.5% increase in NO emissions were observed. In summary, a decreasing trend of BSFC and increasing trend of NO emissions with increase in H₂% was observed. However, the variation in IMEP, BMEP and BP is negligible as shown in Fig. 5.9.

Analysis at 50% load point

- 1) At 50% load point with reference to Fig. 5.10, the effect of 16 to 22% H₂ variation and 1% CH₄ (set A, D and G) resulted in overall 5.3% increase in peak pressure, 33.3% reduction in BSFC, 88.2% reduction in CO, 39% reduction in HC and 70.4% increase in NO emissions.
- 2) With 2.5% CH₄ (set B, E and H) an overall 7.4% increase in peak pressure, 19.86% reduction in BSFC, 68% increase in CO, 11% reduction in HC and 35.2% increase in NO emissions were observed.

*Note: Detailed discussion on emissions is presented in section 5.7 of page 63.

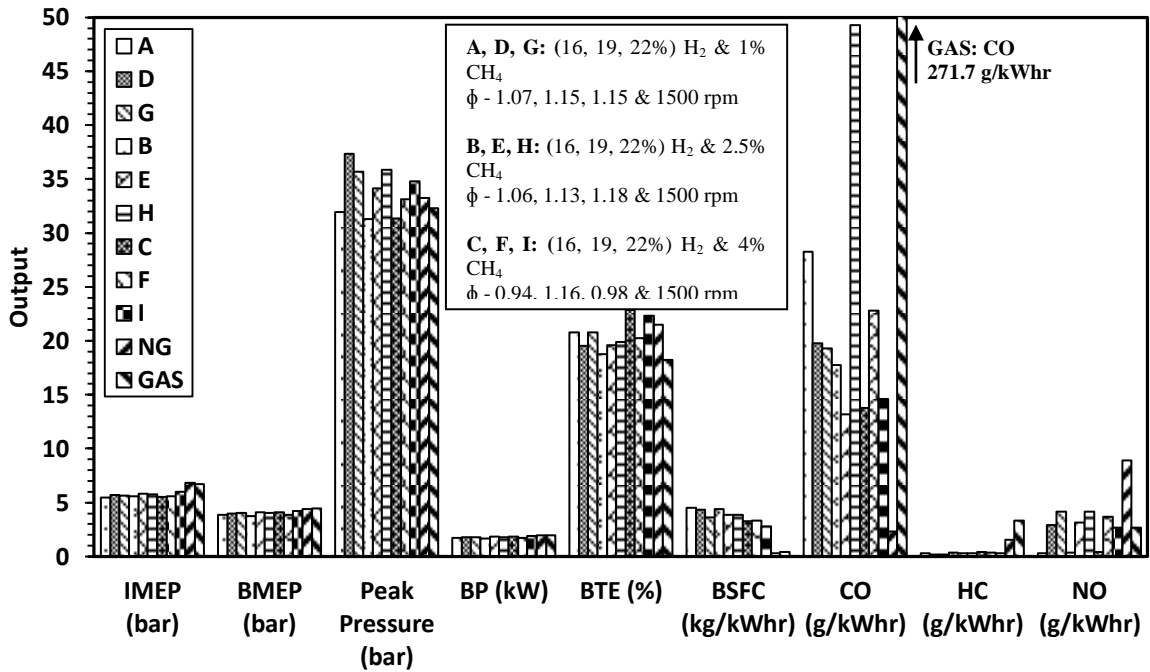


Fig. 5.8 Overall engine response at CR:11, full load for 16 to 22% H₂ and 1 to 4% CH₄

3) With 4% CH₄ (set C, F and I) an overall 17% increase in peak pressure, 18.20% reduction in BSFC, 92.8% decrease in CO, 56% reduction in HC and 82.5% increase in NO emissions was observed. In summary, a decreasing trend of BSFC for all combinations of PG blends, fluctuating CO emissions and slight increase in NO emissions trend with increase in H₂% was observed. However, the variation in IMEP, BMEP and BP and peak pressures is insignificant.

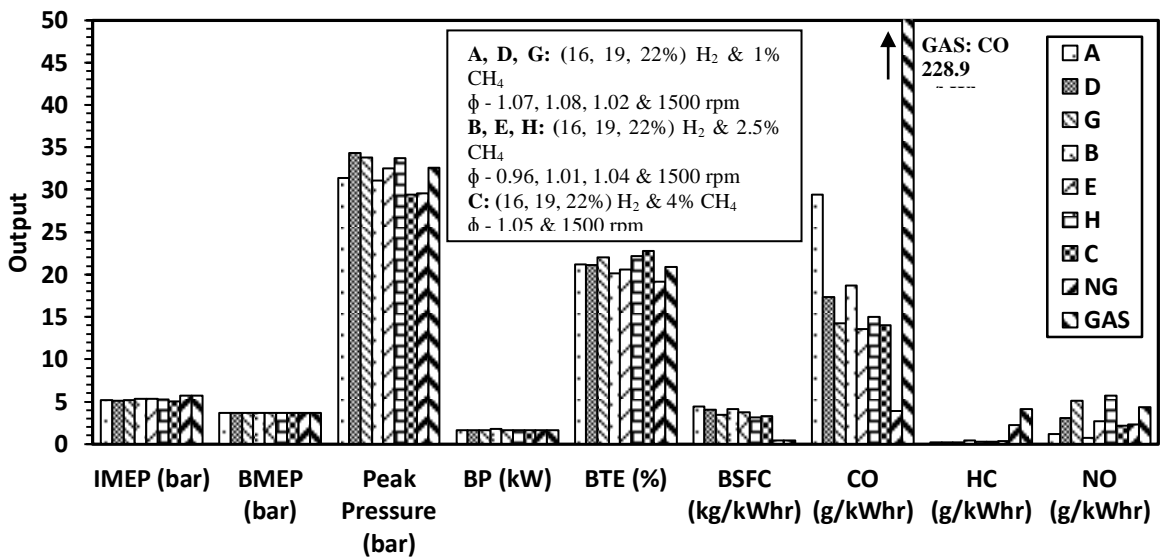


Fig. 5.9 Overall engine response at CR:11, 75% load for 16 to 22% H₂ and 1 to 4% CH₄

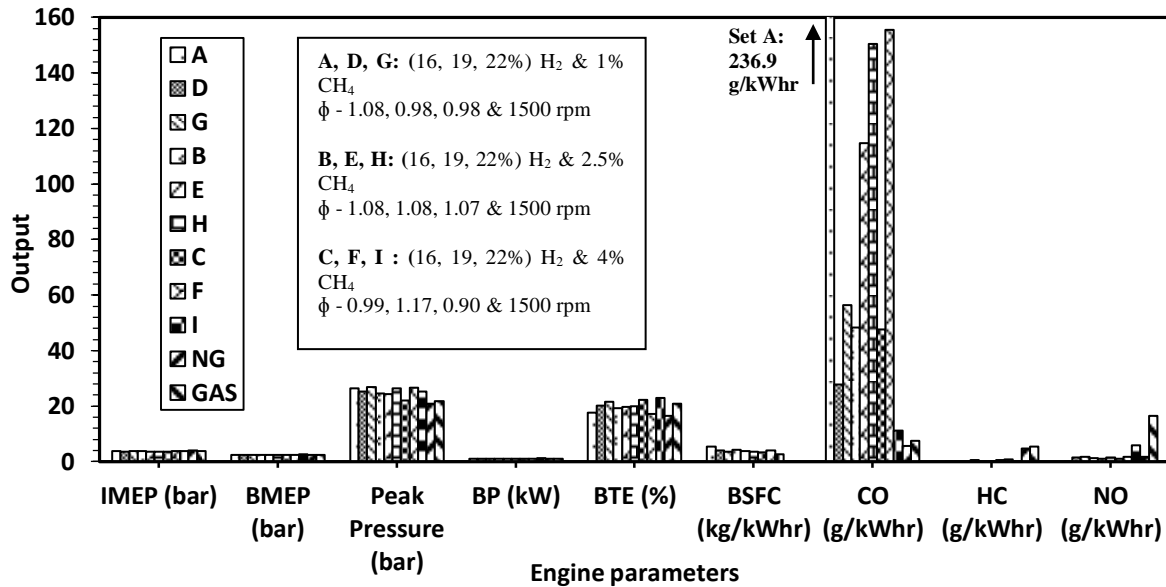


Fig. 5.10 Overall engine response at CR:11, 50% load for 16 to 22% H₂ and 1 to 4% CH₄

5.6.3 Variation of combustion duration (CD)

From the history of mass fraction burnt data, it is observed that the PG combinations with higher H₂% have lower combustion duration (CD). This may be attributed to the presence of O and OH radicals known for accelerating chain reactions and thus completing the combustion process at faster rate (Zhou et al., 2014). In engine combustion process, the initial flame development angle is characterized by 10% MFB point on cumulative heat release curve. For an SI engine, the ignition delay (ID) is mainly associated with chemical process and it is a function of mixture strength, charge pressure, temperature and presence of residual gas. The 10% MFB at CR: 11 ranging from A to I set is shown in Fig. 5.11. The variation of combustion duration at full, 75% and 50% load point is 17.10%, 13.7% and 6.18% respectively. Among the load range, 75% is considered as optimal load point for present engine due to maximum energy conversion in terms of thermal efficiency and minimum fuel consumption. Therefore, analyzing the MFB data at 75% load point reveals that 10% MFB is associated with 28% variation, 50% MFB with 22.5% variation and 90% MFB with 15.85% variation in CD for all combinations of PG blends except F and I set as shown in Fig. 5.12. G and H set undergo least CD at 10% MFB as compared to gasoline, and all PG blends were found to be on lower side of CD at 50% MFB in comparison with NG. Furthermore, 33.3% and 10% variation at overall 10% MFB, 28% and zero at overall 50% MFB and 12.75% and 22.47% at overall 90% MFB variation was observed as compared to NG and gasoline operation. From the above study a crank angle representing 50% MFB can be considered as robust combustion parameter for closed loop control operation.

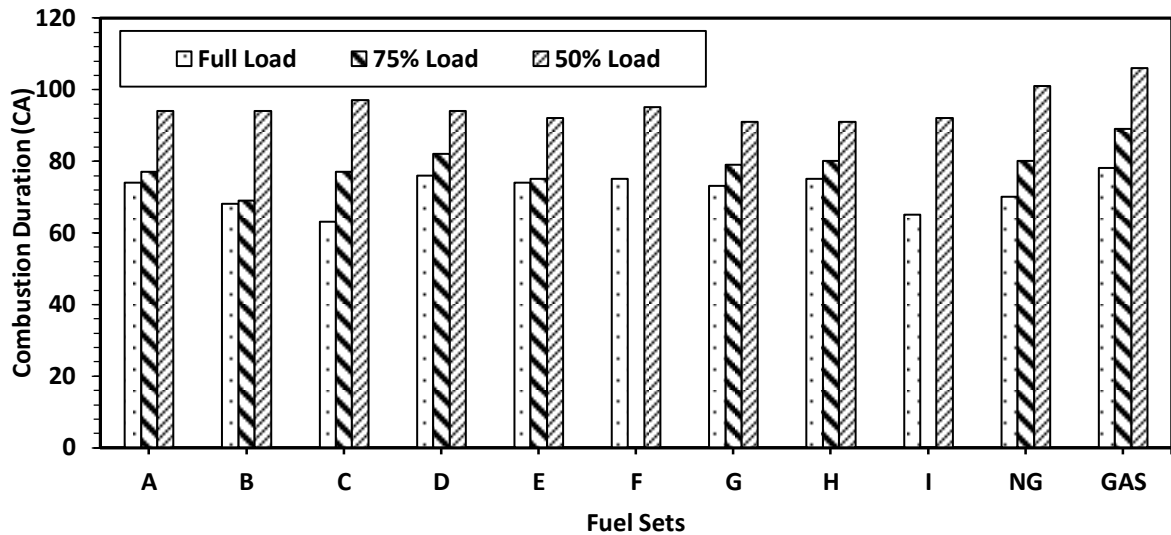


Fig. 5.11 Variation in combustion duration (90% MFB) at full load, CR:11 and 1500 rpm

Along with these findings, the MFB curves were observed to undergo change of slope after 70% MFB. Normally terminal combustion region (around 90% MFB) are known to follow such trend due to near wall quenching phenomena. In present case, the MFB curve undergoes change in slope around 70% MFB. This behavior is attributed to dilution of charge due to internal circulation of residual gas, owing to asymmetrical late valve overlap. This observation forms an additional reason for reduced peak pressures and prolonged combustion durations.

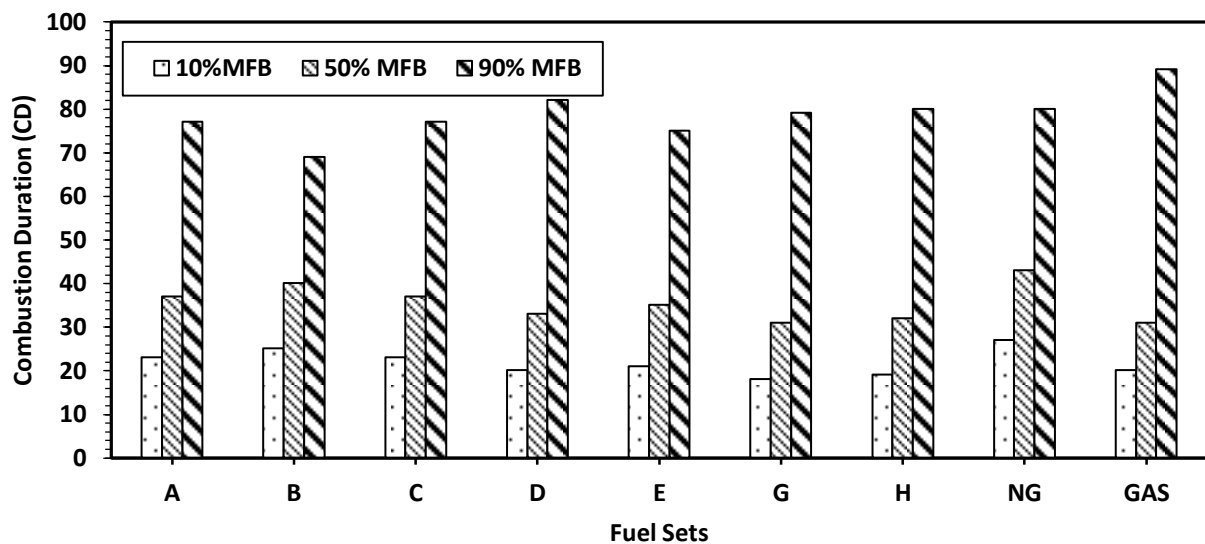


Fig. 5.12 Mass fraction burnt variation at 75% load

5.6.4 Rate of pressure rise (ROPR)

Due to unique combustion properties of hydrogen such as, flame speed and minimum ignition energy (Karim et al., 1996), a variation in combustion process and thus the pressure

rise is expected. Therefore, the rate of pressure rise for all PG blends were estimated as shown in Fig. 5.13 and found to be within 1.35 bar/CA against a knocking limit of 4 bar/CA. Based on this observation, it can be concluded that engine operation was safe without any sign of knock. However, the reason for lower values of $dp/d\theta$ in spite of higher H_2 concentration (22%) may be attributed to the presence of large volume of inert gases ($\approx 55\%$ of CO_2+N_2) in PG fuel sets.

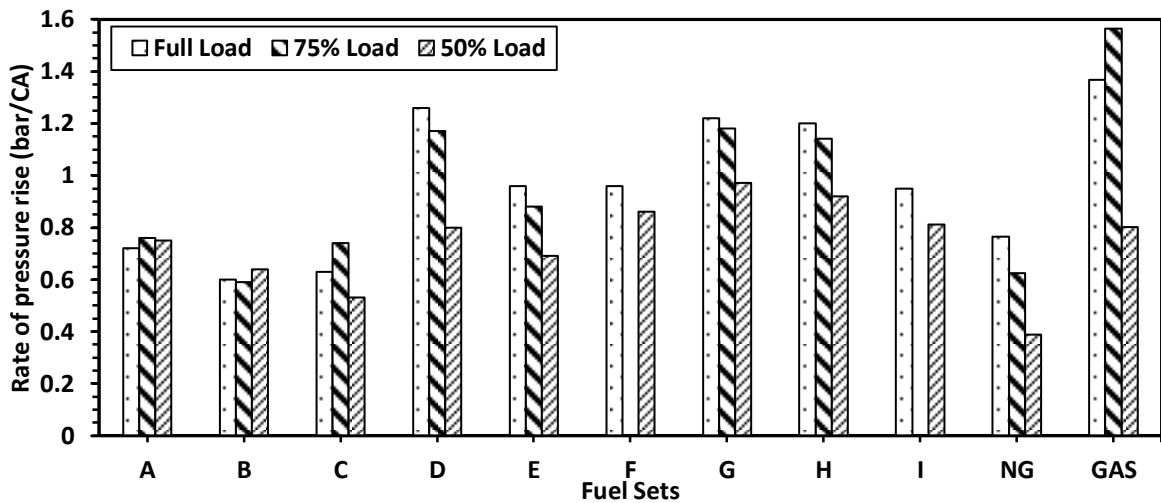


Fig. 5.13 Variation in ROPR at CR:11 and 1500 rpm

5.7 Variation of emissions levels at full, 75% and 50% load points

In the present work, the emissions are compared with Central Pollution Control Board (CPCB - 2016) norms in India. These norms are applicable to converted NG/LPG or gasoline engines used for small ($< 400\text{ cm}^3$) power producing units (gensets).

CO emissions

CO emissions of all fuel sets were found to be well within safe limits of CPCB norms as compared to gasoline but slightly higher than NG as shown in Fig. 5.14. The CO emission of H set was slightly higher, may be due to incomplete combustion at full load owing to fuel rich condition ($\phi=1.15$). This observation on CO emission is in good agreement with earlier work reported (Sridhar et al., 2001). At 75% load point, the CO emissions were well within limits and much lower than full load and 50% load operation as shown in Fig. 5.15 (75% load) and Fig. 5.16 (50% load). A, E, F and H sets gave rise to slightly higher CO ($>100\text{ g/kWhr}$), may be because of incomplete combustion owing to reduced load (7 Nm) and slightly fuel rich operation ($\phi=1.18$). This shows that 75% is the better energy conversion load point as compared to full and 50% load. In summary, CO emissions at all load points were within prescribed limits.

HC emissions

The HC emissions at all load points were well within limits, much lesser than NG/gasoline emissions as shown in Fig. 5.14 and is in good agreement with earlier reported work (Shivapuji et al., 2011). This may be due to efficient combustion process owing to higher diffusivity of hydrogen gas ($0.61 \text{ cm}^2/\text{s}$) as compared to methane ($0.16 \text{ cm}^2/\text{s}$) which generally aids in quick mixing. Further, the rapid combustion processes of hydrogen enriched blends reduce quenching distance and thus lead to much cleaner combustion process (C.G. Bauer et al., 2001).

NO emissions

The NO emissions were found slightly on higher side as shown in Fig. 5.14 for D, E, F and G, H. These fuel sets have 19% and 22% H_2 in common with increasing concentration of CH_4 along with $\phi > 1.1$. This may be attributed to unique combustion properties of hydrogen accompanied with higher adiabatic flame temperature. These observations are coherent with literature (Akansu et al., 2007). At 75% load, G and H set gave rise to higher NO emissions as compared to NG and gasoline operation. At 50% load, very less production of NO was observed as shown in Fig. 5.16. This may be due to reduced cylinder temperatures with engine load. The measured emission values are shown in Table 5.6, 5.7 and 5.8.

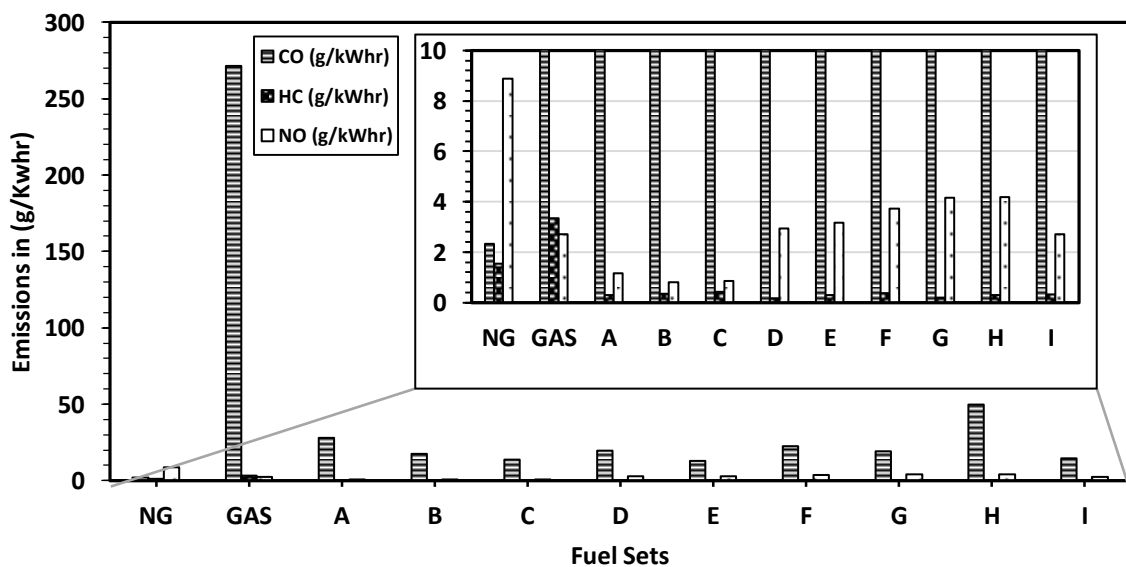


Fig. 5.14 Emissions at full load, CR:11, 1500 rpm

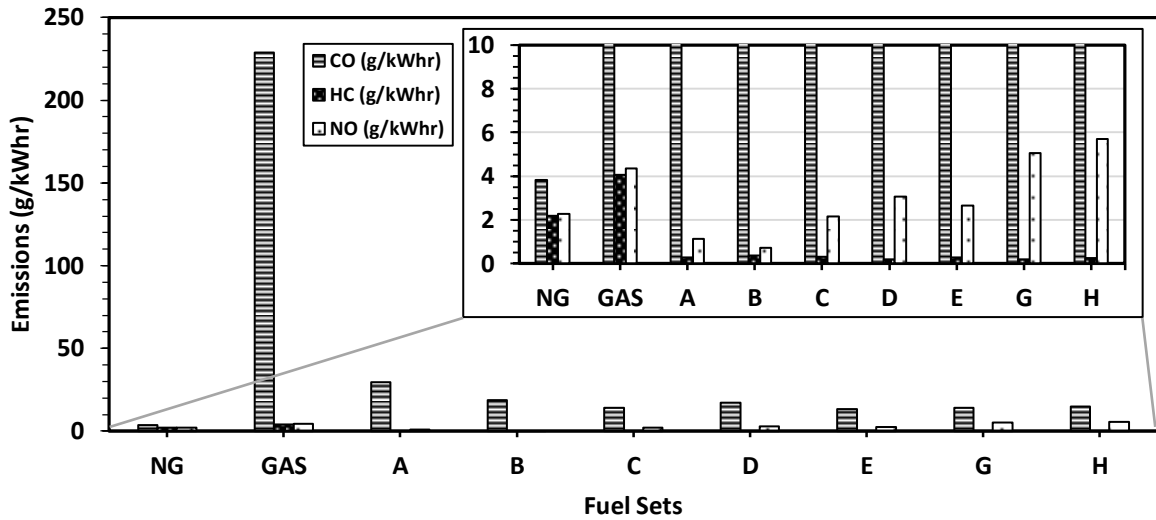


Fig. 5.15 Emissions at 75% load, CR:11, 1500 rpm

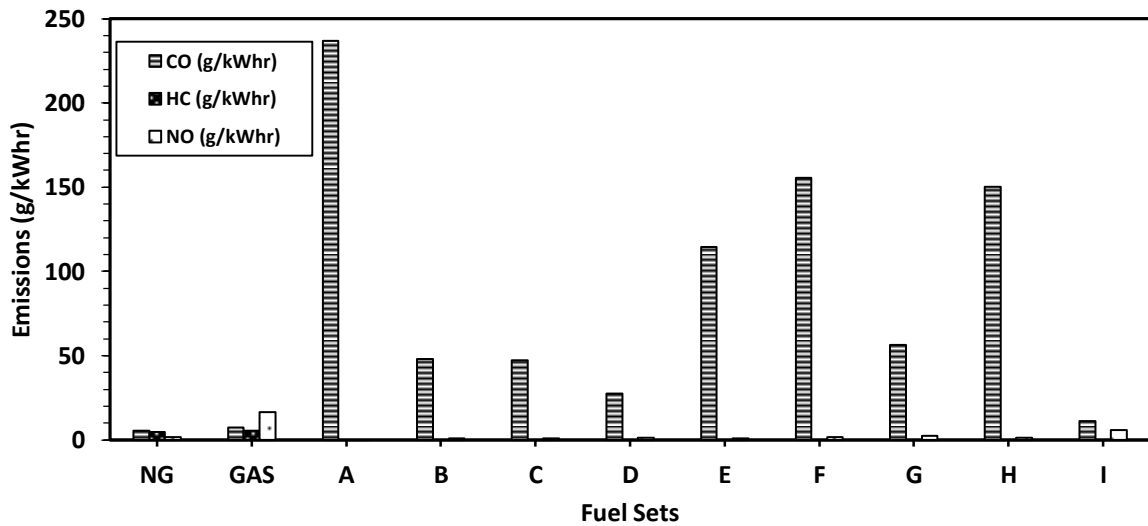


Fig. 5.16 Emissions at 50% load, CR:11, 1500 rpm

Table 5.6 Emissions at full load against CPCB-2016 norms (CPCB-2016)

| Pollutants | CPBP Norms (CNG gensets) | Experimental results (g/kW-hr) | | | | | | | | | | |
|------------|--------------------------|--------------------------------|-------|-------|------|------|-------|-------|-------|------|------|------|
| | | CNG | Gas | A | B | C | D | E | F | G | H | I |
| CO | 250 | 2.33 | 271.7 | 28.3 | 17.8 | 13.8 | 19.76 | 13.2 | 22.81 | 19.3 | 48.8 | 14.6 |
| HC | 8 | 1.56 | 3.36 | 0.31 | 0.36 | 0.43 | 0.18 | 0.313 | 0.37 | 0.20 | 0.31 | 0.32 |
| NO | 8 | 8.9 | 2.72 | 1.158 | 0.81 | 0.87 | 2.95 | 3.17 | 3.73 | 4.17 | 4.2 | 2.72 |

Table 5.7 Emissions at 75% load against CPCB-2016 norms (CPCB-2016)

| Pollutants | CPBP Norms (CNG gensets) | Experimental results (g/kW-hr) | | | | | | | | | | |
|------------|--------------------------|--------------------------------|-------|------|-------|------|------|------|----|------|------|----|
| | | CNG | Gas | A | B | C | D | E | F | G | H | I |
| CO | 250 | 3.84 | 228.9 | 29.4 | 18.7 | 14.0 | 17.3 | 13.5 | -- | 14.2 | 15.0 | -- |
| HC | 8 | 2.18 | 4.07 | 0.27 | 0.38 | 0.32 | 0.20 | 0.28 | -- | 0.19 | 0.25 | -- |
| NO | 8 | 2.27 | 4.36 | 1.13 | 0.709 | 2.16 | 3.06 | 2.65 | -- | 5.07 | 5.7 | -- |

Table 5.8 Emissions at 50% load against CPCB-2016 norms (CPCB-2016)

| Pollutants | CPBP Norms (CNG gensets) | Experimental results (g/kW-hr) | | | | | | | | | | |
|------------|--------------------------|--------------------------------|-------|-------|-------|------|------|-------|-------|------|-------|-------|
| | | CNG | Gas | A | B | C | D | E | F | G | H | I |
| CO | 250 | 5.6 | 7.53 | 236.9 | 48.25 | 47.5 | 27.8 | 114.7 | 155.6 | 56.4 | 150.4 | 11.12 |
| HC | 8 | 4.75 | 5.50 | 0.38 | 0.45 | 0.46 | 0.24 | 0.40 | 0.74 | 0.23 | 0.44 | 0.327 |
| NO | 8 | 1.74 | 16.43 | 0.44 | 1.15 | 1.03 | 1.49 | 0.92 | 1.64 | 2.64 | 1.42 | 5.9 |

5.8 Summary

In this chapter, the effect of variation in hydrogen and methane concentration of producer gas on engine at compression ratio 11 and 1500 rpm was discussed. Based on the experimental results and analysis, the optimal spark time was found to retard with increase in H₂ concentration owing to higher flame speed of H₂.

The MBT ignition time for 9 combinations of PG blends varied from -18 to -14 °CA, -20 to -16° CA and -23 to -20° CA at full, 75% and 50% load point respectively. PG fuel sets C, G and H were found to consume least fuel at 75% load point (1.49, 1.56 and 1.41 kg-wood/kW-hr equivalent) specific to open top, reburn down draft gasifier. Furthermore, estimated F and I set were observed to be potential candidates for achieving lesser fuel consumption (\approx 1.06 and 0.82 kg-wood/kW-hr). From BSEC view point at 75% load, except B and E set rest of the PG blends consumed lesser energy as compared to NG and gasoline. The BTE at 75% load point were found to be within 20 to 23% as compared to 19.16% (NG) and 18.22% (gasoline). The PG fuel sets with higher H₂ concentration produced higher thermal efficiencies due to improved combustion process owing to higher mixture reactivity. The effect of hydrogen and methane concentration on various engine parameters has shown a decreasing trend in BSFC values which was encouraging. However, a steady rise in NO values were also noted owing to slightly lean and higher in-cylinder temperatures that accounts for complete combustion process. The fuel sets, G (22% H₂+1% CH₄), F (19% H₂+4% CH₄), H (22% H₂+2.5% CH₄) and I (22% H₂+4% CH₄) sets have shown remarkably good outcomes in achieving fuel economy (Babu et al., 2016b).

The ignition delay was found to be shorter as compared to NG and gasoline operation, mainly due to the presence of hydrogen – a combustion accelerator. The rate of pressure rise for all PG blends was within 1.35 bar/CA and thus engine was found to operate under normal condition and knock-free. The study of in-cylinder pressure history revealed a smooth variation of pressure at all load points. The variation in pressure was found to be within

16.21%, 14.70% and 22.22% at full, 75% and 50% load points. The D set was found to generate higher pressure (37 bar) as compared to 33 (NG) and 32 bar (gasoline) at full load. The peak pressure of gasoline was found to be on lower side due to fuel rich operation ($\phi=1.44$) on account of factory settings of carburetor. The burn rate profiles were very encouraging upto 50% MFB duration. Beyond 70% MFB region, a negative change in slope (indicating slow burning process) was noticed due to asymmetrical valve overlap period. Considering the influence of valve timing diagram on combustion process, a need for estimating the burn rate or modelling for combustion characterization exists and forms a part of the future work.

On emission front, pollutants (CO, HC and NO) were measured and compared with CPCB norms in India applicable to CNG gensets. At full load, all the emission values were well within the prescribed norms. However, CO was slightly higher as compared to CNG may be due to dissociation effects but well within limits. This indicated a better energy conversion at this load point and could be attributed to typical and inherent characteristics of the basic engines. At 50% load, the CO emissions were found to be on higher side as compared to CNG and gasoline, may be due to incomplete combustion at low loads.

Chapter 6

Effect of Hydrogen Concentration at Higher Compression Ratios in Producer gas Fuelled SI Engine

6.1 Introduction

In the previous chapter, the effect of hydrogen and methane concentration of PG on engine response parameters was discussed in detail. In this chapter, the effects of hydrogen concentration at higher compression ratios (11:1, 15:1 & 18:1) on various in-cylinder and performance parameters are presented.

6.2 Producer gas fuel formulation for higher CRs

From literature survey, it was found that, many researchers explored PG engine operation at various CR's either to study engine performance, emissions or knocking tendency (Gobbato et al., 2015, Arunachalam et al., 2012 and Sridhar et al., 2001). However, the influence of hydrogen alone in PG at higher CR's was not addressed adequately. In this chapter, the effect of hydrogen on engine response parameters at higher CRs was taken up for investigation. Three sets of PG blends were considered with a lowest limit of 16% and highest limit of 22% with a mid-point of 19% of H₂ as shown in Table 6.1. The calculated combustion properties of fuels are listed in Table 6.2.

Table 6.1 Formulation of PG fuel sets

| PG composition (% Vol.) | A | B | C | CNG |
|-------------------------|------|------|------|-----|
| Hydrogen | 16 | 19 | 22 | -- |
| Methane | 2.5 | 2.5 | 2.5 | 95 |
| Carbon-monoxide | 18 | 18 | 18 | -- |
| Carbon-dioxide | 12 | 12 | 12 | -- |
| Nitrogen | 51.5 | 48.5 | 45.5 | -- |
| Ethane | -- | -- | -- | 5 |

Table 6.2 Combustion properties of fuels

| Properties | Units | A | B | C | CNG | Gasoline (C ₈ H ₁₈) |
|-----------------------------|-------------------|-------|-------|-------|-------|--------------------------------------------|
| Molecular weight | g/mole | 25.59 | 24.71 | 23.75 | 16.73 | 114 |
| Density | kg/m ³ | 1.064 | 1.028 | 0.987 | 0.695 | 4.73 |
| (A/F) Stoichiometry | kg/kg | 1.18 | 1.302 | 1.482 | 17:1 | 14.7:1 |
| Adiabatic flame temperature | K | 1950 | 1980 | 2010 | 2230 | 2280 |
| Lower heating value | MJ/kg | 4.283 | 4.712 | 5.361 | 49.88 | *44.4 |
| Mixture heating value | MJ/kg | 2.226 | 2.289 | 2.382 | 2.771 | 2.828 |

* adapted from A.M. Shivapuji et al., 2014.

6.3 Experimental set-up for higher compression ratio work

Owing to higher Octane Number (100 to 105) of producer gas fuel (Banapurmath et. al., 2009), a higher Compression Ratio (CR) single cylinder, four stroke Compression Ignition (CI) engine was considered and modified to SI mode by replacing the fuel injector with a spark plug. The desirable compression ratios were set by varying the thickness of engine head gasket volume as shown in Fig. 6.1. For further details on calculation of compression ratios, reader may refer to Chapter 3. The compression ratios considered in the present study was 11:1, 15:1 and 18:1. Further, the air cooled engine was equipped with two pedestal fans (forced convection) across engine cylinder as shown in Fig. 6.2, primarily to prevent overheating and engine stalling at higher CRs. The cylinder wall surface temperature (thus the heat losses) were not accounted in the present work. The other mandatory arrangements like instrumentation for acquiring engine data are described in Chapter 3.



Fig. 6.1 Head gasket and compression rings for CR:11, 15 and 18

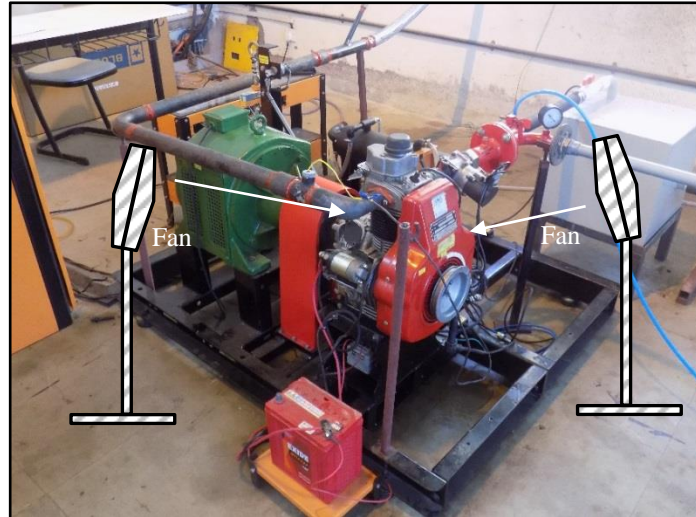


Fig. 6.2 A view of forced convection to support higher CR operation

6.4 Experimental procedure

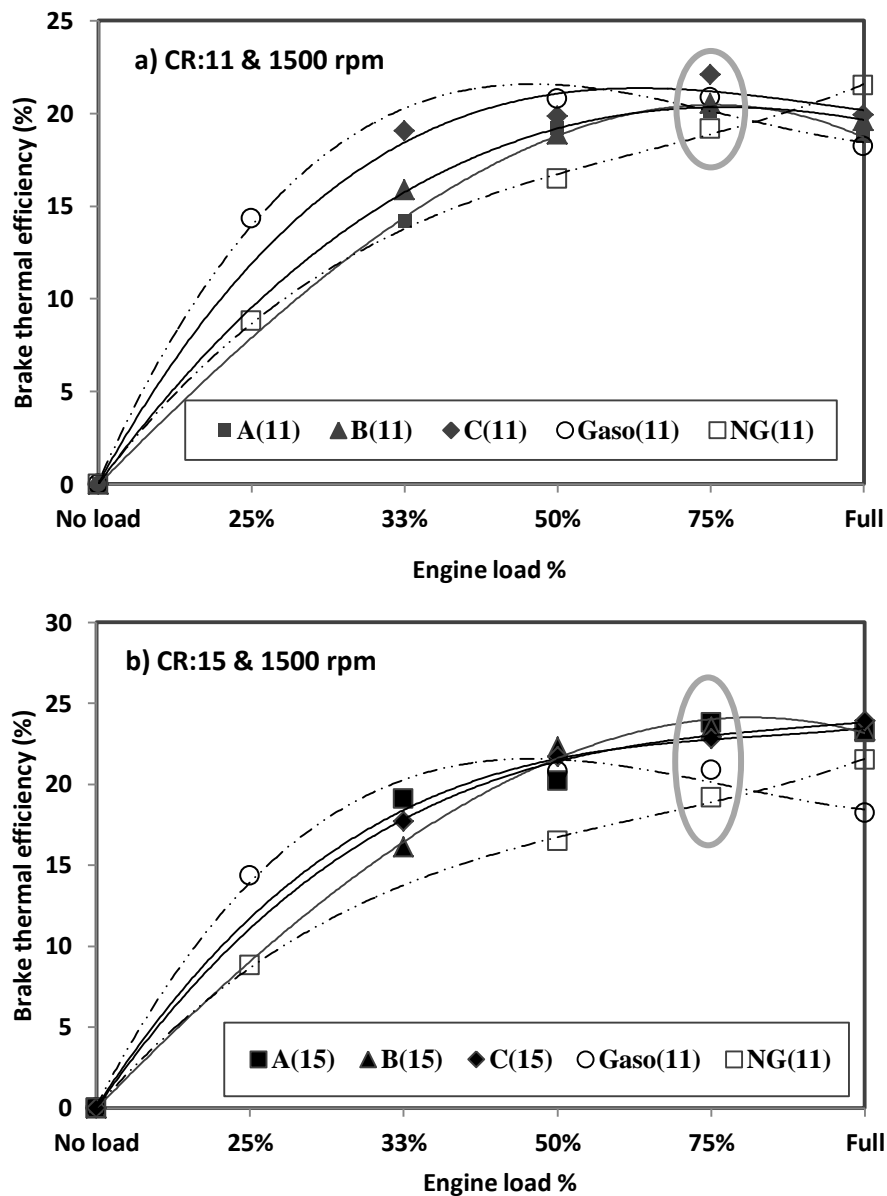
The test rig was interfaced with induction system developed in-house, comprising of few control elements which enable stoichiometry to the engine operation (Babu et al., 2016). For engine operation at CR:11, the two-stage regulator of PG bottle was initially set to 2 bar (gauge) supply pressure. This pressure supply along with throttle valve setting helped in maintaining nearly 150 mm WC flow ahead of air-gas regulator. This arrangement and setting in conjunction with zero pressure regulator, enabled naturally aspirated engine operation. Further, for CR:15 and CR:18, an additional 1 bar pressure was accordingly increased and maintained, to compensate for expanding PG gas, resulting in fall of bottled pressure, and thus affecting the PG density. With this arrangement, all the experiments were conducted ranging from no-load, 33.33%, 50%, 75% and full load engine operation at constant speed of 1500 rpm.

6.5 Analysis of engine performance parameters

6.5.1 Brake thermal efficiencies (BTE)

BTE indicates the effective utilization of supplied thermal energy. Among the tested fuels, for CR: 11, 15 and 18, the overall BTE was found to vary from 16 to 20%, 20 to 24% and 20 to 22.5% respectively as shown in Fig. 6.3abc. 75% load point was found to produce 6% higher BTE as compared to CR:11 and 5% higher as compared to CR:18. Further, PG based fuel sets resulted in 12% and 18% higher BTE as compared to baseline gasoline and NG fuel operation. Efficient utilization of thermal energy was not observed at CR:18 due to

load throw-off conditions experienced beyond 91.66% of rated load (14 Nm). At this load point (91.66%), the peak brake power developed by engine at CR:15 and 18 were identical and therefore similar BTE values were obtained. This is attributable to the basic design of engine used for the testing. Further, the mechanical efficiencies for all three fuel blends at CR:11, 15 and 18 at full load, 75% and 50% load point were in the range of 70 to 64%, 78 to 68% and 77 to 71% of the engine rating respectively. Additionally, the PG engines are generally known to operate with lower volumetric efficiencies (Hagos et al., 2014, Gobbato et al., 2015), owing to its typical A/F ($\approx 1:1$) ratio. All these factors leads to lower energy conversion at higher CR:18. Apart from analyzing thermal efficiencies, a study on fuel consumption trend was also taken up to strengthen the criteria for arriving at optimum CR for present engine on PG operation.



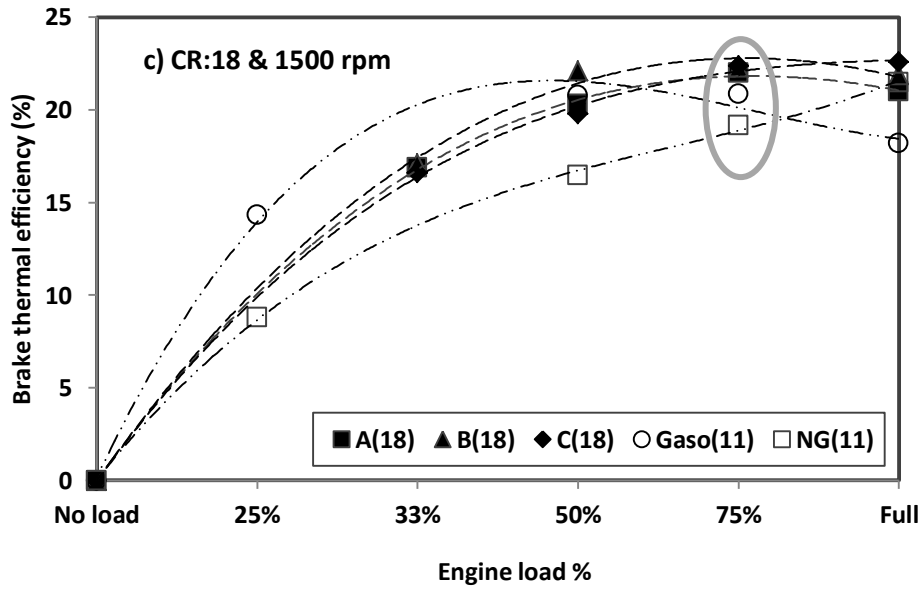


Fig. 6.3abc Brake thermal efficiencies at CR: 11,15 &18

6.5.2 Brake specific fuel consumption (BSFC)

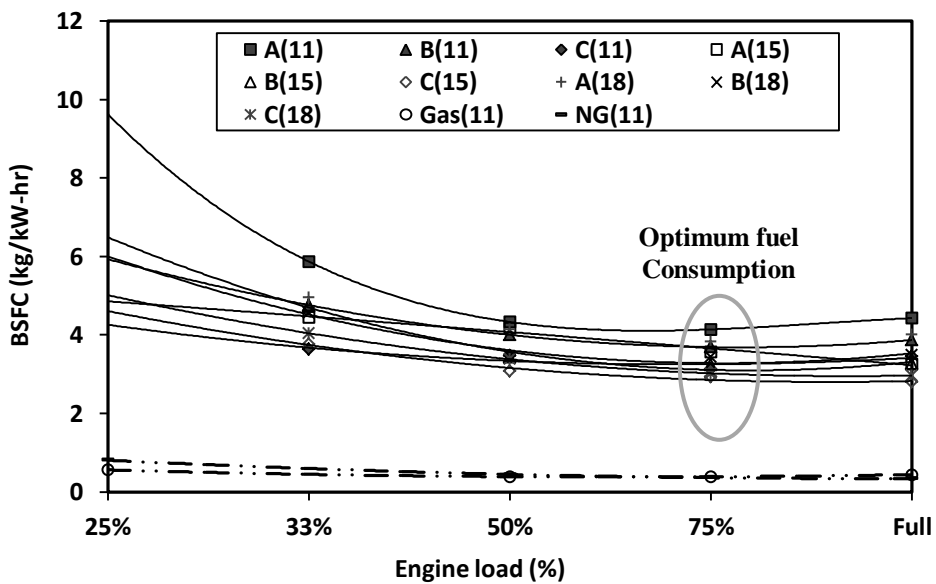


Fig. 6.4 Brake specific fuel consumption at CR: 11, 15 and 18

A study on specific fuel consumption is significant primarily from economic view point. For applications like transportation and power generation the economics are quite important in making decisions for long term utilization. Normally an engine is known to consume minimum fuel at MBT spark time. Therefore, a study on the influence of optimal spark on PG mixtures with steady increase in $H_2\%$ was taken up. From Fig. 6.4, it is observed that the curves approach minimum fuel consumption point with reference to step wise increase in the engine load. Among the fuel blends, C set at CR:15 has consumed the least fuel followed by

CR:18 and 11. Based on the minimum specific fuel consumption data and higher thermal efficiencies at 75% engine load point, CR:15 was considered as the optimum compression ratio for the present engine. Approximately 85% difference in fuel consumption is noticed between PG fuel sets against gasoline and NG owing to vast difference in A/F ratio among fuels. Further, fuel sets with higher H₂% are known to enhance mixture reactivity and thus promote efficient combustion process. Based on BTE and BSFC analysis, CR:15 was considered as an optimum compression ratio for the present engine on formulated PG fuel blends.

6.6 Analysis of combustion parameters

6.6.1 Variation of in-cylinder peak pressures

Study of in-cylinder pressure with crank angle provides significant information on nature of combustion process involved in engine. For CR:11, considering all three fuel blends, the MBT spark time was within 17 to 20° CA BTDC, 15 to 17° for CR:15 and 12 to 13° for CR:18. Further, the field experience has revealed that, the spark time at higher CR's (15 and 18) were highly sensitive. A variation in spark time of $\pm 2^\circ$ CA could abruptly bring engine to halt. This observation suggested for a closed loop dynamic spark time control unit. MBT spark time data is provided in appendix I. A power loss of 15% at CR: 11 and 10% at CR: 15 and 18 was observed against rated power of 2.2 kW. The reason for power loss can be attributed to 9% (average) reduction in product to reactant conversion ratio as compared to NG and 19.6% variation in mixture heating value of PG fuel blends as shown in Table 6.2. With reference to Fig. 6.5, a smooth pressure variation at full load for all compression ratios is observed. The peak pressures of baseline gasoline and NG are comparable to PG fuels at CR:11. This was actually unexpected and may be attributed to reduction in flame speed of gasoline charge on account of fuel rich operating condition ($\phi=1.44$) owing to the settings of gasoline carburetor make.

Further, for NG operation it is attributed to dilution of charge as a result of asymmetrical late valve overlap as shown by Fig. 6.6. Apart from these, the flame speed of PG being 30% higher than NG (methane), a quick combustion process may have resulted in better performance. Further study on this aspect is analyzed and discussed at a later stage with mass fraction burnt (MFB) plots. Referring to Fig. 6.5, at full load for CR:11, the variation of peak pressures of PG fuel blends (A, B and C) was within 31 to 36 bar. Referring to Fig. 6.7, at 75% load and CR:11, all fuels blends including gasoline and NG showed comparable peak

pressures to full load point. This may be due to 6% marginal difference in peak supported load points. At CR:15, no significant pressure variation was observed between PG blends except 8% against full load for B set. However, at CR:18 with full load point, 10% peak pressure variation was noted between A and B set and 8% between A and C sets. From Fig. 6.6 and Fig. 6.7, the peak pressure of C set at CR:18 and full load is 5% lesser than 75% load point due to slightly lean operation ($\phi \approx 0.95$). From the above discussion, 75% load point can be concluded as stable operating load point for the given PG fuel blends. Overall observation for PG fuel blends considering CR:11, 15 and 18 at 75% load point revealed that the difference in combustion peak pressures at three fuel blends were 7.6%, 6.8% and 15.8% respectively.

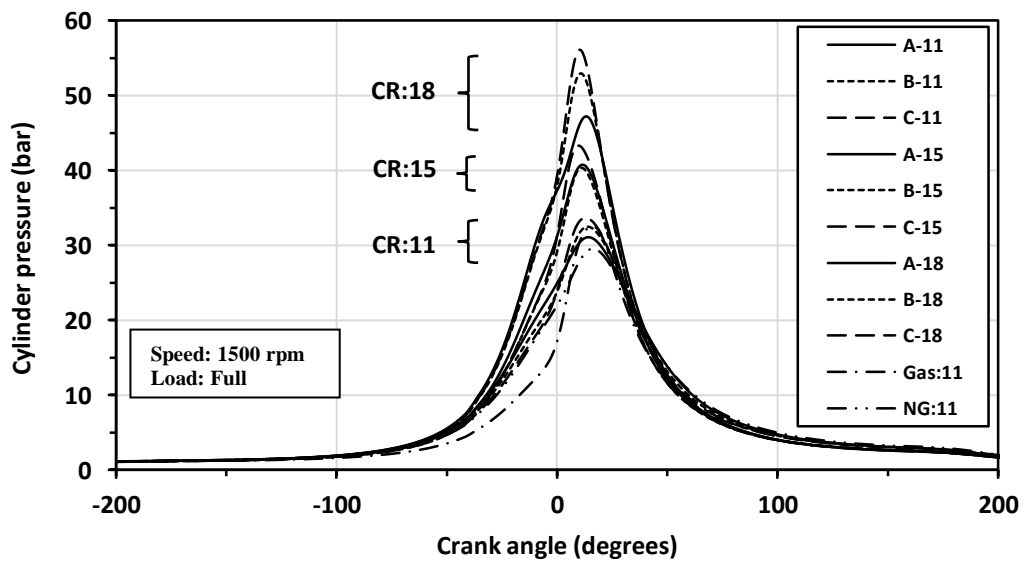


Fig. 6.5 Cylinder pressure variation at full load for various CRs

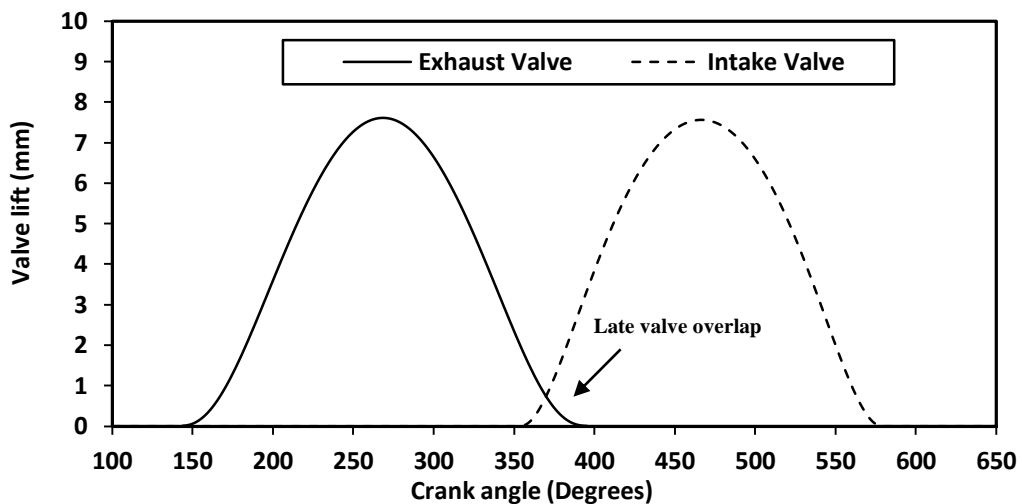


Fig. 6.6 Asymmetrical late valve overlap

This shows that at optimum operating load (75%), there is no significant pressure variation and thus most stable combustion process was achieved with $COV_{imep} < 5\%$. Further, comparing the peak pressure variation across CR:11, 15 and 18 shows an average increment of 2 bar per compression ratio.

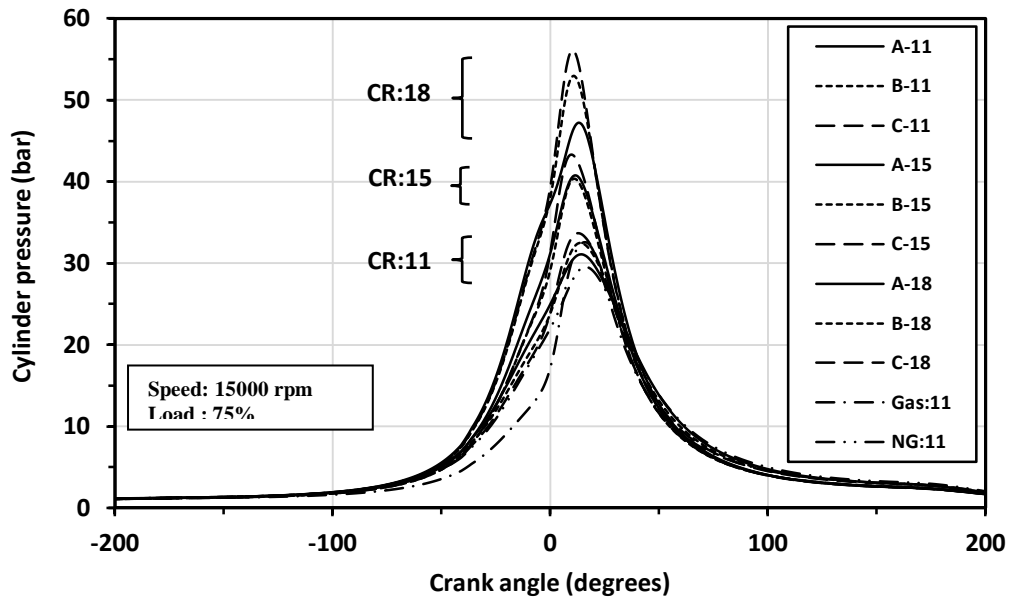


Fig. 6.7 Cylinder pressure variation at 75% load for various CRs

6.6.2 Rate of pressure rise ($dp/d\theta$)

Based on literature review, it is observed that variation in H_2 concentration can potentially alter the combustion process owing to its higher laminar flame speed of 2 m/s against 0.5 m/s of PG at $\phi = 1$ (Sridhar et al., 2003). In this context, a study on rate of pressure rise was taken up to estimate the influence of H_2 (16, 19 and 22% volume) on engine knocking tendency at higher CR's. In the present study at 50%, 75% and full load point, the highest recorded rate of pressure rise did not exceed 2.5 bar/CA. Based on this observation, it may be concluded that the engine operated without any abnormal combustion process. However, the reason for lower values of $dp/d\theta$ in spite of higher H_2 concentration (22%) may be attributed to existence of large amount of inert gases ($\approx 55\%$ of CO_2+N_2) in PG fuel sets. Further detailed study on knocking phenomena is not done in the present work.

6.6.3 Variation of rate of heat release

Rate of heat release (ROHR) is the sole base for development of cylinder pressure and therefore considered as an important parameter in engine combustion analysis. The maximum gross ROHR variation between three PG fuel sets at CR: 11, 15, 18 and at full load are 20%, 7.39% and 3.78% respectively. The variation of ROHR at CR:11 and full load is attributed to variation in A/F ratios across PG fuel blends as depicted in Table 6.3. Further, it is also reported in the literature that, combustion chambers with bowl-in-piston types experience 10% additional heat losses (Heywood, 2011). Another researcher observed that with an increasing amount of H₂% in PG, the heat loss (heat flux) from cylinder walls increases due to higher thermal conductivity of PG mixture, on account of higher H₂% (Shivapuji et al., 2014). These facts further add to reduced performance of PG engines. However, in the present work the heat losses from cylinder walls were not estimated due to the lack of provision to account for temperature measurement on this air cooled engine.

6.6.4 Variation of combustion duration

The study of mass fraction burnt (MFB) indicates the progress of combustion process and events under the regime of overall combustion loop. It is observed that, the PG combinations with higher H₂% have lesser combustion duration (CD) and is in agreement with literature. The parameter which signifies the initial combustion phase is represented by ignition delay (ID) and characterized by 10% MFB on cumulative heat release curve. For an SI engine, the ID is mainly associated with chemical process and it is a function of mixture strength, charge pressure, temperature and presence of residual gas.

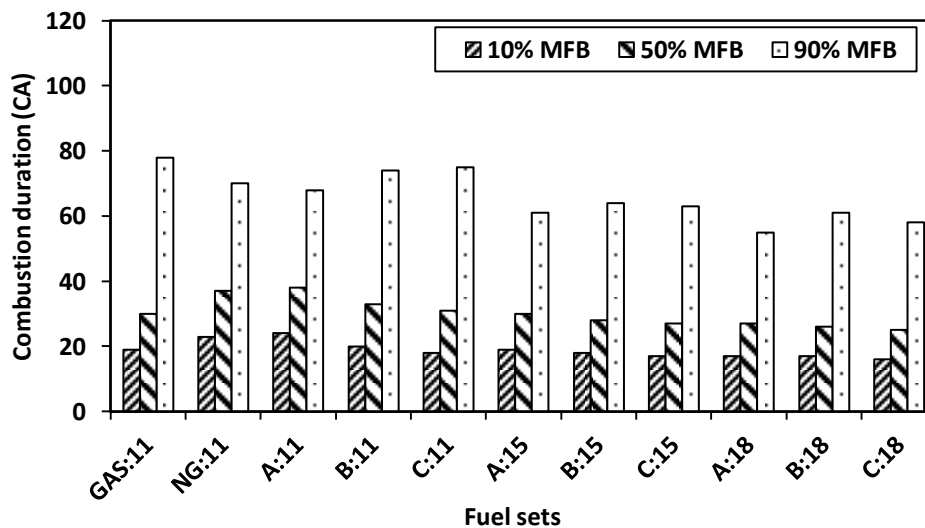


Fig. 6.8 Mass fraction burnt trend at full load

The ignition delay time (CA) at CR: 11, 15 and 18 ranging from A to C fuel sets as shown in Fig. 6.8 are 14%, 10.5% and 5.8%. From Fig. 6.9, the ID at 75% engine load for CR:15 shows a decreasing trend with increasing H₂% and overall CD was comparable to NG operation. Further, comparing all MFB values (from Fig. 6.8, 6.9 and 6.10) at CR:15 and 75% load point shows a uniform 50% MFB values as evident from Fig. 6.9. This suggests that, crank angle at 50% MFB can be considered as a robust combustion parameter for closed loop control operation. Along with these findings, the MFB curves were observed to undergo sharp change in slope after 70% MFB as shown in Fig. 6.11. Normally terminal combustion region (around 90% MFB) are known to follow such trend due to near wall quenching phenomena. In the present case, the MFB curve undergoes change in trend around 70% MFB. This behavior is attributed to dilution of charge due to internal circulation of residual gas, owing to asymmetrical late valve overlap as shown in Fig. 6.6. This observation forms an additional reason for reduced peak pressures and prolonged combustion durations.

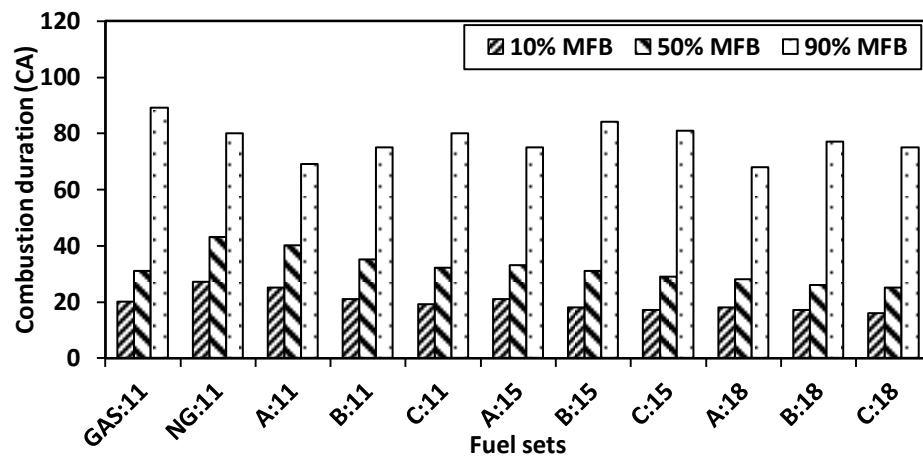


Fig. 6.9 Mass fraction burnt trend at 75% load

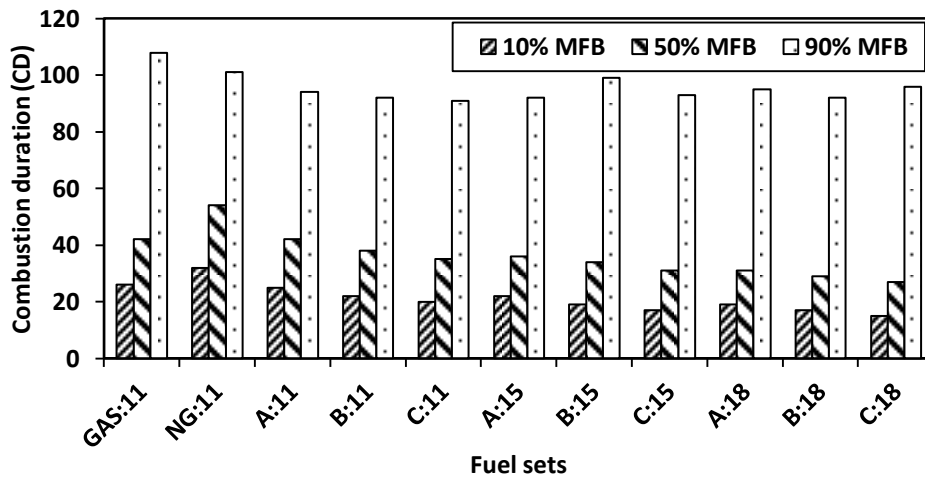


Fig. 6.10 Mass fraction burnt trend at 50% load

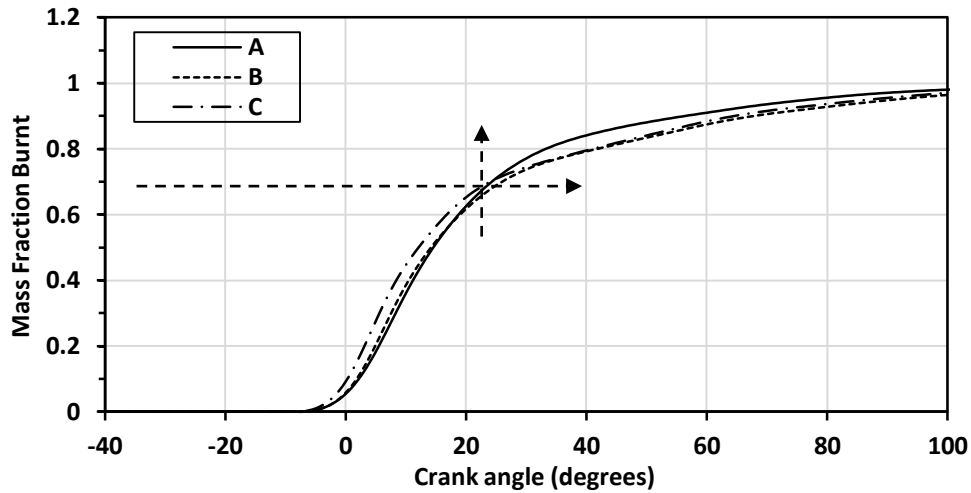


Fig. 6.11 Mass fraction burnt profiles at CR:15 and 75% load point

6.7 Analysis of emissions

6.7.1 CO, HC and NO emissions

The CO emissions were found to be well within permissible limits of CPCB norms as compared to gasoline, but still higher than NG. This observation on CO emission is in good agreement with literature (G. Sridhar et al., 2001). However, the work reported by A. M. Shivapuji et al., 2011, on multi-cylinder engine had resulted higher CO emission and it was attributed to incomplete combustion at higher loads. Further, the CO emission marginally increased with increase in CR. For applications involving fuels like PG, the CO component being one of the main constituents of mixture, there may be a possibility of higher CO emissions, if engine undergoes inefficient combustion process, mostly at higher load points or at fuel rich conditions. Thus for PG operation, medium range speeds seem to be favorable. The HC emission at all PG fuel sets were found to be lesser than gasoline and NG and well within the prescribed limits. These observations are consistent with earlier reported work (Shivapuji et al., 2011). This may be due to efficient combustion process owing to gaseous state of fuels which generally aid in quick mixing and thus lead a much cleaner combustion. The NO emissions were also within safe limits except for C set at CR:15 and 18. This can be attributed to lean operation of engine giving rise to higher in-cylinder temperatures as depicted in Table 6.3. Similar observation was made by G. Sridhar et al., 2001 at MBT operation and CR:13.5 with higher loads. It appears that, the combination of higher H₂% and CH₄ of 2.5% generally promotes quick combustion due to higher reactivity.

6.7.2 Emissions at full load engine operation

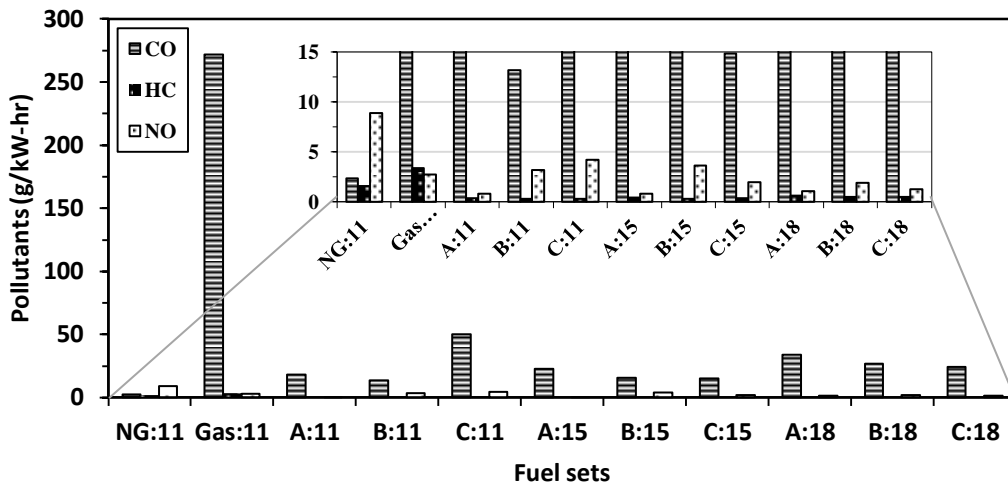


Fig. 6.12 Emissions at full load engine operation

Referring to Fig. 6.12 at full load for CR:11, B set produced lesser CO and HC than A and C set. NO increased steadily as H₂% increased. At CR:15, CO decreased steadily as H₂%, increased but within safe limits. B set produced higher NO compared to A and C set. At CR:18, CO decreased comparatively with increase in H₂% and NO slightly increased for B than A and C set. Overall observation at full load shows that, all the pollutants are within safe limits.

6.7.3 Emissions at 75% and 50% load operation

Referring to Table 6.3 and Fig. 6.13. The NO increased steadily at 75% load point with increase in H₂% at CR:15 and 18. This may be due to higher cylinder temperatures owing to higher CR's. Further, for CR:15 the C set was observed to cross the NO emission limit by almost 20% against permissible limit. Similar observation was made at CR:18 as well. This may be attributed to maximum energy conversion at 75% load point owing to engine design and the presence of higher H₂% in C set. Regarding CO emissions, a decreasing trend with increasing load was observed. It is observed that, B set was the best mixture combination in generating lesser emissions comparatively. At 50% load point with CR:11 as shown in Table 6.4, a higher CO trend as compared to 75% and full load point was observed. B set with CR:18 produced lesser CO and higher NO than CR:11 and 15, but within safe limits.

Table 6.3 Emissions at 75% load against (CPCB-2016 norms)

| Pollutants | CPCB Norms | Experimental results (g/kW-hr) | | | | | | | | | | |
|------------|------------|--------------------------------|-------|------|------|------|-------|-------|-------|-------|-------|-------|
| | | CR:11 | | | | | CR:15 | | | CR:18 | | |
| | | NG | Gas | A | B | C | A | B | C | A | B | C |
| CO | 250 | 3.84 | 228.9 | 18.7 | 13.5 | 15 | 22.16 | 21.17 | 18.22 | 33.2 | 24.84 | 21.63 |
| HC | 8 | 2.18 | 4.07 | 0.38 | 0.28 | 0.25 | 0.45 | 0.34 | 0.3 | 0.67 | 0.53 | 0.47 |
| NO | 8 | 2.27 | 4.36 | 0.71 | 2.65 | 5.7 | 1.75 | 4.8 | 9.9 | 1.84 | 5.98 | 9.95 |

Table 6.4 Emissions at 50% load operation

| Pollutants | CPCB Norms | Experimental results (g/kW-hr) | | | | | | | | | | |
|------------|------------|--------------------------------|-------|-------|-------|-------|-------|------|-------|-------|------|-------|
| | | CR:11 | | | | | CR:15 | | | CR:18 | | |
| | | NG | Gas | A | B | C | A | B | C | A | B | C |
| CO | 250 | 5.6 | 7.53 | 48.25 | 114.7 | 150.4 | 65.2 | 91.5 | 98.82 | 90.9 | 25.4 | 129.2 |
| HC | *8 | 4.75 | 5.50 | 0.45 | 0.4 | 0.44 | 0.62 | 0.47 | 0.43 | 0.91 | 0.48 | 0.67 |
| NO | #8 | 1.74 | 16.43 | 1.15 | 0.92 | 1.42 | 1.15 | 1.73 | 3.76 | 1.8 | 4.17 | 7.37 |

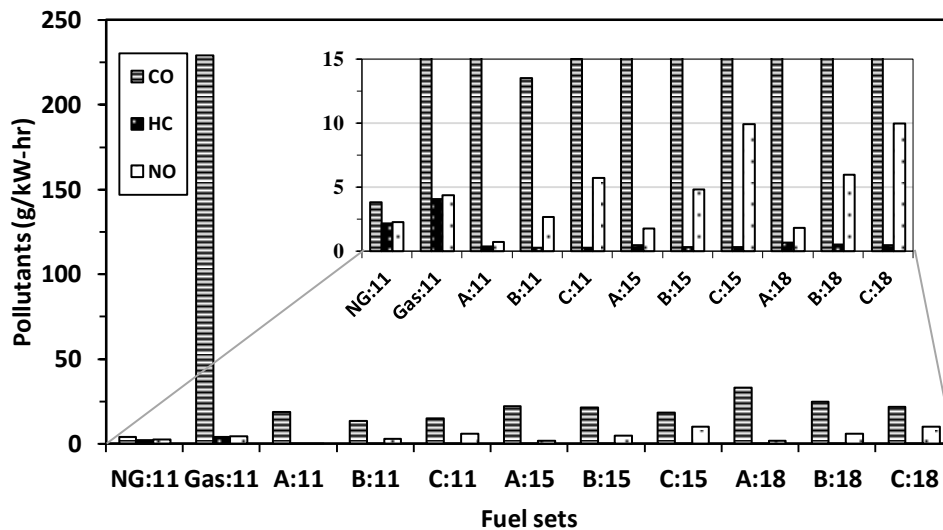


Fig. 6.13 Emissions at 75% engine load

6.8 Summary

In this chapter, the effect of variation in moisture content of biomass leading to variation in H₂ concentration and the influence of higher compression ratios on PG fuelled engine was discussed. Based on the experimental results and analysis, the optimal spark time was found to retard with increase in H₂ concentration owing to higher flame speed of H₂. PG fuel sets B (19% H₂) and C (22% H₂) were observed to promote fuel economy (1.27 and 1.33 kg-wood/kW-hr equivalent) compared to open top, reburn down draft gasifier performance. It was also seen that, the variation of H₂ in the PG mixture blends was favorable in taking up of

higher loads, and resulted in overcoming power loss to the tune of 6% from CR:11 to 15 and 18 due to reduced ignition delay tendency at higher CR's. The rate of pressure rise for all PG mixture blends was within 2.5 bar/CA and thus engine was knock-free. At 75% load point, the COV of IMEP at CR:15 for all PG blends was in the range of 1 to 2% that indicate a stable combustion process. For the optimum CR 15 at 75% load point, 50% MFB crank angle was inferred as a robust combustion parameter for closed loop engine operation. A positive variation in heat release patterns and MFB profiles were noted. However, variation in concentration of H₂ (16, 19 and 22%) was not making significant impact on shaft power output. On emission front, pollutants (CO, HC and NO) were measured and compared with CPCB norms in India, applicable to CNG gensets. At full load for all CRs the emissions were well within the prescribed norms. At 75% load, C set generated slightly higher NO. B set was observed to be the best fuel blend in terms of emissions and engine performance.

Chapter 7

Modeling of Mass Fraction Burn Curves and Parametric Studies

7.1 Introduction

In the previous chapter, a detailed discussion on the effect of hydrogen concentration at higher compression ratios (11:1, 15:1 and 18:1) on PG engine was presented. PG fuel sets B (19% H₂+2.5% CH₄) and C (22% H₂+2.5% CH₄) were observed to promote fuel economy. However, owing to heavy valve overlap in the present modified SI engine, the mass fraction burn curves were observed to be greatly affected (prolonged combustion duration as observed in Fig. 6.11 of Chapter 6). Therefore, modelling of mass fraction burn curves and the parametric studies were taken-up to understand the effect of hydrogen and methane concentration in producer gas.

7.2 Methodology

The modelling study was motivated to mimic the experimental MFB data obtained for all the PG blends. The experimental data presented in Section 5.6.3 of Chapter 5 for full load at CR:11 and 1500 rpm was considered for the present modelling study. For quick reference, the PG blends considered are shown in Table 7.1 and the corresponding combustion properties are listed in Table 7.2. The MFB values were calculated with an in-house developed MATLAB code, based on the well-established Rassweller and Withrow method as described by eq.7.1 (Shayler et al., 1990 & Heywood, 2011).

Table 7.1 Optimal combinations of PG fuel sets

| PG composition (% Vol.) | A | B | C | D | E | F | G | H | I | CNG |
|-------------------------|----|------|----|----|------|----|----|------|----|-----|
| Hydrogen | 16 | 16 | 16 | 19 | 19 | 19 | 22 | 22 | 22 | -- |
| Carbon-monoxide | 18 | 18 | 18 | 18 | 18 | 18 | 18 | 18 | 18 | 95 |
| Methane | 1 | 2.5 | 4 | 1 | 2.5 | 4 | 1 | 2.5 | 4 | -- |
| Carbon-dioxide | 12 | 12 | 12 | 12 | 12 | 12 | 12 | 12 | 12 | -- |
| Nitrogen | 53 | 51.5 | 50 | 50 | 48.5 | 47 | 47 | 45.5 | 44 | -- |
| Ethane | -- | -- | -- | -- | -- | -- | -- | -- | -- | 5 |

Table 7.2 Combustion properties of PG blends

| Properties | Units | A | B | C | D | E | F | G | H | I | CNG | Gasoline (C ₈ H ₁₈) |
|----------------------|-------------------|-------|-------|-------|-------|-------|-------|-------|-------|-------|-------|--------------------------------------------|
| Mol. Wt | g/mole | 25.61 | 25.43 | 25.25 | 24.86 | 24.66 | 24.55 | 24.02 | 23.90 | 23.74 | 16.73 | 114 |
| Phi | Kg/kg | 1.09 | 1.06 | 0.94 | 1.15 | 1.13 | 1.16 | 1.15 | 1.18 | 0.97 | 1.00 | 1.44 |
| Spark | BTDC | 18 | 18 | 16 | 18 | 15 | 16 | 14 | 15 | 15 | 16 | 10 |
| Density | Kg/m ³ | 1.065 | 1.058 | 1.05 | 1.034 | 1.026 | 1.021 | 0.999 | 0.994 | 0.987 | 0.695 | 4.73 |
| (A/F) _{sto} | Kg/kg | 1.028 | 1.189 | 1.36 | 1.133 | 1.308 | 1.484 | 1.276 | 1.438 | 1.614 | 17:1 | 14.7:1 |
| LHV | MJ/kg | 3.850 | 4.318 | 5.066 | 4.224 | 4.742 | 5.257 | 4.738 | 5.204 | 5.717 | 49.88 | *44.4 |
| MHV _{Stoi.} | MJ/kg | 1.898 | 1.973 | 2.044 | 1.98 | 2.055 | 2.116 | 2.082 | 2.135 | 2.187 | 2.771 | 2.828 |

* adapted from A.M. Shivapuji et al., 2014, Mol.Wt: Molecular weight, AFT: Adiabatic flame temperature, LHV: Lower heating value, MHV_{stoi.}: Mixture heating value at stoichiometry.

$$MFB = \frac{m_b(i)}{m_b(total)} = \frac{\sum_{SOC}^{EOC} \Delta p}{\sum_{SOC}^{EOC} \Delta p} \quad (7.1)$$

7.3 Inadequacy of Wiebe single stage function for PG fuel

Literature in the field of combustion modelling was reviewed. It was found that Wiebe correlation was extensively used in zero and one dimensional cycle simulation study both in SI and CI engines. Wiebe model is a well-known mass fraction burn formulation and is a function of shape factor (m) and efficiency factor (a). The combustion parameters like mass fraction burnt (MFB) and rate of heat release (ROHR) are important in research and development of engines to study the overall engine performance, efficiencies and emissions (Yeliana et al., 2008). Miyamoto et al., 1972 used single Wiebe function for predicting the in-cylinder pressure and thermal efficiency of diesel engine. In 1979, Heywood studied the effect of Wiebe function on four stroke SI engine to study the effect of operating conditions on engines performance and NO emissions. Further, specialized applications like TNT explosions was studied by Kuhl et al., 1999, and to generate catalytic conversion efficiency maps (Shaw B., et al., 2002), the single Wiebe function was used. However, single stage Wiebe function was well suited only for limited applications (Ghojel, 2010), mostly dominated by conventional fuels.

Single stage Wiebe function

The single Wiebe function represents the fraction of fuel energy released (mass fraction burnt) against crank angle. The energy released typically takes characteristics S shape in an SI engine. The 'S' shape mass fraction burnt profile is characterized by three parameters namely, (i) Flame development angle – representing the 10% MFB on abscissa, (ii) Rapid

burning angle – representing the combustion duration between 10% to 90% of MFB on abscissa and finally (iii) Overall burning angle – which includes the combustion duration from spark time to 90% MFB. The two coefficients used in Wiebe function, a and m are called as Wiebe efficiency factor and Wiebe form factor respectively. Depending upon the nature of heat release (mass fraction burnt) the coefficients a and m are adjusted to represent the experimental heat release analytically. The single stage Wiebe function is expressed as shown by eq.7.2. For gasoline application, $a = 5$ and $m = 2$ was found to fit the experimental data (B. P Pundir, 2010).

$$x_b = 1 - \exp \left[-a \left(\frac{\theta - \theta_o}{\Delta\theta} \right)^{m+1} \right] \quad (7.2)$$

where, x_b is the mass fraction burnt, θ is the crank angle, θ_o is the start of combustion, $\Delta\theta$ is the total combustion duration and a and m are adjustable parameters.

Recently, Shivapuji et al., 2012, used the single stage Wiebe function for PG application. Owing to thermo-physical properties of PG fuel (due to presence of hydrogen) like heating value, flame speed, adiabatic flame temperature, etc: the heat release curves were different from conventional baseline fuels like gasoline. They observed a change in slope of MFB curve around 50% MFB point and therefore, coefficients a and m were curve fitted accordingly as 2.4 and 0.7.

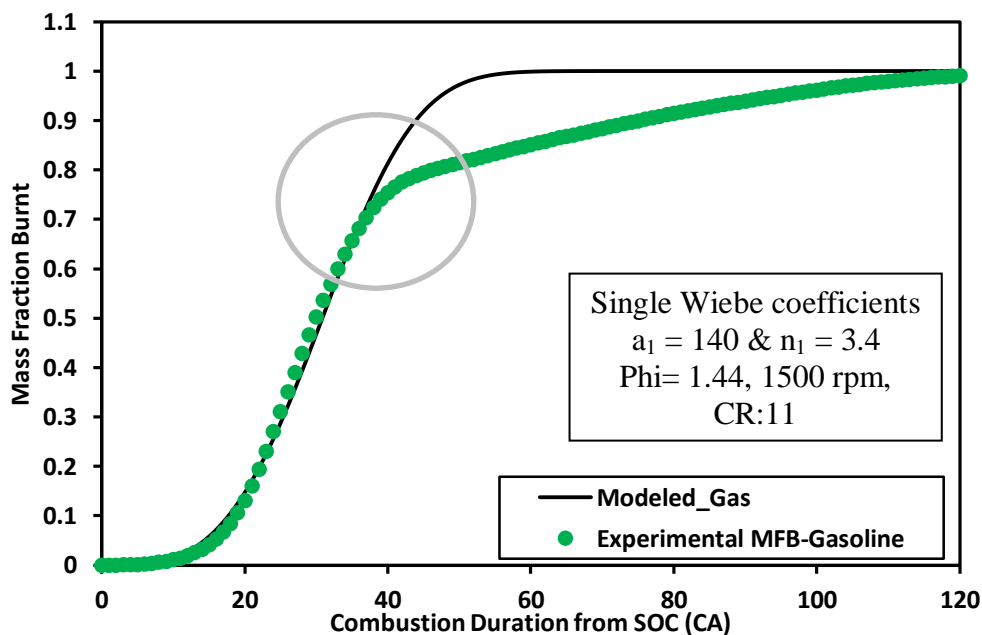


Fig. 7.1 Single Wiebe coefficients for gasoline fuel at full load

However, the exact PG composition for which the MFB curves were analyzed was not clear. The work was carried out on two multi-cylinder engines, one under naturally aspirated mode and the other on turbocharged mode.

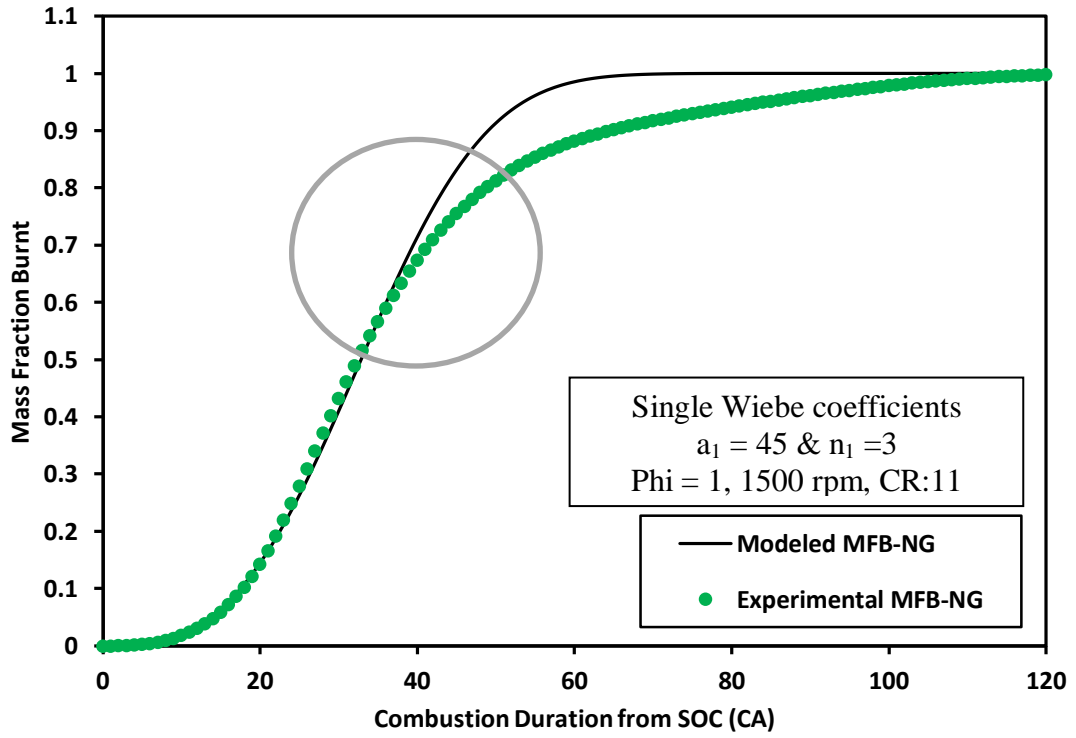


Fig. 7.2 Single Wiebe coefficients for CNG fuel at full load

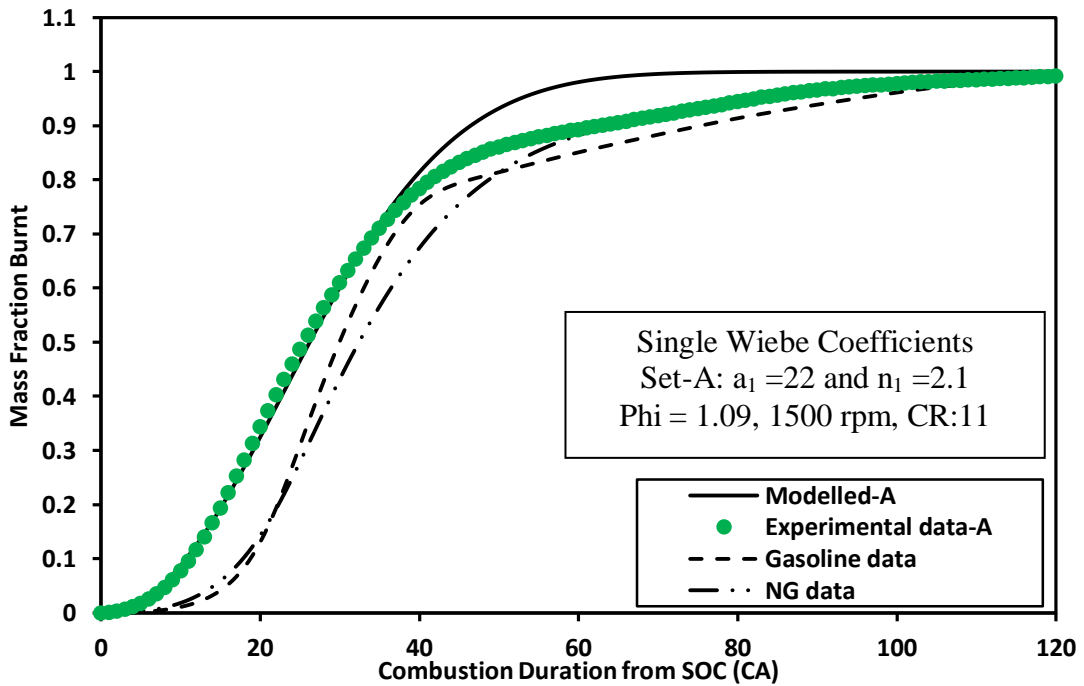


Fig. 7.3 Single Wiebe coefficients for PG: (Set-A) fuel at full load

The engine was operated on gasoline and CNG baseline fuels and PG. From the acquired pressure and crank angle data, the mass fraction burnt curves were analyzed using single stage Wiebe function as shown in Fig. 7.1 to 7.3. Based on the observation from these figures, it is clear that in the present work also the curves have undergone significant change in slope after 50% MFB, indicating a sluggish behavior of combustion process or slow burning of all fuels. The variation in slope is attributed to (i) typical valve lift setting of the engine, since the present engine was modified from CI to SI engine mode, and (ii) unique combustion properties of PG blends. Therefore, based on the above discussion, it is clear that single stage Wiebe function was inadequate to capture the trend and therefore not suitable for the present engine geometry and PG fuel sets.

Influence of valve lift timing on engine operation

The valve lift timing for the present engine is shown in Fig. 7.4. The valve timing depicts a negative asymmetrical overlap period of 41° CA, which typically dilutes the fresh incoming charge by left over residual gases of previous cycle. This argument is further strengthened by observing similar response from gasoline and CNG operation as well as shown in Fig.7.3 Further, a similar observation was reported by Meyer, 2007, when a heavy overlap valve timing engine was operated with gasoline. The researcher proved the inadequacy of single stage Wiebe function to fit the experimental MFB curve as shown in Fig. 7.5. Therefore, from the above discussion, it may be concluded that, irrespective of the fuel used in present engine configuration, the valve lift timing has a significant influence on engine operation and its performance. In literature (Reed, 1988), the optimization of PG engines with reference to valve timing is not sufficiently addressed.

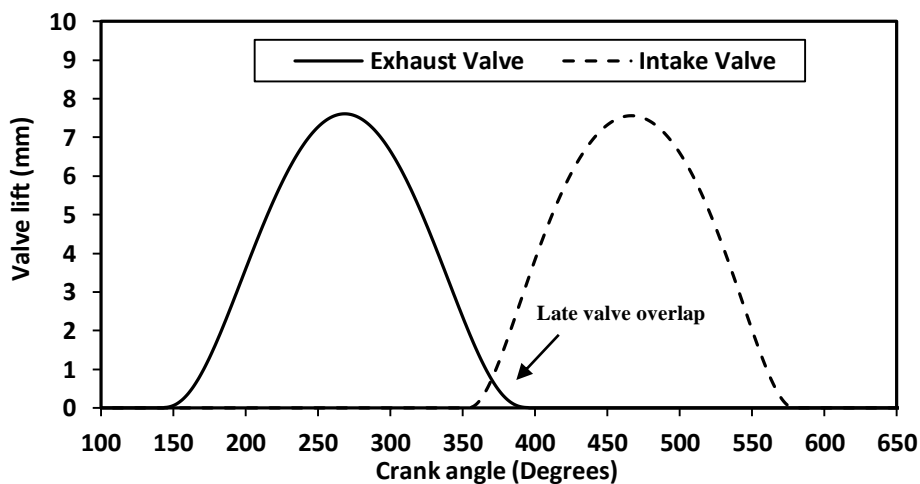


Fig. 7.4 Asymmetrical negative valve overlap

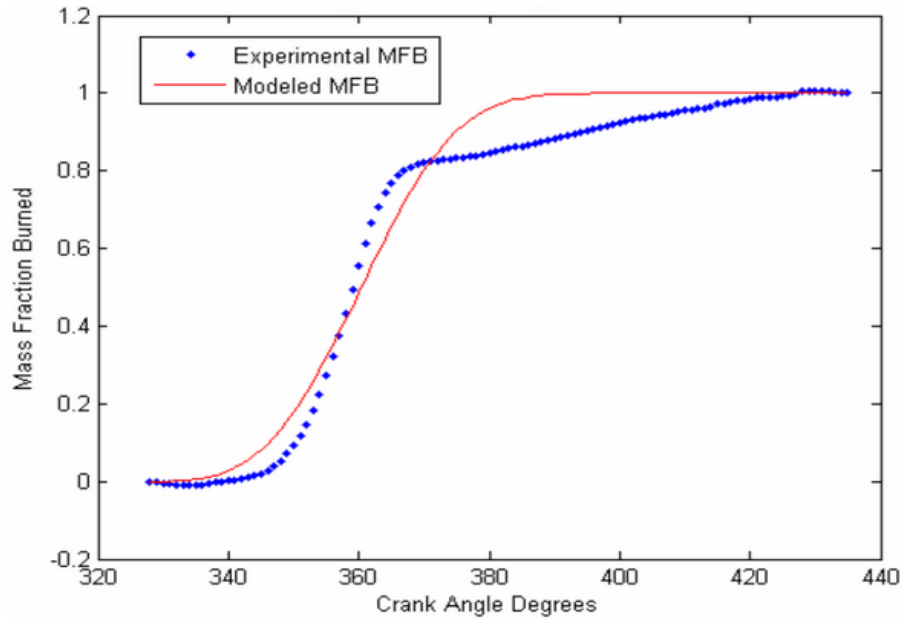


Fig. 7.5 Inadequacy of single stage Wiebe model for heavy valve overlap engines

7.4 Suitability of double stage Wiebe function for PG fuel

Usage of double stage Wiebe function

According to the literature, between 1960 and 1970 the researchers were of the opinion that double stage Wiebe function is more appropriate for diesel engines only (Miyamoto et al., 1972). However, with the advancement in engine technology and also in fuel, the usage of double phase Wiebe function has been extended to dual fuel (NG & Diesel) engine operation (Liu and Karim, 1997), Homogeneous Charge Compression Ignition engines (HCCI) (Firmansyah et al., 2013), Spark ignited CI engines (Hellstrom et al., 2014). Furthermore, the advantage of double phase Wiebe function lies in modelling the complicated mass fraction burnt curves by adjusting the coefficients. For the kind of response shown in Fig. 7.1 to 7.3, a need for modelling the MFB curve in two phases arises, as shown in Fig. 7.6. Therefore, double phase Wiebe function was considered as an ideal model to approximate the MFB trend for fuels like PG. The double stage Wiebe function is expressed by eq.7.3

Double stage Wiebe function

$$x_b = x \left(1 - \exp \left[-a_1 \left(\frac{\theta - \theta_o}{\Delta\theta} \right)^{n_1} \right] \right) + (1-x) \left(1 - \exp \left[-a_2 \left(\frac{\theta - \theta_o}{\Delta\theta} \right)^{n_2} \right] \right) \quad (7.3)$$

where, a_1 , a_2 are model constants, $n_1 = m_1 + 1$ and $n_2 = m_2 + 1$, m_1 and m_2 are index variables and x is a scaling factor.

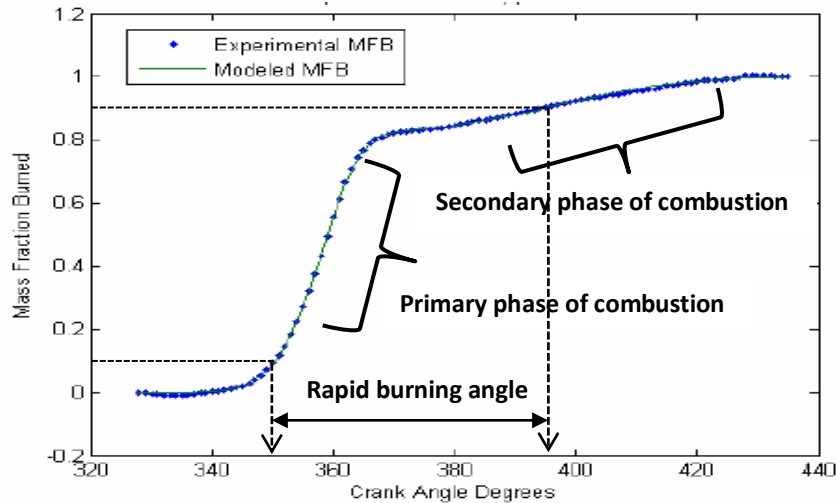


Fig. 7.6 Phases of combustion process

7.5 Result and discussions

In this section, the suitability of double stage Wiebe function for PG fuel is demonstrated considering several PG fuel combinations (set A to I) listed in Table 7.1. Further, the effect of variation in hydrogen and methane concentration on PG combustion process is analyzed through MFB curves. All the MFB data is expressed from the start of combustion (SOC).

Table 7.3 Combustion properties of fuels

| PRM | A | B | C | D | E | F | G | H | I | GAS | CNG |
|-----------------------------------------|------|------|------|------|------|------|------|------|------|------|------|
| Phi | 1.09 | 1.06 | 0.94 | 1.15 | 1.13 | 1.16 | 1.15 | 1.18 | 0.97 | 1.44 | 1.0 |
| Spark Time | 18 | 18 | 16 | 18 | 15 | 16 | 14 | 15 | 15 | 10 | 16 |
| Peak Pr. | 31.9 | 31.3 | 31.3 | 37.3 | 34.1 | 33.1 | 35.6 | 35.8 | 34.8 | 33.2 | 32.3 |
| Experimental MFB values from spark time | | | | | | | | | | | |
| 10% | 12 | 13 | 13 | 10 | 12 | 11 | 10 | 10 | 11 | 19 | 18 |
| 50% | 26 | 27 | 27 | 23 | 25 | 24 | 22 | 23 | 24 | 30 | 32 |
| 90% | 63 | 57 | 54 | 67 | 66 | 66 | 66 | 67 | 57 | 76 | 63 |
| RBA | 51 | 44 | 41 | 57 | 54 | 55 | 56 | 57 | 46 | 57 | 45 |

PRM: Parameter; Spark: °CA BTDC; MHV: Mixture heating value (MJ/kg); Peak Pr.: Peak Pressure (bar); RBA: Rapid burning angle

From Table 7.3, on comparative basis it can be observed that, PG fuel sets with increase in hydrogen concentration consumed 2° CA lesser combustion time for 10% MFB. However, except A, B and C rest of the PG blends consumed similar CA time for completing 50% MFB.

Table 7.4 Curve fitted model constants at full load (Babu, et al., 2017)

| PRM | A | B | C | D | E | F | G | H | I | GAS | CNG |
|-------|------|------|------|------|------|------|-------|-------|------|------|-------|
| x | 0.82 | 0.85 | 0.86 | 0.80 | 0.80 | 0.82 | 0.785 | 0.783 | 0.84 | 0.76 | 0.818 |
| a_1 | 52 | 30 | 35 | 60 | 60 | 66 | 75 | 70 | 65 | 375 | 49 |
| n_1 | 2.43 | 2.31 | 2.35 | 2.26 | 2.41 | 2.35 | 2.38 | 2.35 | 2.45 | 3.77 | 2.93 |
| a_2 | 6 | 5 | 5 | 6.3 | 5.3 | 6 | 5 | 5.7 | 6 | 6.4 | 5.5 |
| n_2 | 3 | 3 | 2.75 | 2.88 | 2.8 | 2.85 | 2.7 | 2.80 | 2.8 | 2.98 | 3 |

where, $n_1 = m_1 + 1$, $n_2 = m_2 + 1$

Table 7.5 Variation of Wiebe model constants

| Model constants | For Gasoline at Full load (J. Meyer, 2007) | Present work at full load for all fuels | Accuracy of constants |
|-----------------|--------------------------------------------|-----------------------------------------|-----------------------|
| x | 0.5 to 0.9 | 0.76 to 0.86 | -- |
| a_1 | 10 to 2000 | 30 to 375 | ± 5 |
| $n_1 = m_1 + 1$ | 3 to 10 | 2.26 to 3.77 | ± 0.02 |
| a_2 | 3 to 37 | 5 to 6.4 | ± 1 |
| $n_2 = m_2 + 1$ | 3 to 9 | 2.7 to 3 | ± 0.02 |

Fig. 7.7, Fig. 7.8 and Fig. 7.9 demonstrate the determinations of model constants through curve fitting based on experimental MFB data. A MATLAB code was written to superimpose the analytical (double stage Wiebe) curve over experimental MFB data and through fine tuning of model constants, their values were predicted. More details of the code is given in Appendix–H. The accuracy of curve fitting through model constants is given in Table 7.5. The PG blends (A, B and C) have same hydrogen concentration (16%) but differ in methane concentration. The parametric studies with blend A, B and C indicates the influence of methane concentration with 16% H₂ on combustion process (thus MFB) and therefore heat release behavior. Similarly, blend D, E and F indicate the effect of methane with 19% H₂ on heat release behavior and finally blends G, H and I indicate the effect of methane with 22% H₂ on heat release behavior. Furthermore, to understand the influence of hydrogen variation with 1% CH₄ on PG combustion process, requires parametric study considering set A, D and G. Similarly, effect of hydrogen variation with 2.5% CH₄ requires parametric study on set B, and H, and finally, hydrogen variation with 4% CH₄ requires parametric study on set C, F and I.

Model constants for Set-A, B and C

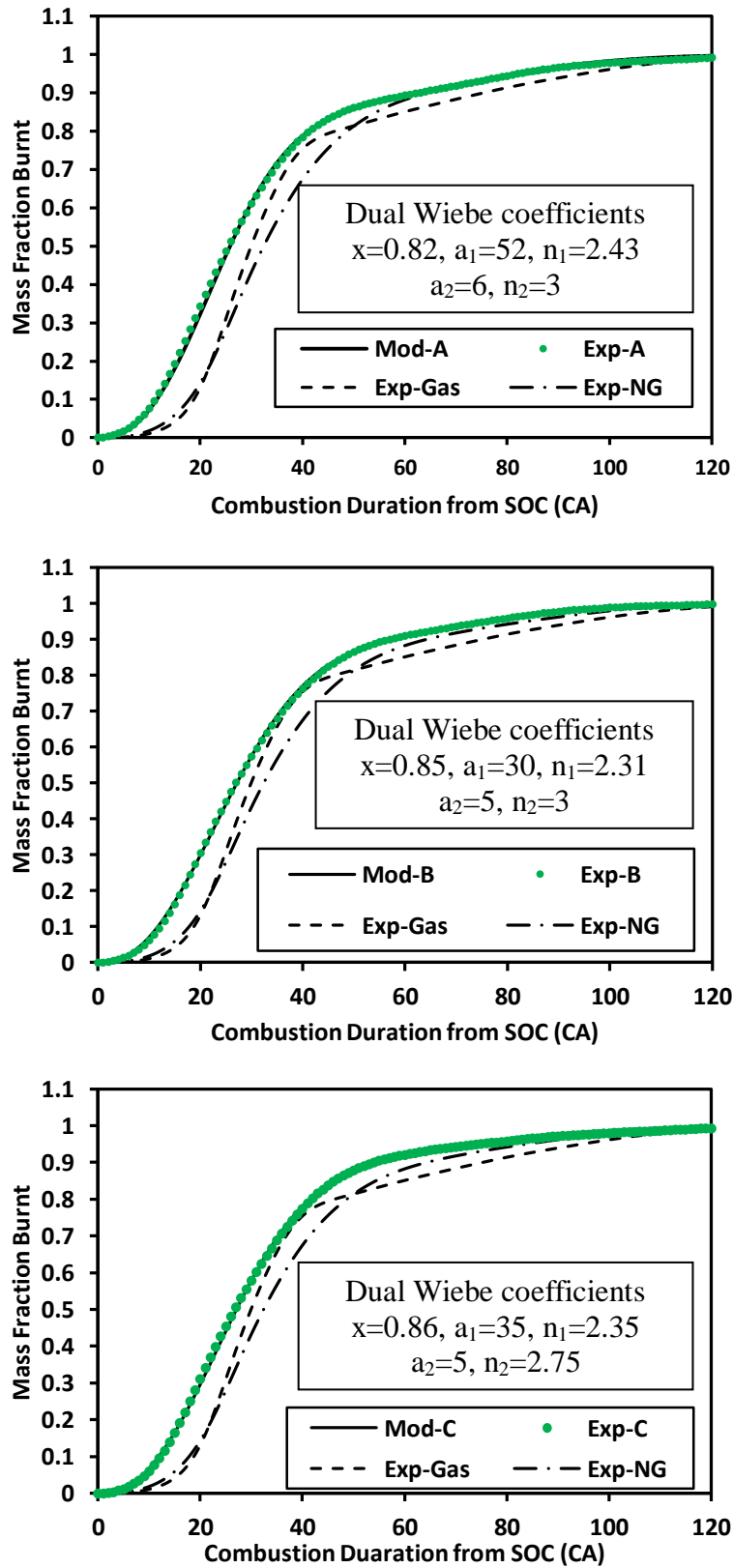


Fig. 7.7 Model constants for PG: Set-A, B and C

Model constants for Set-D, E and F

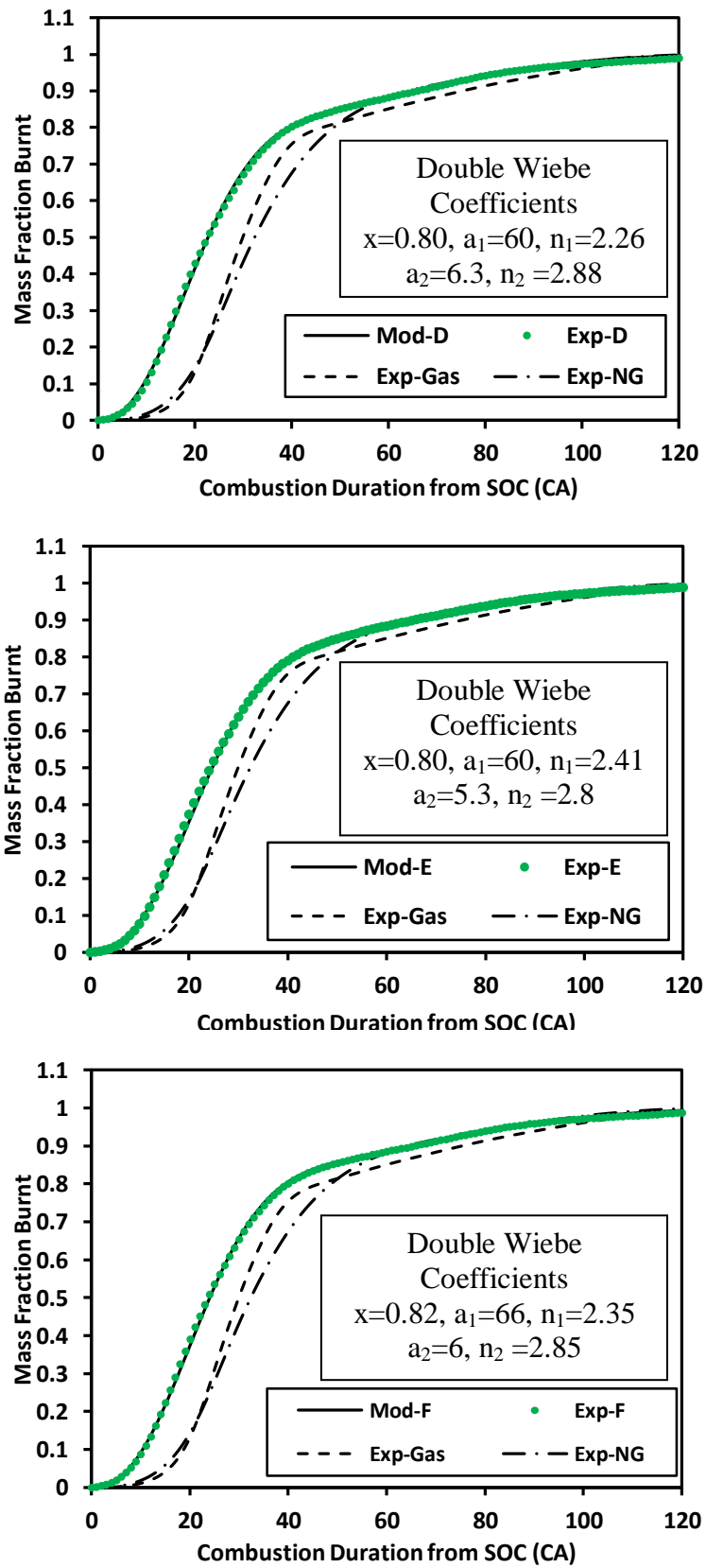


Fig. 7.8 Model constants for PG: Set-D, E and F

Model constants for Set-G, H and I

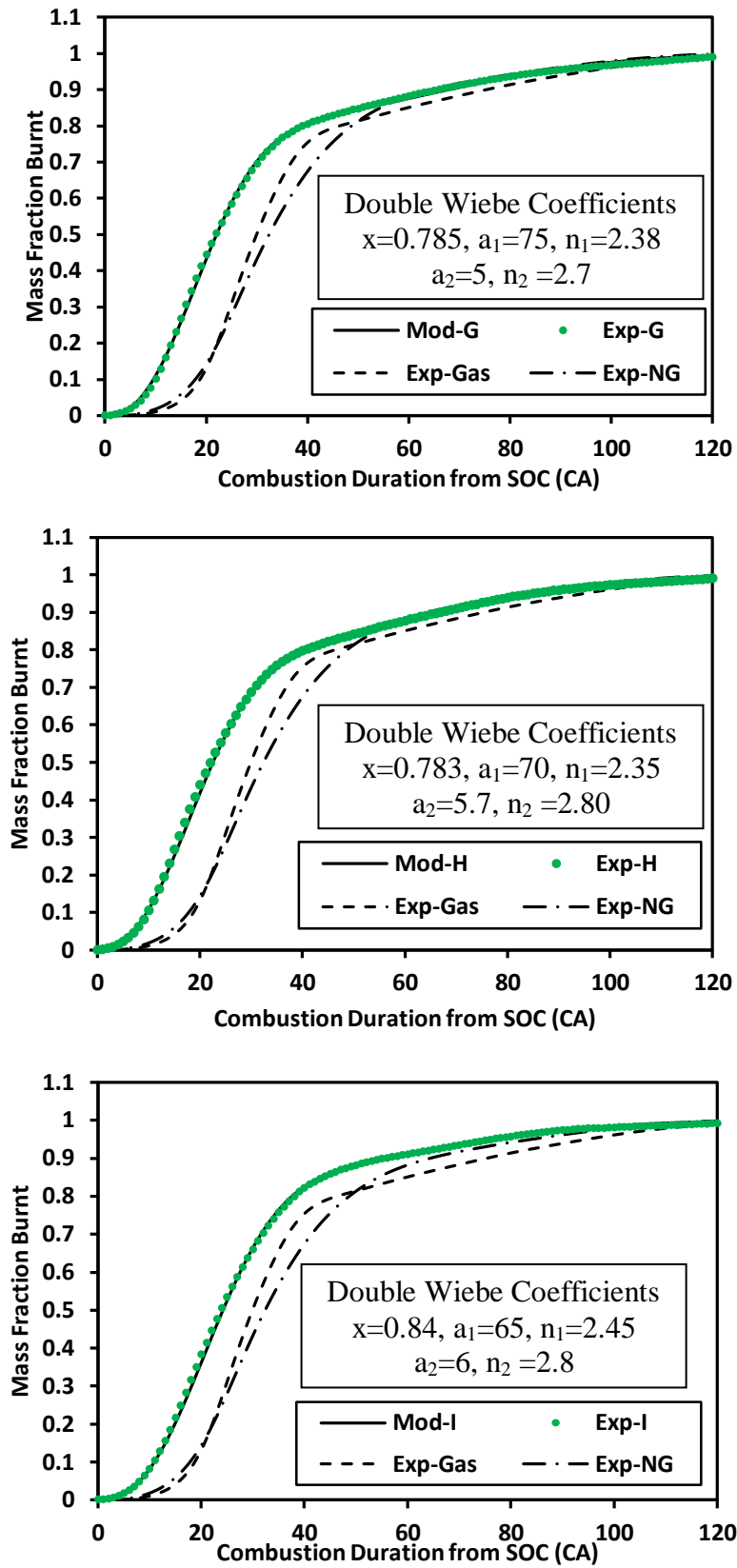


Fig. 7.9 Model constants for PG: Set-G, H and I

Effect of hydrogen variation with 1% CH₄

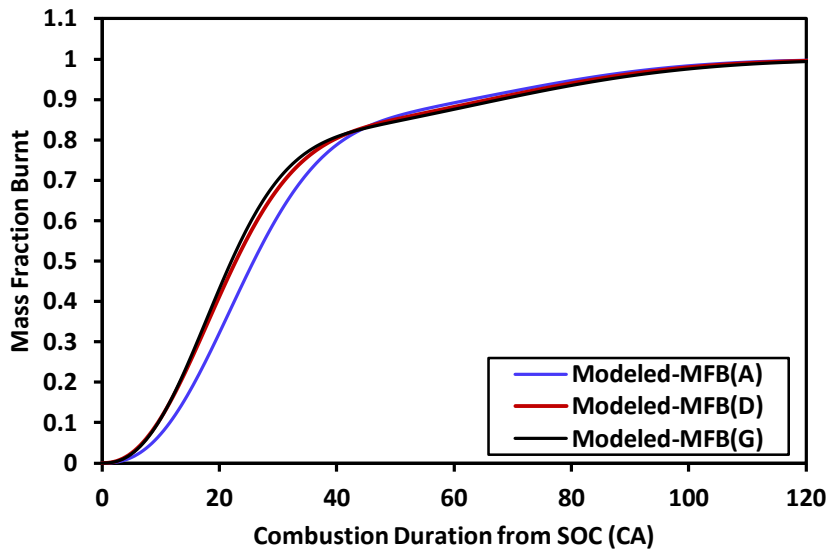


Fig. 7.10 Effect of hydrogen with 1% methane concentration

From Fig. 7.10 it is evident that with an increase in the hydrogen concentration, the slope of MFB curves tend to increase, indicating potential for rapid combustion, owing to higher mixture reactivity. The fuel set D and G have almost similar effect on the combustion process at 50% MFB (22 and 23° CA) and 90% MFB (66 and 67° CA). However, set A has lesser combustion duration (difference of 3° CA) to complete 90% MFB. Among PG fuel sets (A, D and G) with higher hydrogen concentration, set G has undergone quick combustion upto 70% mass fraction and thereafter sluggish response was observed during secondary phase of combustion process.

Effect of hydrogen variation with 2.5% CH₄

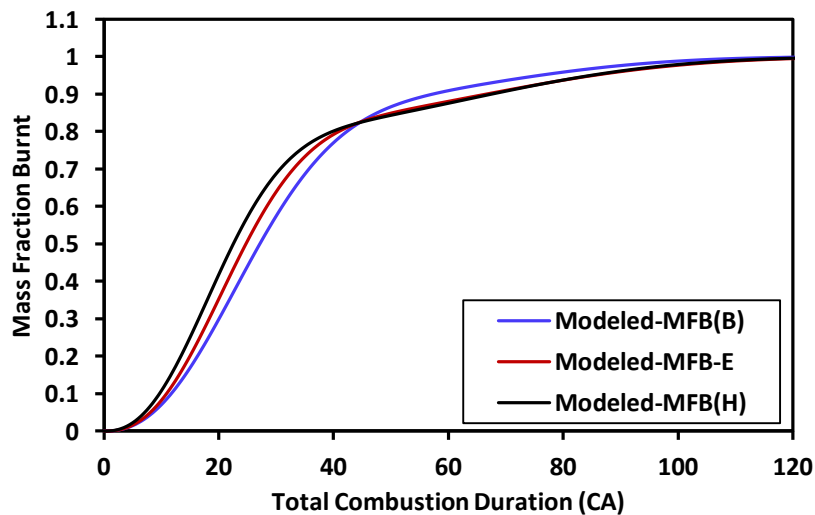


Fig. 7.11 Effect of hydrogen with 2.5% methane concentration

The effect of hydrogen concentration with 2.5% methane is shown in Fig. 7.11. It is clear from the plot that fuel set with 22% hydrogen (set H) has a dominating effect over 19% and 16% hydrogen (set E and B). The combustion duration at 50% MFB shows 2° CA between these sets. Furthermore, the fuel set (B: 16% H₂ + 2.5% CH₄) has shown potential to undergo faster secondary phase combustion almost with a difference of 9° CA at 90% MFB point.

Effect of hydrogen variation with 4% CH₄

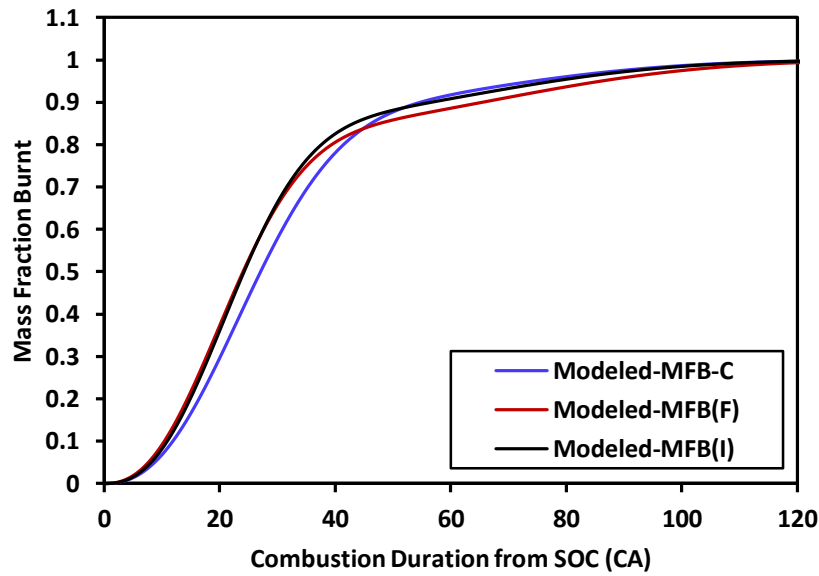


Fig. 7.12 Effect of hydrogen with 4% methane concentration

The effect of hydrogen concentration with 4% methane is shown in Fig. 7.12. It is clear from the plot that, fuel set with 22% and 19% hydrogen (set F and I) has a dominating effect over 16% hydrogen (set C). The combustion duration at 50% MFB has shown identical 24° CA between F and I set. Furthermore, the fuel set C (16% H₂ + 4% CH₄) has shown potential to undergo quick secondary phase combustion almost with a difference of 8° CA at 90% MFB against set F and 3° CA against set I.

From the above plots through modelling studies, it can be concluded that, fuel sets with higher hydrogen concentration, have a potential for faster combustion during primary phase of combustion and therefore result in lesser rapid burning periods. According to literature (Cha et al., 2015 and Karim et al., 1996), the flame propagation speeds up with hydrogen and methane combination and lead to shorter combustion duration. Furthermore, these mixtures help in achieving higher power levels with lower cyclic variations, thus stable combustion process. However, it is observed that fuel sets with higher hydrogen concentration tend to slow down after rapid burning period. The sensitivity of curve fitting for the present work is

set out in Table 7.5. Among the coefficients of double stage Wiebe function, form or shape factors were very sensitive (± 0.02), signifying the importance of combustion dynamics associated with PG fuels with variation in hydrogen and methane concentration. The operating parameters and experimental MFB data are listed out in Table 7.3 for comparison.

Effect of methane variation with 16, 19 and 22% hydrogen

The effect of methane variation (1, 2.5 and 4%) on 16% hydrogen can be seen in Fig. 7.13. The fuel sets which are rich in methane (B and C) have a dominating effect in the secondary phase of combustion process.

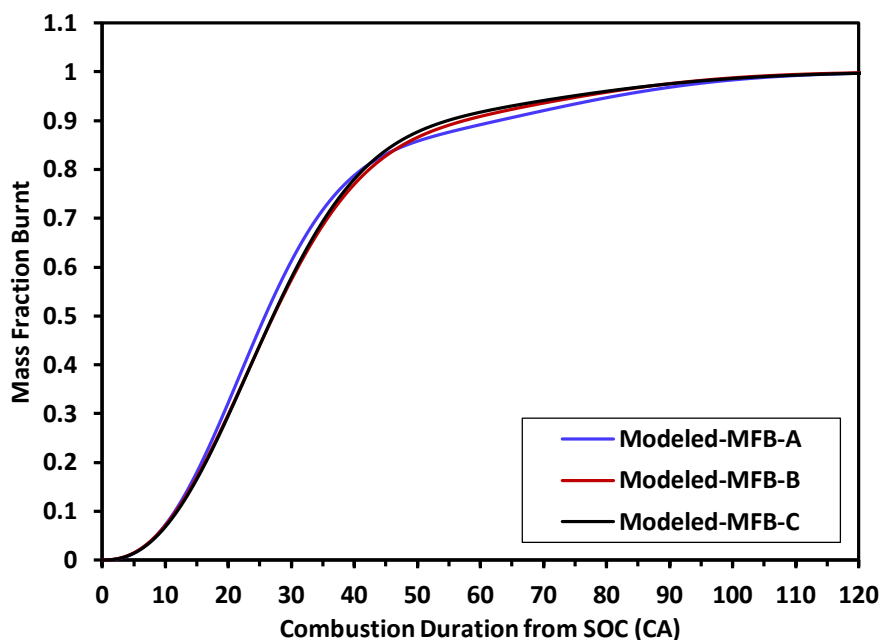


Fig. 7.13 Effect of methane with 16% hydrogen

The curve fitted model constants for set A, B and C are listed in Table 7.4. From Fig. 7.7, comparatively the gasoline MFB curve resulted one of the highest rapid burning angle (57°CA). After 50% MFB duration, the gasoline mixture combustion was sluggish and consumed highest duration (76°CA from SOC) to complete 90% MFB duration as compared to set A (63°CA from SOC) and CNG (63°CA from SOC). Interestingly, the 10% MFB data shows that set A has shortest value as compared to baseline fuels. Furthermore, with increase in CH_4 concentration the MFB curves have shown slightly longer rapid burning angles. This indicates that, set A with 16% H_2 and 1% CH_4 has higher mixture reactivity level as compared to set B and C. On other hand, as $\text{CH}_4\%$ was increasing with constant 16% H_2 as can be seen in Fig.7.13, the MFB curve of set C has undergone lowest combustion duration at 90% MFB values, indicating a better combustion during the secondary phase. This

observation can also be verified from drop in model constant n_I with increase in CH_4 concentration. Therefore, among set A, B and C, the set A has shown a potential for quick combustion at 10% and 50% MFB combustion duration.

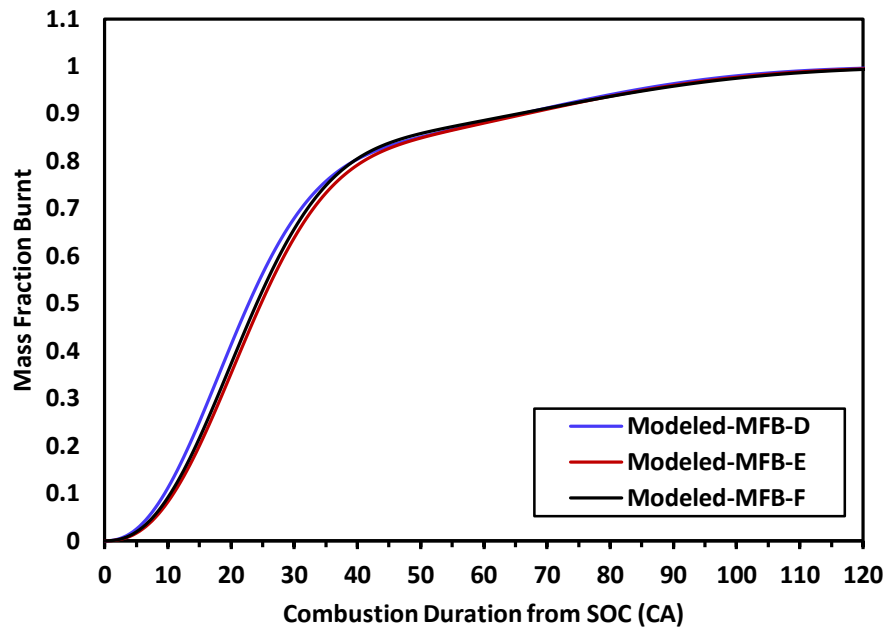


Fig. 7.14 Effect of methane with 19% hydrogen

The model constants for PG fuel sets D, E and F are shown in Table 7.4. With constant 19% hydrogen and step wise increase in $\text{CH}_4\%$ shows that, the 10% MFB from SOC for Set-D is shortest as compared to E and F as shown in Fig. 7.8. Further, the PG sets D, E and F have dominated baselines fuels (gasoline and CNG), which indicates the combination with 19% H_2 has better capability over set A, B and C to undergo quick combustion and therefore shorter rapid burning angles. Furthermore, the secondary combustion phase of PG blends has shown better potential to complete 90% MFB faster as compared to gasoline (9° CA lesser) and 3° CA more than CNG. Therefore, among the PG fuel sets (D, E and F), for quick combustion view point, set D and F are of choice. Very negligible variation in set D, E and F was observed in secondary phase of combustion process. From the above discussion, it can be concluded that, the PG fuel sets (D, E and F) with varying methane concentration was not very significant on combustion characteristics.

From Fig. 7.15, it can be observed that, fuel sets G, H have shown better potential for undergoing quick combustion during the primary combustion phase than set I. However, it is observed that the combustion duration during secondary phase is prolonged by 10° CA over G and H sets at 90% MFB point.

The model constants for PG blends (G, H and I) are shown in Table 7.4. With constant 22% hydrogen and step wise increase in methane (1, 2.5 and 4%) the trend in MFB is shown in Fig. 7.9. The PG blends (G, H and I) have dominating (rapid burning) effect over baseline fuels. Furthermore, set G and H have shown better potential to complete 50% MFB faster as compared to set I. The ability to quickly complete the secondary phase of combustion process is shown by set I and it consumed almost 10° CA lesser than G and H sets.

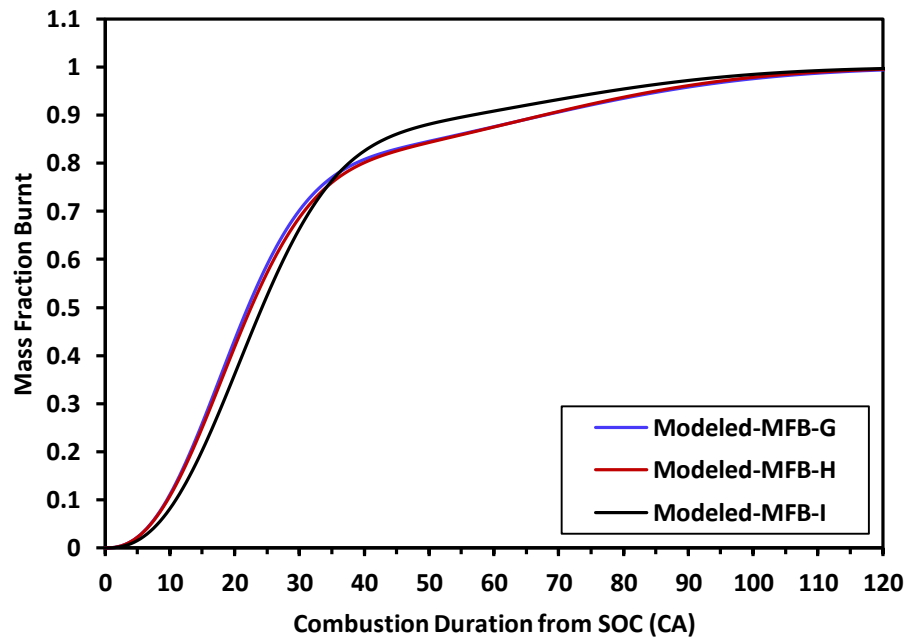


Fig. 7.15 Effect of methane variation with 22% hydrogen

7.6 Summary

In this chapter, the effect of variation in hydrogen and methane concentration on combustion of producer gas through modelling studies was discussed. Owing to asymmetrical negative valve overlap and unique combustion properties of PG, the MFB curves of PG fuel sets were observed to undergo change in slope (thus prolonging combustion duration) after 50% MFB point. Based on the experimental MFB curves, the burnt rate was modeled through double stage Wiebe function to approximate the overall burning trend of PG fuels. The model constants were adjusted to represent experimental MFB.

Among PG fuel sets, A, D and G (hydrogen variation with 1% CH₄), D and G has shown potential for rapid combustion during primary phase of combustion and fuel set A has shown slightly prolonged secondary phase combustion. Fuel set with 22% hydrogen (set H) has

shown a dominating effect over 19% and 16% hydrogen (set E and B). Furthermore, the fuel set B (16% H₂ + 2.5% CH₄) has shown higher potential to undergo quick secondary phase combustion with a rapid burning angle difference of approximately 8° CA. The fuel sets with 22% and 19% hydrogen (set F and I) have shown a dominating effect over 16% hydrogen (set C). The combustion duration at 50% MFB resulted in identical combustion duration of 24° CA between F and I set. Furthermore, the fuel set C (16% H₂ + 4% CH₄) has shown greater potential to undergo quick secondary phase combustion with a rapid burning angle difference of 14° CA as compared to set F and 5° CA against set I.

The effect of methane variation (1, 2.5 and 4%) on 16% hydrogen has shown that fuel sets that are rich in methane (B and C) have higher potential to undergo faster combustion during the secondary phase of combustion process (unlike the effect of hydrogen). This is due to the unique tetrahedral molecular arrangement of methane molecules, requiring larger temperature to break through C-H bond energies. This additional temperature required for efficient methane combustion is gained through hydrogen combustion during primary phase of PG fuel combustion (Mohammad et al., 2015). The effect of methane variation on 19% hydrogen has shown no significant variation in secondary phase of combustion process.

The data from the experiments and the analysis leads to the conclusion that PG mixtures which are dominated by hydrogen concentration tend to undergo faster combustion and thus result in lesser rapid burning angles, owing to higher O and OH radicals which fasten chain reactions (Karagoz et al., 2016). PG mixtures dominated by higher methane concentration tend to relatively slow down the primary phase of combustion and then accelerate it during secondary phase to consume 90% of mass fraction of PG fuels (Babu et al., 2017).

Chapter 8

Conclusions

8.1 Introduction

Producer gas derived from thermo-chemical energy conversion route is a mixture of three combustible and two non-combustible gases namely, hydrogen, methane, carbon-monoxide and carbon-dioxide, nitrogen respectively. The composition of Producer gas (PG) varies widely depending upon the type of feedstock and gasifier design. In this work, the influence of Producer gas composition on combustion characteristics and engine performance has been addressed in detail for modified SI engine fuelled by bottled Producer gas. The major outcomes are given below.

8.2 Work flow

A block diagram representing the overview of work flow to achieve the proposed research objectives is shown in Fig.8.1

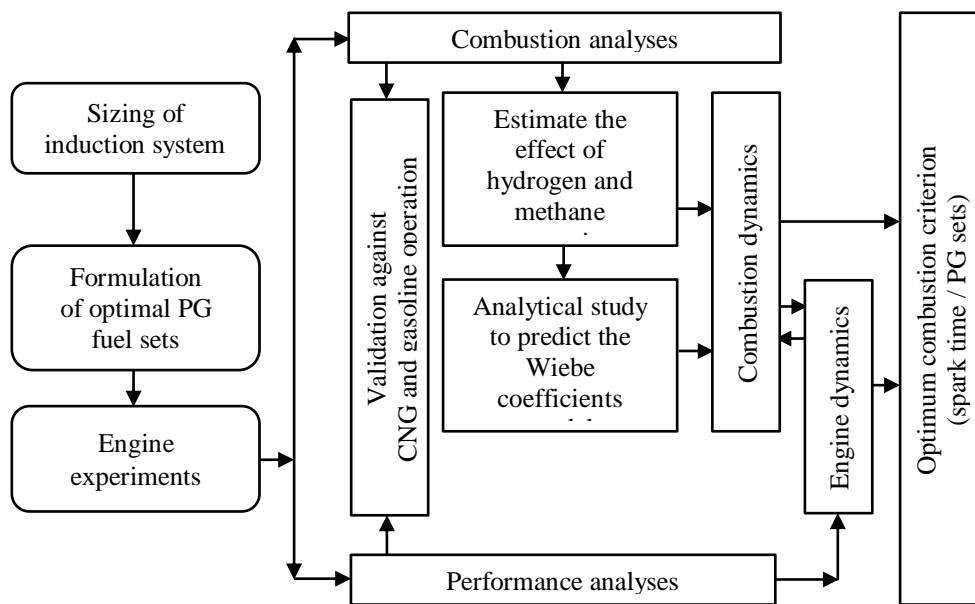


Fig. 8.1 Block diagram of research work

8.3 Development of induction system for bottle fuelled PG engine

The design of test-rig for conventional fuels like gasoline and Diesel are standardized and are readily available in market for end use. However, to interface bottled (high pressure) producer gas with base test-rig was challenging. In view of this, a systematic approach was followed to arrive at a tailor made induction system integrated to the base existing test-rig.

The salient points of developmental activity are as follows. A closed loop arrangement of PG-air mixer and air-gas regulator was essential to enable stoichiometry engine operation. The knowledge of air to fuel ratio (gas composition dependent) and corresponding area ratio of air and fuel ports was required as a guideline in sizing a producer gas-air mixer. These are some of the requirements during the design stages of induction system. The properties of PG like, molecular weight and specific gravity along with engine capacity help in selection of air-gas regulator model. In the present work, the commercial available air-gas regulator was not suitable for engine and therefore called for redesign of valve port area to support stoichiometry operation. To reduce the investments on air and gas flow measurement devices, simple flow measuring devices like orifice-meter can be adapted by incorporating a correction factor accounting for density change between gas and air.

The performance testing resulted in achieving a brake power of 84.54% against the rated gasoline power (2.2 kW) at an MBT spark timing of 16° CA before top dead center. Further a power loss of 15% was observed due to 25% lower mixture calorific value of PG against gasoline and also because of lower product to reactant ratio. The magnitude of power loss was in good agreement with literature reported values. The induction system developed for the producer gas fuel was successfully integrated with the engine.

8.4 Influence of variation in hydrogen and methane concentration

The influence of variation in hydrogen and methane concentration of producer gas fuel on engine was analyzed at compression ratio 11 and 1500 rpm. Owing to moisture variation in biomass (which governs H_2 yield) and methanation reaction (which governs CH_4 production), nine optimal combinations of PG mixtures were formulated. Based on the experimental results, the optimal spark time was found to retard with increase in H_2 concentration, owing to higher flame speed of H_2 . The MBT ignition time for nine combinations of PG blends varied from -18 to -14° CA, -20 to -16° CA and -23 to -20° CA at full, 75% and 50% load point respectively.

PG fuel sets C, G and H were found to consume lowest fuel at 75% load point (1.49, 1.56 and 1.41 kg-wood/kW-hr equivalent) compared to open top, reburn down draft gasifier performance. Furthermore, estimated set F and I were observed to be potential candidate for achieving lesser fuel consumption (\approx 1.06 and 0.82 kg-wood/kW-hr). From brake specific energy consumption view point at 75% load, except set B and E, rest of the PG blends consumed lesser energy as compared to NG and gasoline. The brake thermal efficiency of PG at 75% load point was found to be within 20 to 23% as compared to 19.16% for NG and 18.22% for gasoline. The PG fuel sets with higher H₂ concentration produced higher thermal efficiencies due to improved combustion process owing to higher mixture reactivity. The effect of hydrogen and methane concentration on various engine parameters has shown a decreasing trend in brake specific fuel consumption values. However, a steady rise in NO values was also noted owing to higher cylinder temperatures that accounts for more efficient combustion process. The fuel sets, G (22% H₂ + 1% CH₄), F (19% H₂ + 4% CH₄), H (22% H₂ + 2.5% CH₄) and I (22% H₂ + 4% CH₄) have shown remarkably good outcomes in achieving fuel economy.

The ignition delay was found to be shorter as compared to NG and gasoline operation, mainly due to presence of hydrogen – a combustion accelerator. The rate of pressure rise for all PG blends was within 1.35 bar/CA and thus engine was found to operate normally and knock-free. Study of in-cylinder pressure history revealed a smooth variation of pressure at all load points. The burn rate profiles were consistent upto 50% MFB duration. Near 70% MFB region, a change in slope (indicating slow burning process) was noticed due to asymmetrical valve overlap period. Considering the influence of valve timing diagram on combustion process, a need for estimating the burn rate or modelling and characterization of producer gas existed.

On emission front, all the emission values were well within the prescribed norms at full load. However, CO was slightly higher but within limits as compared to NG, may be due to dissociation effects. At 75% load, a decreasing trend of CO and increasing trend of NO was observed owing to slightly lean operation. A better energy conversion at this load could be attributed to typical and inherent characteristics of the basic engine. At 50% load, the CO emissions were on higher side as compared to NG but lesser than gasoline and well within permissible limits. This may be due to inadequate load on engine leading to incomplete combustion.

8.5 Effect of hydrogen at higher compression ratios

Experiments were conducted under naturally aspirated mode at CR:11, 15 and 18 to quantify the effect of hydrogen variation in PG on engine response. Based on the experimental results, the optimal spark time was found to retard with increase in H₂ concentration owing to higher flame speed of H₂ (2.5 m/s) against NG (0.35 m/s). From, fuel consumption view point, PG fuel sets B (19% H₂+2.5% CH₄) and C (22%H₂+2.5% CH₄) was observed to promote fuel economy (1.27 and 1.33 kg-wood/kW-hr equivalent) compared to open top, reburn down draft gasifier performance. This observation further motivated to study various combinations of H₂ in PG engine. Maximum BTE was observed at 75% load point for CR:15. Set A, B and C produced 4.19%, 3% and 0.6% of higher BP against gasoline and 3%, 1.8% higher BP against NG.

Increase of H₂ in the PG mixture blends was favorable in taking up of higher loads and resulted in overcoming power loss to the tune of 6% at CR: 15 and 18 as compared to CR:11, due to reduced ignition delay and higher peak cylinder pressures at higher CR's. The rate of pressure rise for all PG mixture blends were within 2.5 bar/CA and thus engine was knock-free at higher CR's (15 and 18). At 75% load point, the COV of IMEP for all PG blends was found to vary within 1 to 2% and indicated a very stable combustion process. Based on brake thermal efficiencies and specific fuel consumption values, CR:15 and 75% load point was considered as optimum for the present engine.

Further, 50% MFB crank angle was considered as a robust combustion parameter for closed loop spark control unit based on analysis of combustion durations. Though positive characteristics in heat release patterns and MFB profiles was noted, the formulated variation in H₂ (16, 19 and 22%) was not making significant effect on the shaft power output. On emission front, pollutants (CO, HC and NO) were measured and compared with the Indian CPCB-2016 norms applicable to CNG gensets. At full load for all CR's the measured emissions were much below the prescribed limits. At 75% load, set C generated slightly higher NO. Set B was found to be the best PG fuel blend in-terms of emissions and engine performance.

8.6 Modelling of mass fraction burn curves

Owing to asymmetrical negative valve overlap and unique combustion properties of PG, the MFB curves of PG fuel sets were observed to undergo negative change in slope (thus

prolonging combustion duration) after 50% MFB point. Single stage Wiebe function was found inadequate to approximate the experimentally obtained MFB curves. Therefore, depending on combustion characterization and the fact of existence of primary and secondary phases of combustion process, double stage Wiebe model was considered and found suitable. The burnt rate was modeled by adjusting Wiebe coefficients (model constants) through curve fit for all PG fuels.

Among PG fuel sets, A, D and G (hydrogen variation with 1%CH₄), D and G has shown potential for rapid combustion during primary phase of combustion and fuel set A has shown slightly prolonged secondary phase combustion. Fuel set with 22% hydrogen (set H) has shown a dominating effect over 19% and 16% hydrogen (set E and B). Furthermore, the fuel set B (16%H₂ + 2.5%CH₄) has shown higher potential to undergo quick secondary phase combustion with a rapid burning angle difference of approximately 8° CA. The fuel sets with 22% and 19% hydrogen (set F and I) have shown a dominating effect over 16% hydrogen (set C). The combustion duration at 50% MFB resulted in identical combustion duration of 24° CA between F and I set. Furthermore, the fuel set C (16%H₂+4%CH₄) has shown greater potential to undergo quick secondary phase combustion with a rapid burning angle difference of 14° CA as compared to set F and 5° CA against set I. The reason for faster combustion of hydrogen enriched PG mixtures is attributed to presence of higher O and OH radicals, which quicken chain reactions and accelerate flame propagation, especially during primary phase of combustion.

The effect of methane variation (1, 2.5 and 4%) on 16% hydrogen have shown that, fuel sets that are rich in methane (B and C) have shown higher potential to undergo faster combustion during the secondary phase of combustion process (unlike the effect of hydrogen). This is attributable mainly to unique tetrahedral molecular arrangement of methane molecules, which require higher temperature for breaking C-H bond energies. This temperature is gained from primary combustion phase of PG for efficient methane combustion. The effect of methane variation on 19% hydrogen has shown no significant variation in secondary phase of combustion process. In summary, it can be concluded that, PG mixtures which are dominated by higher hydrogen concentration tend to undergo quick combustion and thus result in lesser rapid burning angles. On the other hand, PG mixtures dominated by higher methane concentration tend to behave sluggish during primary phase of combustion and then accelerate during secondary phase to complete 90% of mass fraction of PG fuels.

8.7 Contribution of the thesis

1. Designed and successfully developed and deployed the induction system suitable for bottled fuelled producer gas engine operation, used as the research workbench.
2. Worked with higher compression ratio (CR:15) that resulted in showcasing of minimizing the power loss to the tune of 6% as compared to CR:11. The fuel sets B (19% H₂+2.5% CH₄) and C (22% H₂+2.5% CH₄) were identified as optimal composition for achieving fuel economy. The variation of hydrogen concentrations from 16% to 22% in producer gas was found to be knock free.
3. Experiments with nine selective combinations of PG blends at CR:11, led to identify variation of optimal (MBT) spark time with variation in concentrations of hydrogen and methane, that served to be input parameter for the closed loop engine operation, a significant input for designing efficient PG engines.
4. Application of double stage Wiebe combustion model for producer gas fuel was successfully implemented, and Wiebe model constants were established and are validated with the experimental results. This aspect is another important parameter for design of PG engines and for optimizing their performance.
5. The experimental results and analyses presented in the thesis can be used for validating many model studies and in design data for producer gas engines including suitable electronic control units.

8.8 Recommendations

1. For economic reasons and also taking their reliability into considerations, it is recommended to adapt simple flow control meters like orifice-meters based on the guidelines provided in this thesis.
2. For achieving higher power levels with reduced emissions, it is recommended to operate producer gas engines at CR:15 instead of restricting to CR:10 or 11:1.
3. 50% mass fraction burnt (MFB) point on CR:15 is recommended to be used as closed loop controls for the naturally aspirated producer gas engine operations.
4. The variation in concentrations of hydrogen (16 to 22%) and methane (1 to 4%) does not cause significant effect on engine power output.

8.9 Scope for future work

1. Experimental studies can be extended to study the effect of twin spark plug on reduction in combustion durations and also to measure experimental flame speed.
2. Optimizations studies with valve lift timing could be taken up for higher power output and safe emission limits.
3. Effect of piston shapes on burn rate can be studied to arrive at suitable combustion chamber design for producer gas fuel, which reduces heat losses and promote efficient combustion process.

References

Akansu S.O., Nafiz K., Çeper B. (2007), “Experimental study on a spark ignition engine fuelled by methane-hydrogen mixtures”, *Int. J. of Hydrogen Energy*, vol. 33, pp. 4279 – 4284.

Amann C.A. (1985), "Cylinder-pressure measurement and its use in engine research," SAE Paper 852067.

Andrea T.D., Henshaw P.F., Ting D.S.K. (2004), “The addition of hydrogen to a gasoline-fuelled SI engine”, *Int. J. of hydrogen Energy*, vol. 29, pp. 1541 – 1552.

Arunachalam A., Oslen D.B. (2012), “Experimental evaluation of knock characteristics of producer gas”, *Int. J. of Biomass and Bioenergy*, vol. 37, pp. 169 – 176.

Available from: <http://www.intechopen.com/books/advances-in-natural-gastechnology/application-of-natural-gas-for-internal-combustion-engines>

Babu M.S., Clement S., Rajan N.K.S. (2011), “Biomass based green technologies: Potential and sustainability”, *Bio-energy India*, M.N.R.E, Govt. of India, Issue 9 & 10, July-December, pp. 20 – 23.

Babu M.S., Clement S., Rajan N.K.S. (2012), " A parametric study on biomass fuelled producer gas engine", National Conf. on Energy and Sustainable Development, College of Engg., Pune.

Babu M.S., Clement S., Rajan N.K.S. (2016), “Development and testing of laboratory scale induction system fuelled with bottled producer gas”, *Int. J. of Applied Mechanics and Materials*, vol. 852, pp. 659 – 665.

Babu M.S., Clement S., Rajan N.K.S. (2016b), “Fuel conversion benefit of producer gas over gasoline”, *Energy Procedia*, vol. 100, pp. 203 - 210.

Babu M.S., Garg V., Akella S.B., Clement S., Rajan N.K.S. (2017), "Influence of valve lift timing on producer gas combustion and its modelling using double stage Wiebe function", 19th Int. Conf. on Thermal Engineering, March, 2017.

Bakar R.A., Kadirgama K., Rahman M.M., Sharma K.V., Semin (2012), “Application of Natural Gas for Internal Combustion Engines, *Advances in Natural Gas Technology*, Dr. Hamid Al-Megren (Ed.), ISBN: 978-953-51-0507-7.

Banapurmath N.R., Prakash T., Yaliwal V.S., Basavarajappa Y.H. (2009), “Combustion characteristics of a 4-stroke CI engine operated on Honge oil, Neem and Rice barn oils when

directly injected and dual fuelled with producer gas induction”, *Int. J. of Renewable Energy*, vol. 33, pp. 1877 – 1884.

Banapurmath N.R.B., Tewari P.G., Hosmath R.S. (2008), “Experimental investigations of a four stroke single cylinder direct injection diesel engine operated on dual fuel mode with producer gas as inducted fuel and Honge oil and its methyl ester (HOME) as injected fuels”, *Int. J. of Renewal Energy*, vol. 33, pp. 2007 – 2018.

Bauer C.G., Forest T.W. (2001), “Effect of hydrogen addition on the performance of methane-fuelled vehicles. Part I: Effect on S.I. engine performance”, *Int. J. of Hydrogen Energy*, vol. 26 pp. 55 – 70.

Bilger R.B. (2000), “Future progress in turbulent combustion research”, *Progress in Energy and Combustion Science*, vol. 26, pp. 367-380.

Brown W.L. (1973), “The caterpillar IMEP Meter and engine friction”, SAE paper 730150 presented at the SAE Annual Congress, Detroit.

Catania, Misul A.E., Spessa D., Vassallo E. (2004), “Analysis of combustion parameters and their relation to operating variables and exhaust emissions in an upgraded multivalve bi-fuel CNG SI engine”, SAE Paper 2004-01-0983.

Ceper B.A., Akansu S.O., Kahraman (2009), “Investigations of cylinder pressure for H₂/CH₄ mixtures at different loads”, *Int. J. of Hydrogen Energy*, vol. 34, pp. 4855 – 4861.

Cha H., Eom T., Song S., Chun M.W. (2015), “An experimental study on the fuel conversion efficiency and NO_x emissions of a spark ignition engine for power generation by fuel mixture of methane and model syngas (H₂/CO)”, *Int. J. of Natural Gas Science and Engineering*, vol. 23, pp. 517 – 523.

Chen K.K., Krieger R.B. (1976), “A statistical analysis of the influence of cyclic variation on the formation of nitric oxide in SI engines”, *Comb. Sci. Tech.*, vol. 12, pp. 125–34.

Cho. H.M., He B.Q. (2006), “Spark ignition natural gas engines - A review”, *Int. J. of Energy Conversion and Management*, vol. 48, pp. 608–618.

Christodoulou F., Margaritis A. (2014), “Experimental investigations of the effects of separate hydrogen and nitrogen addition on the emissions and combustion of diesel engines”, *Int. J. of Hydrogen Energy*, vol. 39, pp. 2692 - 2702.

Cornelius W., John Caplan D. (1952), “Some effects of fuel structure, Tetra ethyl lead and engine deposits on precombustion reactions in a firing engine”, SAE Technical Paper 520250.

CPCB-2016 Norms: Online: http://cpcb.nic.in/LPG_and_CNG_Generator_Set.pdf

Dasappa S., Mukunda H.S., Paul J.P., Rajan N.K.S., Sridhar G., Sridhar H.V. (2008), “A process and apparatus for cleaning Tar and Dust laden gas to highest level of purity using Cn Technology”, Indian Patent granted No. 215917 DATE 2008.

Dasappa S., Paul P.J., Mukunda H.S., Rajan N.K.S., Sridhar G., Sridhar H.V. (2004), “Biomass gasification technology – a route to meet energy needs, Applications of S & T to rural areas”, Current science, vol. 87, No.7.

Dasappa S., Sridhar G., Paul P.J. (2011), “Adaptation of small capacity natural gas engine for producer gas operation”. Proc. IMechE, Part C, Mechanical Engineering Science, vol. 226 pp 1568-1578.

Energy statistics- Report (2012), Ministry of statistics and programme implementation, Govt. of India.

Energy statistics- Report (2014), Ministry of statistics and programme implementation, Govt. of India.

F.V. Tinaut (2006), “Method for Predicting the Performance of an Internal Combustion Engine Fuelled by Producer Gas and Other Low Heating Value Gases,” Fuel Processing Technology, vol. 87, pp. 135 –142.

FAO-Report (1972), “Wood gas as engine fuel, Rome”, Food and Agricultural Organization of the United Nations.

Ferguson C.R., Kirkpatrick A.T., “Internal combustion engines”, Wiley India Publications, 2nd Edi., India.

Firmansyah, Rashid A., Aziz A., Heikal M.R. (2013), “Double stage Wiebe: An approach to single zone modelling of Dual fuel HCCI combustion”, Asian J. of Scientific Research, vol. 6(2), pp. 388 – 394.

Flekiewicz M., Kubica G., Flekiewicz B. (2014), “The analysis of energy conversion efficiency in SI engines for selected gaseous fuels”, SAE transactions 2014-01-2692.

Ganesan V. (1999), Internal Combustion Engines. Tata McGraw Hill Publications, New Delhi.

Ghojel J.I. (2010), “Review of the development and applications of the Wiebe function: a tribute to the contribution of Ivan Wiebe to engine research”, Int. J. of Engine Research, vol.11, pp. 297 – 312.

Gish R.E., McCullough J., Retzloff J., Mueller H. (1958), “Determination of true engine friction”, SAE Transaction, vol. 66, pp. 649 – 667.

- Gobatto P., Massi M., Bernetti M. (2015), "Performance analysis of a producer gas-fuelled heavy duty SI engine at full load operation", *Energy Procedia*, vol. 82, pp. 149 – 155.
- Hackett C., Durbin T.D., Welch W., Pence J. (2004), "Evaluation of conversion technology processes and products", Integrated waste management board publication, California.
- Hagos F.Y., Aziz A. (2014). "Trends of syngas as a fuel in internal combustion engines", *Advances in Mechanical Engineering*, Hindawi Publishing Corporation, ID:401587.
- Hellstrom H., Stephanopoulou A., Jiang Li (2014), "A linear least squares algorithm for double Wiebe functions applied to spark assisted compression ignition", *J. of Engineering for Gas Turbines and Power*, vol. 136, 091514-1.
- Heywood J.B. (2011), *Internal combustion engine fundamentals*, Tata McGraw Hill, New Delhi, 2011.
- Heywood J.B., Higgins J.M., Watts P.A., Tabaczynski R.J. (1979), "Development and use of a cycle simulation to predict SI engine efficiency and NO_x emissions". SAE paper 790291.
- Holman J.P. (2015), "Experimental methods for engineers", 7th Edi., McGraw and Hill Publications, New York.
- Homdoun N., Tippayawong N., Dussadee N. (2014), "Effect of ignition timing advance on performance of a small producer gas engine", *Int. J. of Applied Engineering Research*, vol. 9, Issue 13, pp. 2341-2348.
- Horton S., "The 1973 Oil Crisis" <http://www.envirothonpa.org/documents/The1973OilCrisis.pdf>
- Jonas U., Matthias A., Martin T., Johansson B., Jesper A., Franz X.S. and Henriksen U. (2011), "SI gas engine: Evaluation of engine performance, efficiency and emissions comparing producer gas and natural gas", SAE paper 2011-01-0916.
- Kanitkar S., Chakravarthy P., Paul P.J., Mukunda H.S. (1993), "The flame speeds, Temperature and limits of flame propagation for producer gas air mixtures –Experiments results", *Proc. of fourth national meet on biomass gasification and combustion*, Mysore, India, Vol.4, pp. 50 – 62.
- Karagöz Y., Güler İ., Sandalcı T., Yüksek L., Dalkılıç A.S., Wongwises S. (2016), "Effects of hydrogen and methane addition on combustion characteristics, emissions and performance of a CI engine", *Int. J. of Hydrogen Energy*, vol. 41, pp. 1313 – 1325.
- Karim G.A., Wierzba I., Al-Alousi Y. (1996), "Methane-Hydrogen mixtures as fuels", *Int. J. of Hydrogen Energy*, vol. 21, No.7, pp. 625 – 631.
- Kaupp A. (1984), "Small scale gas producer engine system", Biomass energy foundation. RPS84100.

- Khan B.H. (2014), "Non-conventional energy resources", Tata McGraw Hill publications, 2nd Edi., New-Delhi, India.
- Kishore V.R., Ravi M.R., Ray A. (2008), "Effect of Hydrogen Content and Dilution on Laminar Burning Velocity and Stability Characteristics of Producer Gas-Air Mixtures," Int. J. of Reacting Systems, Paper ID: 310740.
- Kline S.J., McClintock FA (1953), "Describing uncertainties in single sample experiments", Mechanical Engineering, vol. 75, pp. 3 – 8.
- Krieger R.B., Gary L B. (1966), "The computation of apparent heat release for internal combustion engines", ASME paper 66-WA/DGP-4.
- Kuhl A.L., Ferguson R. E., Oppenheim A. K. (1999), "Combustion of TNT products in a confined explosion", In Proc. of the 17th International Colloquium on Dynamics of explosions and reactive systems, Heidelberg, Germany.
- Kumar A., Kumar K., Kaushik N., Mishra S. (2010), "Renewable energy in India: Current status and future potentials", Int. J. of Renewable and Sustainable Energy Reviews, vol. 14, pp. 2434–2442.
- Lancaster D.R., Krieger R.B., Lienesch J.H. (1975), "Measurement and Analysis of Engine Pressure Data", SAE Paper 750026.
- Laurence, Ashenafi D. (2012), "Syngas Treatment Unit for Small Scale Gasification - Application to IC Engine Gas Quality Requirement", Int. J. Journal of Applied Fluid Mechanics, vol. 5, pp. 95 – 103.
- Litak G., Kamiński T., Czarnigowski J., Sen A.K., Wendeker M. (2009), "Combustion process in a spark ignition engine: analysis of cycle peak pressure and peak pressure angle oscillations", Int. J. of Meccanica, vol. 44, pp. 1 -11.
- Liu Z., Karim G.A. (1997), " Simulation of combustion process in gas-fuelled diesel engines", Proc. IMechE, Part A: Int. J. of Power and Energy, vol. 211 (A2), pp. 159 – 169.
- Melgar A. (2007), "Thermochemical equilibrium modelling of a gasifying process", Int. J. of Energy Conversion and Management, vol. 48, pp. 59–67.
- Meyer J. (2007), "Engine modeling of an internal combustion engine with twin independent cam phasing", Undergraduate thesis, Ohio State University, 2007.
- Miyamoto N., Murayama T., Fukazawa (1972), "Studies on low compression ratio diesel engines". Bull. JSME, vol. 15(90), pp. 1603–1616.

- Mohammed K., Rahman M.M. (2015), "Performance prediction of spark-ignition engines running on gasoline-hydrogen and methane –hydrogen blends", *Int. J. of Applied Energy*, vol 158, pp. 556 – 567.
- Mukunda H.S. (2011), "Understanding clean energy and fuels from biomass" Wiley India, Publications, New Delhi, India.
- Mukunda H.S., Dasappa S., Shrinivasa U. (1993), "Open-top wood gasifiers, renewable energy – Sources for fuels and electricity", Washington DC., Island press.
- Mukunda HS., Paul P.J., Dasappa S., Shrinivasa U., Sharan H. (1994), "Results of Indo-Swiss programme for quantification and testing of a 300 Kw IISc-gasifier, *Int. J. of Energy for Sustainable Development*, Vol. 4, pp. 46-9.
- Murugan S., Ramaswamy M. C., Nagarajan G. (2008), "A comparative study on the performance, emission and combustion studies of a DI diesel engine using distilled tyre pyrolysis oil-diesel blends". *Fuel*, vol. 87, pp. 2111-2121.
- Nakazono T., Watanabe Y. (2015), "A study of stoichiometry bio-mass gas engine", *SAE transaction* 2015-32-0831.
- Ouellette, Patric (2000), "High Pressure Direct Injection (HPDI) of Natural Gas in Diesel Engines", *Proc. ANGVA 2000 Conference*. Yokohama.
- Patterson D.J. (1967), "Cylinder pressure variations - A fundamental combustion problem", *SAE paper*, Vol. 75.
- PischingerS., Umierski U., Hüchtebrock B. (2003), "New CNG concepts for passenger cars: High torque engines with superior fuel consumption". *SAE Paper* 2003-01-2264.
- Poonam G. (2011), "Opportunities for biomass energy in rural India", *Bio-energy India*, M.N.R.E, Govt. of India, Issue-7, January-March, pp. 28 - 30.
- Poulton M.L., (1994), "Alternative Fuels for Road Vehicles", *Computational Mechanics Publication*, London. 1994.
- Pulkarbek W.W. (2009), "Engineering fundamentals of the internal combustion engine", 2nd Edi., Eastern Economy Edition, New Delhi, India.
- Pundir B.P. (2010), "IC Engines: Combustion and Emissions", Narosa publications, 1st Edi., India.
- Rajvanshi A.K. (1986), "Alternative Energy in Agriculture", vol. II, CRC Press, pp. 83-102.
- Reed T.B., Das A. (1988), "Handbook of biomass downdraft gasifier engine systems", SERI, SP-271-3022, Colorado.

- Rifken E.B. (1952), "Early combustion reactions in engine operation", SAE paper 3, vol. 6.
- Roger D.R., (2010), "Engine Combustion: Pressure measurement and analysis", SAE International Publication, R-388, USA.
- Roy M.M., Tomita E., Kawahara N., Harada Y., Sakane A. (2009), "Performance and Emission Comparison of a Supercharged Dual-Fuel Engine Fuelled by Producer Gases with Varying Hydrogen Content," Int. J. of hydrogen energy, vol. 34, pp. 7811–7822.
- Sera M.A., Bakar R.A., Leong S.K. (2003), "CNG engine performance improvement strategy through advanced intake system", SAE Paper 2003-01-1937.
- Sharma A.K. (2006), "Simulation of biomass gasifier-engine system", PhD. thesis, Indian Institute of Technology, Delhi, India.
- Sharma A.K. (2011), "Experimental Investigations on a 20 kWe Solid Biomass Gasification System", Int. J. of Biomass and Bioenergy, vol.35, pp.421-428.
- Shashikantha, Parikh P.P. (1999), "Spark ignition producer gas engine and dedicated compressed natural gas engine -Technology development and experimental performance optimization", SAE Paper 1999-01-3515.
- Shaw B.T., Fischer G.D., Hedrick J.K. (2002), "Simplified cold start catalyst thermal model to reduce hydrocarbon emissions", Proc of 15th Triennial World Congress of the International Federation of Automatic Control, Barcelona, Spain.
- Shayler P.J., Wiseman M.W. (1990), "Improving the determination of mass fraction burnt", SAE paper 900351.
- Sheth P.N., Babu B.V. (2005), "Effect of Moisture Content on Composition Profiles of Producer Gas in Downdraft Biomass Gasified," Proc. of International Congress Chemistry and Environment (ICCE), pp. 356 – 360.
- Shivapuji A.M. and Dasappa S. (2012), "Experiments and zero D modelling studies using specific Wiebe coefficients for producer gas as a fuel in spark ignited engines", Proceedings of IMechE, Part C: Journal of mechanical engineering science, vol. 227 (3), pp.504 - 519.
- Shivapuji A.M., Dasappa S., (2011), "Experimental studies on multi-cylinder natural gas engine fuelled with producer gas", 19th European biomass conference and exhibition, Berlin, Germany.
- Shivapuji A.M., Dasappa S., (2014), "In-cylinder investigations and analysis of a SI gas engine fuelled with H₂ and CO rich syngas fuel: Sensitivity analysis of combustion descriptors for engine diagnostics and control", Int. J. of Hydrogen Energy, vol. 39, pp. 15786-15802.

Shivapuji A.M., Kumar A., Prakash E.S., Dasappa S., (2013), “Experiments and CFD simulation of producer gas fuelled SI engine: Towards addressing high exhaust enthalpy and cooling loads”, 23rd National conference on IC engine and combustion, SVNIT, Surat, India.

Shivapuji A.M., Dasappa S., (2015), “Influence of fuel hydrogen fraction on syngas fuelled SI engine: Fuel thermo-physical property analysis and in-cylinder experimental investigations”, Int. J. of Hydrogen Energy, vol.40, pp. 10308 – 10328.

Shrestha S.O.B., Karim G.A. (1999), “Hydrogen as an additive to methane for spark ignition engine applications”, Int. J. of Hydrogen Energy, vol. 24, pp. 577-586.

Sridhar G. (2003), “Experiments and modeling studies of producer gas based spark-ignited reciprocating engines”, PhD thesis, Indian Institute of Science, India.

Sridhar G., Dasappa S., Sridhar H.V., Paul P.J., Rajan N.K.S. (2005b), " Gaseous emissions using producer gas as fuel in reciprocating engine", SAE Paper 2005-01-1732.

Sridhar G., Paul P.J., Mukunda H.S. (2001), “Biomass derived producer gas as a reciprocating engine fuel – An experimental analysis”, Int. J. of Biomass and Bioenergy, vol. 21, pp. 61 – 72.

Sridhar G., Paul P.J., Mukunda H.S. (2005c), “Computational studies of the laminar burning velocity of a producer gas and air mixture under typical engine conditions”, Proc. IMechE, Int. J. of Power and Energy, vol. 219(3), pp. 195 – 201.

Sridhar G., Sridhar H.V., Dasappa S., Paul P.J., Subbukrishna D. and Rajan N.K.S. (2005), “Green Electricity from Biomass Fuelled Producer Gas Engine”, 14th European Biomass Conference & Exhibition Biomass for Energy, Industry and Climate Protection, Paris, France.

Stone C.R., Armytage G. (1987), “Comparison of methods for the calculation of mass fraction burnt from engine pressure time diagrams”, Proc. IMechE, Part D: Int. J. Transport Engineering, vol. 201(14), pp. 61–67.

Tewari P.G., Subrahmanyam J.P., Babu M.K.G. (2001), “Experimental investigations on the performance characteristics of a producer gas fuelled spark ignition engine”, SAE transactions 2001-01-1189.

Turare C. (1997), “Biomass Gasification Technology and Utilization”, Artes Institute, University of Flensburg, Flensburg, Germany.

US IEA (2014), International energy data and analysis. <http://www.eia.gov/beta/international/analysis.cfm?iso=IND>

Wayne W.S., Clark N.N., Atkinson C.M. (1998), “A parametric study of knock control strategies for a bi-fuel engine”, SAE Paper 980895.

Yaliwal V.S., Banapurmath N.R., Girish N.M., Tewari P.G. (2014), “Production and utilization of renewable and sustainable gaseous fuel for power generation applications: A review of literature”, *Renewable and Sustainable energy reviews*, vol. 34, pp. 608 – 627.

Yeliana, Cooney C., Worm J., Michalek D., Naber J. (2008),” Wiebe function parameter determination for mass fraction burn calculation in an ethanol- gasoline fuelled SI engine”, *Int. J. of KONES Power Trains and Transportation*, vol. 15, pp. 567 – 574.

Zhou J.H., Cheung C.S., Leung C.W. (2014), “Combustion, performance and emission of a diesel engine with H₂, CH₄ and H₂+CH₄ addition”. *Int. J. of Hydrogen Energy*, vol.39, pp. 4611-21.

LIST OF PUBLICATIONS

Publications in International / national Journal and Conferences

1. **M. Sreedhar Babu**, S. Clement and N.K.S. Rajan (2016), "Fuel conversion benefit of Producer gas over Gasoline - An experimental analysis ", *Energy Procedia*, Vol. 100, pp. 203 – 210. [Scopus]
2. **M. Sreedhar Babu**, S. Clement and N.K.S. Rajan (2016), "Development and Testing of a Laboratory Scale Induction System for a Bottled Producer gas Fuelled IC Engines", *Journal of Applied Mechanics and Materials*, Vol. 852, pp. 659 – 665. [Scopus]
3. **M. Sreedhar Babu**, V. Garg, S.B. Akella, S. Clement and N.K.S. Rajan (2016), "Influence of valve lift timing Valve timing on producer gas combustion and its modelling using two-stage Wiebe function". 19th Int. Conf. on Thermal Engineering, Czech Republic, 23-24th March, 2017.
4. **M. Sreedhar Babu**, S. Clement and N.K.S. Rajan (2012), "A Parametric Study on Biomass Fuelled Producer Gas Engine," National Conference on Energy and Sustainable Development, 28 - 29th February, College of Engineering, Pune, India.
5. **M. Sreedhar Babu**, S. Clement and N.K.S. Rajan (2011), "Biomass Based Green Technologies-Potential and Sustainability," *Bio-energy India Magazine*, Ministry of New & Renewable Energy, Govt. of India, Issue 9 and 10, pp. 20-23.
6. **M. Sreedhar Babu**, S. Clement and N.K.S. Rajan (2016), "Influence of hydrogen and methane concentration on a producer gas fuelled spark ignition engine", *Int. J. of Hydrogen Energy*. [Under review – SCI]
7. **M. Sreedhar Babu**, S. Clement and N.K.S. Rajan (2016), "Effect of hydrogen concentration at higher compression ratio of a producer gas fuelled SI engine". *Int. J. of Hydrogen Energy*. [Under review - SCI]

Appendices

Appendix – A

Estimating the amount of bottled producer gas required

Total volume of air = (Engine capacity × Volumetric efficiency × Effect of CR)

Total volume of air = $\left(359 \text{ cc} \times 0.45 \times \frac{10}{11}\right)$, Assumed vol. efficiency = 0.45

Total volume of air = 146.86 cc

$\left(\frac{A}{F}\right)_{\text{Stoichiometry volume}} = \left[\frac{\text{Volume flow of air in cc}}{\text{Volume flow of PG in cc}}\right]$, (A/F) ratio for Set – A is 0.928

Volume of PG in cc = $\left[\frac{146.86 \text{ cc}}{0.928}\right] = 158.25 \text{ cc}$

Volume of PG in cc/min = $158.25 \text{ cc} \times \frac{1500}{2} = 118687.5 \text{ cc/min}$

Volume of PG in Lit/min = 118.687 Lit/cc

Volume of PG in $\frac{m^3}{hr} = 118.687 \times 0.06 = 7.12 \text{ m}^3/hr$

Appendix – B

Piezoelectric pressure transducer (Kistler Make)

7. Technical Data Type 6613CA

| | | | |
|-----------------------------|------------------------------------------|--------------------|------------------|
| Measuring range | Range I | bar | 0 ... 250 |
| | Range II | bar | 0 ... 100 |
| Sensitivity | Range I ($\pm 0,5$ %) | mV/bar | 10 |
| | Range II ($\pm 0,5$ %) | mV/bar | 25 |
| Measuring frequency | (-3 dB) | Hz | 0,016 ... 20 000 |
| Linearity | $^{\circ}\text{C}$ 20 | %FSO | $\leq \pm 1$ |
| Operating temperature range | mounting location | $^{\circ}\text{C}$ | -50 ... 350 |
| | electronic | $^{\circ}\text{C}$ | -10 ... 110 |
| | Viton [®] cable connection max. | $^{\circ}\text{C}$ | 200 |
| Sensitivity shift | 200 \pm 150 $^{\circ}\text{C}$ | % | $\leq \pm 2,5$ |
| | 200 \pm 50 $^{\circ}\text{C}$ | % | $\leq \pm 1$ |
| Time constant | for cylinder measuring | s | ≈ 5 |
| | for calibration | s | >2 500 |
| Signal output (at 1mA load) | max. | V | 4,4 ... 5 |
| | min. | V | >0 |
| Signal span | | V | 2,5 |
| Zero line | | V | 2 ... 2,2 |
| Supply voltage | | V | 7 ... 32 |
| Supply current | | mA | 6 |
| Output impedance | | Ω | 100 |
| Mounting torque | | N·m | 15 |
| Connector | | | Lumberg M12 IP67 |

Accessories Included

- Cr-Ni-St.seal

Type 1100A3

Optional Accessories

- Torque wrench 8 ... 40 N·m *
- Fork wrench SW 12 for 1300A11*
- Adapter M14 x 1,25 – M10x1
- Adapter BSP R 1/2" - M10x1 1/2
- Adapter for M20x1,5; for BSF 3/4"; for 6 1/2"
- Connecting cable 4-pin, one free cable end, length = 10 m, 1, 2, 5, 8
- Connecting cable 3-pin, one free cable end, length = 10 m, 1, 5, 8
- Connecting cable 3-pin, one free cable end, length = 20 m, 1, 5, 8
- Tubular socket wrench

Type

1300A11
 1300A13
 6582A1
 6582A2
 7523B01/B02/B03
 1700A71
 1700A69
 1700A69A1
 1300A6

* refer to data sheet about Special Tools and Sensor Dummies (000-068)

Calibration certification of pressure transducer



Werkszeugnis Test Report

Type Kistler 6613CQ18

Serial No. 4556097

| | | |
|---------------------------------------------------|----------------------------------------------|---------------------------------|
| geprüft durch tested by | Datum Date | |
| M. Bernardin | 09. Dec. 2013 | |
| Referenzgeräte Reference Equipment | Typ Type | Serien-Nr. Serial No. |
| Gebrauchsnormal Working Standard | Kistler 6961A250 | 1213533 |
| Ladungskalibrator Charge Calibrator | Kistler 5395A | 605260 |
| Umgebungstemperatur Ambient Temperature | Relative Feuchte Relative Humidity | |
| °C | % | |
| 27 | 51 | |

Technische Daten Technical Data

| | | | |
|-------------------------|---------------------------------------|------------------------------------------|--------------------------------|
| Bereich Range | Empfindlichkeit Sensitivity | Empf. Toleranz Sens. Tolerance | Linearität Linearity |
| bar | mV / bar | ≤ ± % | ≤ ± %FSO |
| 0 ... 100 (200°C) | 40,00 | 0,50 | 1,00 |

Messverfahren Kontinuierliche Kalibrierung mit sinusförmigem Druckverlauf, Vergleichsverfahren. Kalibriert und abgeglichen im Bereich 0 ... 100 bar bei 200°C und 2 Hz.

Measurement Procedure Continuous Calibration with sinusoidal pressure profile, Comparison Method. Calibrated and adjusted in the range 0 ... 100 bar at 200°C and 2 Hz.

Kistler betreibt die SCS Kalibrierstelle Nr. 049, akkreditiert nach ISO 17025. SCS Kalibrierzertifikate sind auf Bestellung erhältlich.

Kistler operates the SCS Calibration Laboratory No. 049, which is accredited per ISO 17025. SCS Calibration Certificates are available on request.

Bestätigung Confirmation

Das oben durch die Seriennummer identifizierte Gerät entspricht der Vereinbarung der Bestellung und hält die Herstellertoleranzen gemäss den Spezifikationen der Datenblätter ein. Dieses Dokument erfüllt die Anforderungen von EN 10204 Werkszeugnis "2.2". Alle Messmittel sind auf nationale Normale rückverfolgbar. Das Kistler Qualitätsmanagement System ist nach ISO 9001 zertifiziert. Dieses Dokument ist ohne Unterschrift gültig.

The equipment mentioned above and identified by Serial Number complies with the agreement of the order and meets the manufacturing tolerances specified in the data sheets. This document fulfils the requirements of EN 10204 Test Report "2.2". All measuring devices are traceable to national standards. The Kistler Quality Management System is certified per ISO 9001. This document is valid without a signature.

Kistler Instrumente AG

Eulachstrasse 22 Tel. +41 52 224 11 11 ZKB Winterthur BC 732 IBAN: CH67 0070 0113 2003 7462 8
PO Box Fax +41 52 224 14 14 Swift: ZKBKCHZZ80A VAT: 229 713
CH-8408 Wintherthur info@kistler.com Account: 1132-0374.628 ISO 9001 certified

www.kistler.com

Appendix – C

Crank angle encoder (Kuebler Make)



Technical Specification

| | |
|----------------------------------|------------------------------------------------------------------------------|
| General specifications | |
| Pulse count (ppr) | 360 |
| Electrical specifications | |
| Operating voltage | 5 V DC \pm 5 % |
| No-load supply current I_0 | Max. 70 mA |
| Output | |
| Output type | Pulse |
| Operating current | max. per channel 20 mA , conditionally short-circuit proof (not with U_b) |
| Output frequency | max. 200 kHz |
| Rise time | 100 ns |

| | |
|---------------------------|---------------------------------------------|
| Connection | |
| Connector | type 9416, 12-pin, type 9416L, 12-pin |
| Cable | Ø7.8 mm, 6 x 2 x 0.14 mm ² , 1 m |
| Standard conformity | |
| Protection degree | DIN EN 60529, IP65 |
| Climatic testing | DIN EN 60068-2-3, no moisture condensation |
| Emitted interference | DIN EN 61000-6-4 |
| Interference rejection | DIN EN 61000-6-2 |
| Shock resistance | DIN EN 60068-2-27, 100 g, 3 ms |
| Vibration resistance | DIN EN 60068-2-6, 10 g, 10 ... 2000 Hz |
| Ambient conditions | |
| Operating temperature | -20 ... 60 °C (253 ... 333 K), fixed cable |
| Storage temperature | lens -40 ... 70 °C (233 ... 343 K) |
| Mechanical specifications | |
| Material | |
| Housing | aluminium, powder coated |
| Flange | aluminium 3.1645 |
| Shaft | stainless steel 1.4305 |
| Mass approx. | 350 g |
| Rotational speed. | max 12000 min ⁻¹ |
| Moment of inertia | ≤ 25 gcm ² |
| Starting torque | ≤ 1.5 Ncm |

Appendix – D

MATLAB code for in-cylinder data processing

```
%Creating a function which reads the given .csv source file.
%The inputs: STBTDC = Spark time (-ve before TDC and +ve after TDC), mass
=Mass flow rate of fuel
%CV = Calorific Value, Engine Specs, Filename, 'a' from graph
%function [Gc , Ge] = readmyfile (STBTDC,mass,CV)
%clearvars -except STBTDC mass CV
% a =          start angle of upper loop of p-v curve (see the intersecting
region)
% b = a+360 closing angle of upper loop of p-v curve (see the intersecting
region)
% N = number of cycles

clear all
clc
STBTDC = -14;      % spark time BTDC
massfuel= 7.0352; % kg/hr fuel
CV = 4715000;     % J/kg
massair = 8.6988; % mass flow rate air kg/hr
BP = 1.8;         % Brake power kW
A_Fs = 1.27;     % Stoichiometric Air/Fuel ratio
P_amb = 101;     % Pressure ambient kPa
T_amb = 28;      % Temperature Ambient deg C
%~~~~~Enter the engine specifications #0~~~~~
EVO=504;
Vswept=0.000359; %swept volume m^3
CR=11;          %compression ratio
rpm=1500;

%~~~~~Extracting data from the original file #1~~~~~
filename = 'FL-1.csv';
sheet = 'FL-1';
xlRange = 'D92:E812';
PV = xlsread(filename,sheet,xlRange);

%~~~~~Converting P from bar to pascal #2~~~~~
PV(:,2) = PV(:,2)*101325 ;

%~~~~~Filling the empty space in last row of second column #3~~~~~
PV(720,2)= PV(719,2);

%~~~~~Creating the PV sheet in the excel file #4~~~~~
filename = 'FL-1.xlsx';
xlRange = 'A1';
sheet = 'PV';
```

```

xlswrite(filename,PV, sheet,xlRange);
warning('off','MATLAB:xlswrite:AddSheet');

%~~~~~Creating a new Gamma file - This is log10 values of P and V
#5~~~~~
PV(:,1) = log10(PV(:,1));
PV(:,2) = log10(PV(:,2));
filename = 'FL-1.xlsx';
xlRange = 'A1';
sheet = 'Gamma';
xlswrite(filename,PV, sheet,xlRange);
warning('off','MATLAB:xlswrite:AddSheet');
lx = PV(:,1);
ly = PV(:,2);
scatter(lx,ly);

%~~~~~Creating sheet for Gc
#6~~~~~
filename = 'FL-1.xlsx';
sheet = 'Gamma';
n = 360- abs(STBTDC) ;
xlRange = strcat('A310:B', int2str(n));
dataGc = xlsread(filename,sheet,xlRange);
filename = 'FL-1.xlsx';
xlRange = 'A1';
sheet = 'Gc';
xlswrite(filename,dataGc,sheet,xlRange);
warning('off','MATLAB:xlswrite:AddSheet');
x=dataGc(:,1);
y=dataGc(:,2);
fitvars = polyfit(x, y, 1); % linear straight line fit of Gc data
Gc = abs(fitvars(1)) % slope of the best fit line
%c = fitvars(2); % intercept if needed

%~~~~~Creating sheet for Ge #7~~~~~
filename = 'FL-1.xlsx';
sheet = 'Gamma';
xlRange = 'A411:B505';
dataGe = xlsread(filename,sheet,xlRange);
filename = 'FL-1.xlsx';
xlRange = 'A1';
sheet = 'Ge';
xlswrite(filename,dataGe,sheet,xlRange);
warning('off','MATLAB:xlswrite:AddSheet');
x=dataGe(:,1);
y=dataGe(:,2);
fitvars = polyfit(x, y, 1); % linear straight line fit of Ge data
Ge = abs(fitvars(1)) % slope of the best fit line
%c = fitvars(2); % intercept if needed

%~~~~~Reading data to create covfiledata.xlsx
#8~~~~~
filename = 'FL-1.csv';
xlRange = 'B818:GS1536';
covfiledata1 = xlsread(filename,xlRange);
xlRange = 'D93:D811';

```

```

vdata = xlsread(filename,xlRange);

%~~~~~Creating covfiledata.xlsx to execute the COVimep matlab code #9~~~~~
filename = 'cov file data.xlsx';
xlRange = 'A1';
xlswrite(filename,covfiledata1,',xlRange);
warning('off','MATLAB:xlswrite:AddSheet');
xlRange = 'GS1';
xlswrite(filename,vdata,',xlRange);
warning('off','MATLAB:xlswrite:AddSheet');

%~~~~~Importing data from covfiledata for cov_imep execution
#10~~~~~
filename = 'cov file data.xlsx';
xlRange = 'A1:GS719';
covfiledata = xlsread(filename,xlRange);
prompt = 'What is the observed value of a ?\n';
a = input(prompt);
b=a+360

%~~~~~Executing the file cov_imep with 'a' as an input
#11~~~~~
clearvars -except a b Gc Ge massfuel CV STBTDC covfiledata BP massair A_Fs
EVO Vswept CR rpm T_amb P_amb
N=200;

for i=1:200

    P(:,i)=covfiledata(:,i);
    V(:,i)=covfiledata(:,201);

    %~~~~~Performance code~~~~~
    %calculate volume change
    Vchange(1,i)=max(V(:,i))-min(V(:,i));

    %calculate peak pressure
    Peakpressure(1,i)= max(P(:,i));

    di=b-a+1;
    %Volume range for indicated work
    V1(1:di,i) = V(a:b,i);

    %Pressure range for indicated work
    P1(1:di,i) = P(a:b,i);

    %Calculated Indicated work
    WorkInd(1,i) = -trapz(V1(1:di,i),P1(1:di,i)) .* 100;

    % Calculate Indicated MEP
    MepInd(1,i) = (WorkInd(1,i)/Vchange(1,i)) ./ 100;

    ddi=a-b+720;
    %Volume range for pump work
    V2(1:ddi,i)=[V(1:a,i);V(b:719,i)];

```

```

%Pressure range for pump work
    P2(1:ddi,i)=[P(1:a,i);P(b:719,i)];

%Calculated indicated work
    WorkPump(1,i) = -trapz(V2(1:ddi,i),P2(1:ddi,i)) .* 100;

% Calculate Pumping MEP
    MepPump(1,i) = (WorkPump(1,i)/Vchange(1,i)) ./ 100;

%Calculated net work kJ, here pumping work is negative, refer to
workspace
    Worknet(1,i) = WorkInd(1,i) + WorkPump(1,i);

% Calculate Net MEP bar
    MepNet(1,i) = (Worknet(1,i)/Vchange(1,i)) ./ 100;
end

for i=1:N
    X(1,i)=MepNet(1,i);
end
    Xtotal=0;
for i=1:N
    Xtotal=MepNet(1,i)+Xtotal;
end
    Xmean=Xtotal/N;
    temp=0;
for i=1:N
    alpha(1,i)=(X(1,i)-Xmean)^2;
    temp=alpha(1,i)+temp;
end
    SD=sqrt(temp/N);

for i=1:N
    COVimep=SD*100/Xmean;      %where x is an property ex. IMEP, BMEP,
(dp/dtheta)max
end

COVimep          %Printing COVimep value

%~~~~~Executing the thermodynamic file #12~~~~~
clearvars -except a b STBTDC massfuel CV Gc Ge covfiledata BP massair A_Fs
COVimep EVO Vswept CR rpm P_amb T_amb

%~~~~~Creating a PV.xlsx with data V and P as columns #13~~~~~
filename = 'FL-1.xlsx';
xlRange = 'A1:B720';
sheet = 'PV';
PVdata = xlsread(filename,sheet,xlRange);
filename = 'PV.xlsx';
xlRange = 'A1';
xlswrite(filename,PVdata,'',xlRange);
V = PVdata(:,1);
P = PVdata(:,2);

```



```

ST = 360 + STBTDC; %Engine property
%~~~~~Enter the fuel properties #14~~~~~
mf=(massfuel*2)/(60*rpm); %mass of fuel going inside the cylinder per
power stroke

%~~~~~PERFORMANCE Code #15~~~~~

%Calculate Volume change
Vchange = max(V) - min(V);

%Calculate Peak Pressure
PeakPressure = (max(P)/101325);

%Plot the P-V curve
%plot(V,P);

%Volume range for indicated work
V1 = V(a:b);

%Pressure range for indicated work
P1 = (P(a:b)/101325);

%this plots indicated work diagram
%uncomment below line as per need
%plot(V1,P1)

%Calculated Indicated work
WorkInd = trapz(V1,P1) .* 100;

% Calculate Indicated MEP
MepInd = (WorkInd/Vchange) ./ 100;

%Volume range for pump work
V2=[V(1:a);V(b:719)];

%Pressure range for pump work
P2=( [P(1:a);P(b:719)]/101325);

%this plots pump work diagram
%uncomment below line as per need
%plot(V2,P2)

%Calculated indicated work
WorkPump = trapz(V2,P2) .* 100;

% Calculate Pumping MEP
MepPump = (WorkPump/Vchange) ./ 100;

%Calculated net work kJ, here pumping work is negative, refer to workspace
Worknet = WorkInd + WorkPump;

```

```

% Calculate Net MEP bar
MepNet = (Worknet/Vchange) ./ 100;

IP= Worknet*750/60;
%~~~~~COMBUSTION code #16~~~~~
%~~~~~calculation of logP~~~~~
logP=log10(P);

%~~~~~calculation of logV~~~~~
logV=log10(V);

%~~~~~calculation of dp/dtheta #17~~~~~
for i=1:(length(P)-1)
dpdtheta(i)=P(i+1)-P(i);
end
dpdtheta(length(P))= dpdtheta (length(P)-1);

%~~~~~calculation of dv/dtheta #18~~~~~
for i=1:(length(V)-1)
dvdtheta(i)=V(i+1)-V(i);
end
dvdtheta(length(V))= dvdtheta (length(V)-1);

%~~~~~calculation of End of coombustion (EOC) #19~~~~~

%%calculation of pressure due to piston

PP(ST)=P(ST);
for i=ST:539
    PP(i+1)=P(i)*(V(i)/V(i+1))^1.35;
without combustion is taken as 1.35
end
%PP is pressure due to piston
%Gamma value of PG air mixture

%%calculation of pressure due to combustion
for i=ST:540
    PC(i)=P(i)-PP(i);
end
%PC is pressure due to combustion

tempa=0;
for i =ST:360
    if PC(i)>0
%To find out where the positive values of PC are starting due to Ignition
delay
        tempa=i;
        break;

```

```

    end
end
ID=tempa-ST;          %How much diff is there in from ST to positive value
point of PC (actual start of combustion).

t=0;
%Use of sum negative approach discussed by P.J.Shayler and M.W.Wiseman
for i =360:537
%The limits are put from 360 to 537 because the EOC will generally occur
after TDC.
    if PC(i)<=0 && PC(i+1)<=0 && PC(i+2)<=0
%This condition can be improved as discussed by the author bu using
standard error.
        t=i;
%Also, this loop is based on the assumption that PC will definitely be
negative for three consecutive values before end of expansion stroke
        break;
    end
end
EOC=t;
%this is just a reference and not to be taken as End of Combustion.
Further code is written on the basis of MFB to calculate EOC.

%%~~~~~calculation of combustion pressure at constant volume by taking
Vref as volume at TDC #20~~~~~
    %for more detail on Vref please refer above mentioned publication
PP(ST+ID)=P(ST+ID);
%As this value is already calculated in the previous loop of this code.
Vref=Vswept/(CR-1);
%The values after (ST+ID) are considered for PC,PCA or totalPCA (basically
combustion starts from here so all the values should remain same for p and
pp)
for i=(ST+ID):EOC
%The values of PP before this point (ST+ID) does not matter
PCA(i+1-(ST+ID))=(P(i)-PP(i))*(V(i)/Vref);
%PCA is combustion pressure at constant volume condition
end
%PCA values are taken from the point of ST+ID where combustion actually
started.

%%~~~~~calculation of mass fraction burnt
#21~~~~~
%%calculating sum of combustion pressures at const vol for MFB

for i=1:(ST+ID-1)
%The combustion pressure is considered to be zero before (ST+ID) point or
say the difference between pp and p is zero.
totalPCA(i)=0;
end

```

```

for i=(ST+ID):EOC
    totalPCA(i)=totalPCA(i-1)+PCA(i+1-(ST+ID));
end

for i=(EOC+1):720
    totalPCA(i)=totalPCA(EOC);
end

%%~~~~~code          for          calculation          of          MFB
#22~~~~~

for i=1:720
    if i>=(ST+ID) && i<=EOC
        x(i)=totalPCA(i)/totalPCA(EOC);
    elseif i>EOC
        x(i)=1;
    else
        x(i)=0;
    end
end

for i=1:720
    if x(i)>1
        x(i)=1;
    elseif x(i)<0
        x(i)=0;
    else
        x(i)=x(i);
    end
end

tempe=0;
for i=1:720
    if x(i)>=0.9999999
        tempe=i;
        break
    end
end
EOC=tempe;

%%~~~~~code for calculation of cummulative heat through MFB
#23~~~~~

for i=1:720
    if i>=(ST+ID) && i<=EOC
        Q(i)=x(i)*mf*CV;
    elseif i>EOC
        Q(i)=mf*CV;
    end
    %Without accounting for heat losses the code is developed.
    else
    %If the code is accounted for Heat loss, the values can be subtracted from
    the code written on the left side accordingly.
    Q(i)=0;
end

```

```

    end
end

for i=1:720
    if Q(i)>(mf*CV)
        Q(i)=(mf*CV);
    elseif Q(i)<0
        Q(i)=0;
    else
        Q(i)=Q(i);
    end
end

%%~~~~~`calculation of the combustion duration
#24~~~~~
tempf=0;
for i=1:720
    %If the value of MFB reaches more than the value that is needed for
    combustion duration(MFBforCD.
        if x(i)>0.9
            %Then the code will save the point where it is more than MFBforCD.
            tempf=i;
            %The difference between the saved point and the ST will give ud CD.
            break
        end
    end
    CD90_MFB=tempf-ST;           %CD represents combustion duration
    EOCforMFBforCD90=tempf;

    tempf=0;
    for i=1:720
        %If the value of MFB reaches more than the value that is needed for
        combustion duration(MFBforCD.
            if x(i)>0.1
                %Then the code will save the point where it is more than MFBforCD.
                tempf=i;
                %The difference between the saved point and the ST will give ud CD.
                break
            end
        end
        CD10_MFB=tempf-ST;           %CD represents combustion duration
        EOCforMFBforCD10=tempf;

        tempf=0;
        for i=1:720
            %If the value of MFB reaches more than the value that is needed for
            combustion duration(MFBforCD.
                if x(i)>0.5
                    %Then the code will save the point where it is more than MFBforCD.
                    tempf=i;
                    %The difference between the saved point and the ST will give ud CD.
                    break
                end
            end
        end
end
end

```

```

CD50_MFB=tempf-ST;           %CD represents combustion duration
EOCforMFBforCD50=tempf;

%~~~~~calculation of dq/dtheta
#25~~~~~`

%%cal of dq/dtheta before compression stroke

for i=1:179
dqdtheta(i)=0;
end

%%cal of dq/dtheta for compression stroke (from start of comp storke to
S.T)
for i=180:(ST+ID)
dqdtheta(i)=((V(i)*dpdtheta(i))/(Gc-1))+((Gc*P(i)*dvdtheta(i))/(Gc-1));
end

for i=(ST+ID+1):EOC
dqdtheta(i)=Q(i+1)-Q(i);
end

%%cal of dq/dtheta for expansion stroke (from EOC storke to EVO)

for i=(EOC+1):540
%we had to use this loop upto EVO but our EVO angle is lesser than EOC
(done this on basis of set b coposition).
dqdtheta(i)=((V(i)*dpdtheta(i))/(Ge-1))+((Ge*P(i)*dvdtheta(i))/(Ge-1));
end

%%cal of dq/dtheta after expansion stroke

for i=541:720
dqdtheta(i)=0;
end

%calculation of gamma value from start of compression to end of expansion
for i=1:180
G(i)=0;
end

for i=180:(ST+ID)
G(i)=Gc;
end

for i=(ST+ID+1):EOC
G(i)=(dqdtheta(i)+(V(i)*dpdtheta(i)))/(dqdtheta(i)-
(P(i)*dvdtheta(i)));
end

```

```

for i=(EOC+1):540
    G(i)=Ge;
end

for i=540:720
    G(i)=0;
end

dqthetamax=max(dqdtheta);
dpdthetamax=max(dpdtheta)/101325;

for i=1:720
    if dqdtheta(i)==max(dqdtheta)
        dqdthetaalpha=i-360;
        break
    end
end

for i=1:720
    if dpdtheta(i)==max(dpdtheta)
        dpdthetaalpha=i-360;
        break
    end
end

%~~~~~code for writing the excel file for outputs
#26~~~~~
values={};

for i=1:length(P)

temp={P(i),V(i),logP(i),logV(i),dpdtheta(i),dvdtheta(i),dqdtheta(i),x(i),Q
(i),G(i)};
    values=[values;temp];
end
mecheffi = BP*100/IP;
P_Peak_Cycle = max(P)/101325; % bar
dens_inlet_air = (P_amb*29)/(8.314*(273.15+T_amb));
Vol_Effi = 2*(massair/3600)*100/(dens_inlet_air*Vswept*(rpm/60));
phi_stoich = 1/A_Fs;
phi = (massfuel/massair)/(phi_stoich);

headers={'P(Pa)', 'V(m^3)', 'logP',
'logV', 'dp/dtheta (bar/CA)', 'dv/dtheta (m^3/CA)', 'dq/dtheta_gross (J/CA)', 'MF
B', 'cummulative heat (J)', 'Gamma'};
xlswrite('CombustionAnalysis',[headers;values]);

%~~~~~Creating xlsx file with Crank angle data
included~~~~~
filename = 'CombustionAnalysis.xls';
xlRange = 'A1:J721';
CAnalysis = xlsread(filename,xlRange);
filename = 'CombustionAnalysis.xls';

```

```

xlRange = 'D2';
sheet = 'Final';
dump_CA = CAnalysis(:,1);
xlswrite(filename,dump_CA,sheet,xlRange);
warning('off','MATLAB:xlswrite:AddSheet');

filename = 'CombustionAnalysis.xls';
xlRange = 'E2';
sheet = 'Final';
dump_CA = CAnalysis(:,2);
xlswrite(filename,dump_CA,sheet,xlRange);
warning('off','MATLAB:xlswrite:AddSheet');

filename = 'CombustionAnalysis.xls';
xlRange = 'G2';
sheet = 'Final';
dump_CA = CAnalysis(:,3);
xlswrite(filename,dump_CA,sheet,xlRange);
warning('off','MATLAB:xlswrite:AddSheet');

filename = 'CombustionAnalysis.xls';
xlRange = 'H2';
sheet = 'Final';
dump_CA = CAnalysis(:,4);
xlswrite(filename,dump_CA,sheet,xlRange);
warning('off','MATLAB:xlswrite:AddSheet');

filename = 'CombustionAnalysis.xls';
xlRange = 'K2';
sheet = 'Final';
dump_CA = CAnalysis(:,5);
xlswrite(filename,dump_CA,sheet,xlRange);
warning('off','MATLAB:xlswrite:AddSheet');

filename = 'CombustionAnalysis.xls';
xlRange = 'N2';
sheet = 'Final';
dump_CA = CAnalysis(:,6);
xlswrite(filename,dump_CA,sheet,xlRange);
warning('off','MATLAB:xlswrite:AddSheet');

filename = 'CombustionAnalysis.xls';
xlRange = 'Q2';
sheet = 'Final';
dump_CA = CAnalysis(:,7);
xlswrite(filename,dump_CA,sheet,xlRange);
warning('off','MATLAB:xlswrite:AddSheet');

filename = 'CombustionAnalysis.xls';
xlRange = 'T2';
sheet = 'Final';
dump_CA = CAnalysis(:,8);
xlswrite(filename,dump_CA,sheet,xlRange);
warning('off','MATLAB:xlswrite:AddSheet');

```



```

filename = 'CombustionAnalysis.xls';
xlRange = 'V2';
sheet = 'Final';
dump_CA = CAnalysis(:,9);
xlswrite(filename,dump_CA,sheet,xlRange);
warning('off','MATLAB:xlswrite:AddSheet');

filename = 'CombustionAnalysis.xls';
xlRange = 'W2';
sheet = 'Final';
dump_CA = CAnalysis(:,10);
xlswrite(filename,dump_CA,sheet,xlRange);
warning('off','MATLAB:xlswrite:AddSheet');
%~~~~~Adding Crank Angle Value ~~~~~
filename = 'FL-1.csv';
xlRange = 'J93:J812';
CAdata = xlsread(filename,xlRange);
filename = 'CombustionAnalysis.xls';
xlRange = 'J2';
sheet = 'Final';
xlswrite(filename,CAdata,sheet,xlRange);
warning('off','MATLAB:xlswrite:AddSheet');

xlRange = 'M2';
sheet = 'Final';
xlswrite(filename,CAdata,sheet,xlRange);
warning('off','MATLAB:xlswrite:AddSheet');

xlRange = 'P2';
sheet = 'Final';
xlswrite(filename,CAdata,sheet,xlRange);
warning('off','MATLAB:xlswrite:AddSheet');

xlRange = 'S2';
sheet = 'Final';
xlswrite(filename,CAdata,sheet,xlRange);
warning('off','MATLAB:xlswrite:AddSheet');

%~~~~~ Printing Final parameters ~~~~~
Finalinfo = {'Calorific Value J/kg' CV;'Mass Flow Rate Fuel kg/hr'
massfuel;'Mass Flow Rate Air kg/hr' massair;'Gc' Gc;'Ge' Ge;'Spk Time
BTDC' STBTDC;'phi' phi;'a' a;'b' b;'Mech Effi., %' mecheffi;'10% CD'
CD10_MFB;'50% CD' CD50_MFB;'90% CD' CD90_MFB;'ID (CA)' ID;'IMEP(bar)'
MepNet;'IP(kW)' IP;'dq/dtheta_max(J/CA)' dqthetamax;'dq/dtheta_alpha (CA)'
dpdthetaalpha;'COVimep %' COVimep;'dp/dtheta(bar/CA)'
dpdthetamax;'dp/dtheta_alpha(ATDC)' dpdthetaalpha;'Peak Pressure in
Cycle(bar)' P_Peak_Cycle;'Volumetric Effi.,%' Vol_Effi;} ;
header = {'Parameter','Value','','P(Pa)', 'V(m^3)', '', 'logP',
'logV', '', 'Crank Angle', 'dp/dtheta(bar/CA)', '', 'Crank
Angle', 'dv/dtheta(m^3/CA)', '', 'Crank Angle', 'dq/dtheta_gross(J/CA)', '', 'Crank Angle', 'MFB', '', 'cumulative
heat(J)', 'Gamma'};
xlswrite('CombustionAnalysis',header,'Final','A1')
xlswrite('CombustionAnalysis', Finalinfo,'Final','A2')

%~~~~~Request for plot graphs ~~~~~

```

```

reply_plot = input('Do you wish to generate plots, (Y/N):','s')

if reply_plot == 'Y' | 'y'
    prompt = 'Press 1 for Crank Angle vs dp/dtheta(bar/CA)\nPress 2 for
Crank Angle vs dv/dtheta(m^3/CA)\nPress 3 for Crank Angle vs
dq/dtheta_gross(J/CA)\nPress 4 for Crank Angle vs MFB\n'
    dump_ans = input(prompt);
    if dump_ans == 1
        filename = 'CombustionAnalysis.xls';
        xlRange = 'J2:K721';
        sheet = 'Final';
        Plot_dump = xlsread(filename,sheet,xlRange);
        Plot_dumpx = Plot_dump(:,1);
        Plot_dumpy = Plot_dump(:,2);
        scatter(Plot_dumpx,Plot_dumpy);
    elseif dump_ans == 2
        filename = 'CombustionAnalysis.xls';
        xlRange = 'M2:N721';
        sheet = 'Final';
        Plot_dump = xlsread(filename,sheet,xlRange);
        Plot_dumpx = Plot_dump(:,1);
        Plot_dumpy = Plot_dump(:,2);
        scatter(Plot_dumpx,Plot_dumpy);
    elseif dump_ans == 3
        filename = 'CombustionAnalysis.xls';
        xlRange = 'P2:Q721';
        sheet = 'Final';
        Plot_dump = xlsread(filename,sheet,xlRange);
        Plot_dumpx = Plot_dump(:,1);
        Plot_dumpy = Plot_dump(:,2);
        scatter(Plot_dumpx,Plot_dumpy);
    elseif dump_ans == 4
        filename = 'CombustionAnalysis.xls';
        xlRange = 'S2:T721';
        sheet = 'Final';
        Plot_dump = xlsread(filename,sheet,xlRange);
        Plot_dumpx = Plot_dump(:,1);
        Plot_dumpy = Plot_dump(:,2);
        scatter(Plot_dumpx,Plot_dumpy);
    else prompt = 'Please check value entered'
    end
end
elseif reply_plot == 'N' | 'n'
    break
end

```

Appendix – E

Flue Gas Analyzer (AVL-444)

9. Technical Specifications

| Measured quality: | Measuring range: | Resolution: | Accuracy: |
|------------------------|-------------------------------------------|------------------------------------------|-------------------------------------------------------------------|
| CO: | 0... 10 % vol | 0.01 % vol | < 0.6 % vol: ± 0.03 % vol ≥ 0.6 % vol: ± 5 % of ind. val. |
| CO ₂ : | 0... 20 % vol | 0.1 % vol | < 10 % vol: ± 0.5 % vol ≥ 10 % vol: ± 5 % v. M. |
| HC: | 0... 20000 ppm vol | ≤ 2000: 1 ppm vol, > 2000: 10 ppm vol | < 200 ppm vol: ± 10 ppm vol ≥ 200 ppm vol: ± 5 % of ind. val. |
| O ₂ : | 0... 22 % vol | 0.01 % vol 100 ppm | < 2 % vol: ± 0.1 % vol ≥ 2 % vol: ± 5 % v. M. |
| NO: | 0... 5000 ppm vol | 1 ppm vol | < 500 ppm vol: ± 50 ppm vol ≥ 500 ppm vol: ± 10 % of ind. val. |
| Engine speed: | 400... 6000 min ⁻¹ | 1 min ⁻¹ | ± 1 % of ind. val. |
| Oil temperature: | - 30... 125 °C | 1 °C | ± 4 °C |
| Lambda : | 0... 9.999 | 0.001 | Calculation of CO, CO ₂ , HC, O ₂ |
| Power Supply: | | | |
| Voltage: | 11... 22 V DC | | |
| Power consumption: | ≈ 25 W | | |
| Miscellaneous: | | | |
| Warm up time: | ≈ 7 min | | |
| Connector CAL. GAS: | 60... 140 l/h, max. overpressure 450 hPa! | | |
| Connector Gas In: | ≈ 180 l/h, max. overpressure 450 hPa! | | |
| Response time: | t ₉₅ ≤ 15 s | | |
| Operating temperature: | 5... 45 °C | | |
| Storage temperature: | 0... 50 °C | | |
| Relative humidity: | ≤ 95 %, non-condensing | | |
| Inclination: | 0... 90°∠ | | |
| Dimension (WxDxH): | 270 x 320 x 85 mm ³ | | |
| Weight: | 4.5 kg net weight without accessories | | |
| Interfaces: | RS 232 C, Pick up, Oil Temperature Probe | | |

Technical details may be subject to change.


Calibration certificate of AVL-444 Digas Analyzer



Test/Calibration Report

Ref: 05_16_CC075_BITS-Goa_444-5G

Date: 21-03-2016

| | |
|-----|--------------------------------------------------------------------------------------------------------------------------------------------------------------------------------------------------------|
| 1.0 | Component : Model Name: AVL 444 -5 Gas Analyzer Model Sr. No.: 3270 |
| 2.0 | Test sponsored by: BITS Pilani – K.K. Birla Goa BIRLA INSTITUTE OF TECHNOLOGY & SCIENCE Location: K.K. BIRLA GOA CAMPUS, Near NH17B, Buypass Road, Zuarinagar, Goa - 403726 |
| 3.0 | Objective of the Test : To carry out Physical check and calibration of gas Analyzer as per the test procedure specified in annexure 1 of CMVR/TAP 115-116 Part-8 |
| 4.0 | Detailed Observations: |
| 4.1 | Checking of supply/earthing: OK |
| 4.2 | A) Checking of Accessories |
| | 1. Leak Test Cap OK |
| | 2. Power supply OK |
| | 3. Filters OK |
| | 4. Sampling hose & probes OK |
| | B) Functional Check |
| | 1. Leak Test OK |
| | 2. Auto Zero Test OK |
| | 3. Printer Check OK |
| | 4. Date/Time Check OK |
| | 5. Sampling Pipe(Leakage/Damage) OK |
| | C) Span Calibration |
| | 1. Details of the Gas Concentration: CO-3.51%, Co2-14.2%, HC-2030ppm, NO-2060ppm |
| | 2. Calibration gas cylinder no. : CAN-104, 6576 |
| | 3. Calibration gas cylinder make : Bhuruka Gases Ltd. Bangalore |
| | Result : OK |
| 4.3 | Electrical Calibration : Ok |
| 5.0 | One no of petrol vehicle checked for idling Emission measurement. |
| 6.0 | Conclusion : M/C working OK |
| 7.0 | Calibration due date: 20-03-2017 |
| |  Signature & seal of Manufacturer/Supplier |

Appendix – F

Uncertainty Analysis

Demonstration considering emissions with CNG operation

HC emission

Range : 0 to 20000 ppm
Accuracy : ± 10

$$\text{Uncertainty} = \left(\frac{\text{Accuracy}}{\text{Minimum measured value}} \right)$$

$$\text{Uncertainty} = \left(\frac{10}{89.3} \right) = 0.11$$

CO emission

Range : 0 to 10 %
Accuracy : 0.03

$$\text{Uncertainty} = \left(\frac{0.03}{0.04} \right) = 0.75$$

NO emission

Range : 0 to 5000 ppm
Accuracy : ± 50

$$\text{Uncertainty} = \left(\frac{50}{203.6} \right) = 0.24$$

$$\text{Uncertainty in emissions} = \left(\sqrt{(0.11)^2 + (0.75)^2 + (0.24)^2} \right) = 0.79$$

Appendix – G

A) Calibration certificate - air orifice-meter for gasoline operation

COMMERCIAL - IN - CONFIDENCE
FLUID CONTROL RESEARCH INSTITUTE, PALAKKAD
 An ISO 9001 Establishment
 (A Govt. of India R & D Organisation)
 Autonomous body under Ministry of Heavy Industries & Public Enterprises
 KANJIKODE WEST, PALAKKAD - 678 623, KERALA, INDIA.
 ☎ 91-491-2569010, 2566120, 2566206 📠 91-491-2566326 ✉ customercare@fcriindia.com 🌐 www.fcriindia.com

Air Flow
एफ.सी.आर.आई.
FCRI
 Laboratory

CERTIFICATE OF CALIBRATION

on
ORIFICE METER
 for
**M/s. BIRLA INSTITUTE OF TECHNOLOGY AND SCIENCE,
 PILANI, GOA.**



Page 1 of 5 pages

| | | | |
|-----------------|---------------------|---------------|--------------------|
| DATE OF RECEIPT | DATE OF CALIBRATION | DATE OF ISSUE | CERTIFICATE NUMBER |
| 19.05.2016 | 19.05.2016 | 30.05.2016 | CAH 305 1605 015 |

NABL C-0026
 Approved Signatory
 C.B.SURESH, SRE / A.S.M. / CRE
 FCRI, KANJIKODE, PALAKKAD

SUMMARY

Item : Orifice Meter
Tag No : FE-2
Size : 2" NB
Pipe diameter, mm : 34
Orifice diameter, mm : 18
Witnessed by : Mr. M. Sreedhar
Reference / Standard : Critical Flow Venturi Nozzle / ISO 9300
Calibration medium : Air
Laboratory : Air Flow Laboratory
FCRI Procedure : WP/HPB/C01

Results

Mean C = 0.6951
Expanded uncertainty, U (k=2) : 0.22 % reading

| | | |
|--------------------------------------------------------------------------------------------------------|--------------------------------------------------------------------------------------------------------|------------------------------------------------------------------------------------------------------|
| Calibrated by | Certificate Prepared by | Certificate Checked by |
|  Sandeep. A. Y |  Aswathi Mohan M |  C.B. Suresh |
|  Aswathi Mohan M | | |

All the instruments/ Reference flow meters used are traceable to national standards through reference standards and their calibrations are valid.
 satisfactory test / Calibration in no way implies that the product so tested or equipment calibrated is approved by NABL.
 Results presented in this certificate relate only to the items mentioned & calibrated at FCRI.
 This certificate shall not be reproduced except in full without written approval of FCRI.
 The uncertainties are for a confidence probability not less than 95% confidence level unless specified otherwise.

B) Calibration certificate - producer gas orifice-meter

COMMERCIAL - IN - CONFIDENCE
FLUID CONTROL RESEARCH INSTITUTE, PALAKKAD
 An ISO 9001 Establishment
 (A Govt. of India R & D Organisation)
 Autonomous body under Ministry of Heavy Industries & Public Enterprises
 KANJIKODE WEST, PALAKKAD - 678 623, KERALA, INDIA.
 ☎ 91-491-2569010, 2566120, 2566206 ☎ 91-491-2566326 ✉ customercare@fcriindia.com 🌐 www.fcriindia.com

CERTIFICATE OF CALIBRATION

on
ORIFICE METER
 for
**M/s. BIRLA INSTITUTE OF TECHNOLOGY AND SCIENCE,
 PILANI, GOA.**

NABL C-0026

| | | | |
|-----------------|---------------------|---------------|--------------------|
| DATE OF RECEIPT | DATE OF CALIBRATION | DATE OF ISSUE | CERTIFICATE NUMBER |
| 19.05.2016 | 20.05.2016 | 30.05.2016 | CAH 305 1605 016 |

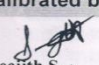
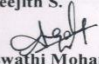
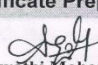
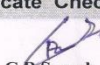
Approved Signatory
 C.B.SURESH, SRE / A.S.M. SURESH, CRE
 FCRI, KANJIKODE, PALAKKAD

SUMMARY

Item : Orifice Meter
Tag No : FE-1
Size : 1" NB
Pipe diameter, mm : 15.798
Orifice diameter, mm : 6.874
Witnessed by : Mr. M. Sreedhar
Reference / Standard : Critical Flow Venturi Nozzle / ISO 9300
Calibration medium : Air
Laboratory : Air Flow Laboratory
FCRI Procedure : WP/HPB/C01

Results

Mean C = 0.6925
 Expanded uncertainty, U (k=2.11) : 0.51 % reading

| | | |
|---------------------------------------------------------------------------------------------------------------------------------------------------------------------------------------------------------------------------------------|-------------------------------------------------------------------------------------------------------------------------------------------|--------------------------------------------------------------------------------------------------------------------------------------|
| Calibrated by  Sreejith S.  Aswathi Mohan M. | Certificate Prepared by  Aswathi Mohan M. | Certificate Checked by  C.B.Suresh |
|---------------------------------------------------------------------------------------------------------------------------------------------------------------------------------------------------------------------------------------|-------------------------------------------------------------------------------------------------------------------------------------------|--------------------------------------------------------------------------------------------------------------------------------------|


All the instruments/ Reference flow meters used are traceable to national standards through reference standards and their calibrations are valid.
 Satisfactory test / Calibration in no way implies that the product so tested or equipment calibrated is approved by NABL.
 Results presented in this certificate relate only to the items mentioned & calibrated at FCRI.
 This certificate shall not be reproduced except in full without written approval of FCRI.
 The uncertainties are for a confidence probability not less than 95% confidence level unless specified otherwise.

Note: Primarily designed for air and converted to PG operation by incorporation density ratio correction factor

C) Calibration certificate - air orifice-meter for CNG operation

COMMERCIAL - IN - CONFIDENCE
FLUID CONTROL RESEARCH INSTITUTE, PALAKKAD
 An ISO 9001 Establishment
 (A Govt. of India R & D Organisation)
 Autonomous body under Ministry of Heavy Industries & Public Enterprises
 KANJIKODE WEST, PALAKKAD - 678 623, KERALA, INDIA.
 ☎ 91-491-2569010, 2566120, 2566206 ☎ 91-491-2566326 ✉ customercare@fcriindia.com 🌐 www.fcriindia.com

CERTIFICATE OF CALIBRATION
 on
ORIFICE METER
 for
M/s. BIRLA INSTITUTE OF TECHNOLOGY AND SCIENCE,
PILANI, GOA.



Page 1 of 5 pages NABL C-0026

| | | | |
|-----------------|---------------------|---------------|--------------------|
| DATE OF RECEIPT | DATE OF CALIBRATION | DATE OF ISSUE | CERTIFICATE NUMBER |
| 30.08.2016 | 29.08.2016 | 22.09.2016 | CAH 1197 1608 083 |


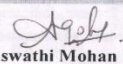
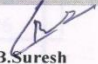
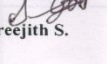
Approved Signatory
ए. एस. मुरली / A. S. MURALI
 उप निदेशक / DEPUTY DIRECTOR

SUMMARY

| | |
|----------------------|-------------------------------------------|
| Item | : Orifice Meter |
| Tag No | : FE-01 |
| Size | : 1½" NB |
| Pipe diameter, mm | : 34 |
| Orifice diameter, mm | : 24 |
| Reference / Standard | : Critical Flow Venturi Nozzle / ISO 9300 |
| Calibration medium | : Air |
| Laboratory | : Air Flow Laboratory |
| FCRI Procedure | : WP/HPB/C01 |

Results

Mean C = 0.6730
 Expanded uncertainty, U (k=2) : 1.48 % reading

| | | |
|---------------------------------------------------------------------------------------------------------|---------------------------------------------------------------------------------------------------------|-----------------------------------------------------------------------------------------------------|
| Calibrated by | Certificate Prepared by | Certificate Checked by |
|  Aswathi Mohan M. |  Aswathi Mohan M. |  C.B.Suresh |
|  Sreejith S. | | |

All the instruments/ Reference flow meters used are traceable to national standards through reference standards and their calibrations are valid.
 Satisfactory test / Calibration in no way implies that the product so tested or equipment calibrated is approved by NABL.
 Results presented in this certificate relate only to the item/s mentioned & calibrated at FCRI
 This certificate shall not be reproduced except in full without written approval of FCRI
 The uncertainties are for a confidence probability not less than 95% confidence level unless specified otherwise.

Appendix – H

MATLAB code for curve fitting (Wiebe model)

```
% Every document must be in the working directory %
% Default working directory is C:\Users\"USERNAME HERE"\Documents\MATLAB"
%
% To select data, double click the relevant document from the %
% 'current folder' section on the left %
% Select all the values between 0 and 1. %
% Also select the last zero and the first one %

%Key Factors%
y=SetA; %name should be changed to SetA or SetB or SetC as per data
selected%
setNo=1; %value should be changed with respect to sets. example: for
y=SetC, setNo=3%

%input from selected data%
theta = 0:1:length(y)-1;
cd =length(y);
is = 0;

%input form user%
a1 = input('input a1: ');
n1 = input('input n1: ');
a2 = input('input a2: ');
n2 = input('input n2: ');

%Wiebe function%
factor=0.80;
z = factor.*(1 - exp(-a1 * ((theta - is)/cd).^n1)) + (1-factor).*(1 -
exp(-a2 * ((theta - is)/cd).^n2));

%code for writing in the excel file%
header={'CA(theta)', 'SetA', 'SetB', 'SetC', 'SetD', 'SetE', 'SetG', 'SetH'};
xlswrite('newData.xlsx',header,1);
xlswrite('newData.xlsx',transpose(theta),1,'A2');
xlswrite('newData.xlsx',transpose(z),1, strcat(char('A'+ setNo),'2'));
plot (theta, z);
hold on;

%code for experimental curve%
x=0:1:length(y)-1;
plot(x,y,'red');
legend('Modeled MFB', 'Experimental MFB');
```

Appendix – I

Data table for MBT spark time and brake power

| CR and (Max. supported load %) | Fuel | Equivalence ratio (ϕ) | | | MBT spark time ($^{\circ}$ CA) | | | Brake Power (kW) | | |
|--------------------------------|------|------------------------------|------|-----------|---------------------------------|-----|-----------|------------------|------|-----------|
| | | 50% | 75% | Full Load | 50% | 75% | Full Load | 50% | 75% | Full Load |
| CR:11 (78 - 83%) | A | 1.08 | 0.96 | 1.06 | 22 | 20 | 18 | 1.11 | 1.65 | 1.70 |
| | B | 1.08 | 1.02 | 1.14 | 19 | 17 | 15 | 1.09 | 1.63 | 1.85 |
| | C | 1.07 | 1.04 | 1.18 | 20 | 17 | 15 | 1.09 | 1.64 | 1.83 |
| CR:15 (91.6%) | A | 1.14 | 1.05 | 1.03 | 18 | 17 | 12 | 1.09 | 1.67 | 1.99 |
| | B | 1.09 | 1.05 | 1.06 | 17 | 15 | 11 | 1.14 | 1.65 | 2.01 |
| | C | 1.11 | 1.07 | 0.96 | 17 | 15 | 10 | 1.13 | 1.61 | 2.01 |
| CR:18 (91.6%) | A | 1.18 | 1.03 | 1.10 | 15 | 12 | 10 | 1.13 | 1.68 | 2.01 |
| | B | 1.02 | 1.02 | 1.04 | 14 | 13 | 11 | 1.11 | 1.64 | 1.97 |
| | C | 1.19 | 0.99 | 0.95 | 15 | 13 | 10 | 1.11 | 1.61 | 1.95 |
| CR:11 (91.6%) | Gas | 1.01 | 1.21 | 1.44 | 22 | 17 | 10 | 1.08 | 1.60 | 2 |
| | NG | 0.95 | 1.02 | 1.01 | 24 | 22 | 16 | 1.12 | 1.62 | 1.98 |

Note: ϕ – Equivalence ratio based on fuel to air ratio basis, MBT – Maximum brake torque, Gas – Gasoline, NG – Natural Gas, Rated power output: 2.2 kW on Gasoline

Brief Biography of Supervisor

Prof. Shibu Clement is an Associate Professor and Head of Mechanical Engineering Department at BITS Pilani KK Birla Goa Campus. He has completed his Ph.D. from IIT Kanpur on “Passive controls for Jet Mixing”. He has over 10 years of teaching and 2 years of industrial experience. His research area includes Investigation into direct absorption of solar energy using nanofluids, Computational and experimental analysis of an alternate fuel based Internal combustion engine, Laminar Separation Bubble: Its structure, dynamics and control, Design, analysis and fabrication of a Lifting-Canard aircraft, Modeling, analysis and fabrication of a thrust vectoring spherical VTOL Aerial Vehicle, Passive controls for jet control and Jet acoustic study. He has research grants from DST FIST Scheme of 25 lakhs in the area of Thermal sciences. He is actively involved in Center for Research Excellence in waste, Water and Energy management – BITS Pilani. He has published over 38 research papers in the international/national journal / conferences of repute. He is actively guiding 4 PhD (2 completed and 1 submitted) and number of first degree academic thesis.

Brief Biography of Co-Supervisor

Dr. N.K.S. Rajan is a Chief Research Scientist at Combustion Gasification & Propulsion Laboratory, Department of Aerospace Engineering, IISc. Bengaluru. He has completed his bachelor of science degree from University of Mysore and PhD from Department of Aerospace Engineering, IISc. He has about 20 years of experience in academic research and R&D in sponsored projects (Government Sponsored & Industrial Consultancy) and he is also an expert member of several committees of the Institute and outside governmental and autonomous institutions. His research area includes, Combustion; Heat Transfer; Fluid Dynamics (Experimental and Computational); Biomass Gasification; Advanced CFD Simulations, Instrumentation; Numerical Modelling (Analysis and Simulation); RSD Analysis, GIS Application Development; Advanced Application Software Development. He has published over 60 research publications (Journals and Conferences – International & National) and about 10 Internal (Departmental) Publications. He is actively guiding 8 PhD (4 completed); 4 MSc (Engg); 50 ME; several batches of B.E. (for their dissertation projects of their degree.). He is a principal investigator for 30 Sponsored R&D projects and

Co-Investigator of about 10 other R&D projects with a total of operating projects outlay of about Rs.50 Crores.

Brief Biography of Candidate

Mr. M. Sreedhar Babu is a lecturer in the department of Mechanical Engineering at the Birla Institute of Technology and Science, Pilani, KK Birla Goa campus, Goa, India. He has over 8 years of teaching experience. He has been teaching core mechanical courses like Basic Thermodynamics, Applied Thermodynamics, Internal Combustion Engines and Advances in IC Engines etc. He completed his graduation in Mechanical Engineering in 2006 and Masters in Energy Systems Engineering from Visveswaraya Technological University, Belgaum in 2008. He secured University 3rd rank during his master's degree. His area of research includes development of Producer gas engines and emission control. He has published over 6 research papers in the peer reviewed international journal / conferences.